# FUNCTIONAL ANALYSIS OF SYP1, A NOVEL SUBSTRATE OF THE SERINE/THREONINE KINASE PRK1

**QIU WENJIE**

**NATIONAL UNIVERSITY OF SINGAPORE**

**2007**

# FUNCTIONAL ANALYSIS OF SYP1, A NOVEL SUBSTRATE OF THE SERINE/THREONINE KINASE PRK1

**QIU WENJIE**

**A THESIS SUBMITTED**
**FOR THE DEGREE OF DOCTOR OF PHILOSOPHY**
**INSTITUTE OF MOLECULAR AND CELL BIOLOGY**
**NATIONAL UNIVERSITY OF SINGAPORE**

**2007**

# Acknowledgements

Foremost, I would like to express my sincere gratitude to my supervisor A/P Mingjie Cai, for providing me the opportunity to continue my Ph.D. research work in his laboratory after my former supervisor left IMCB. I am deeply grateful to A/P Cai for his guidance, tolerance, encouragement and support throughout my graduate studies. Heartfelt appreciation also goes to my graduate supervisory committee members, A/P Thomas Leung and A/P Uttam SURANA, for their invaluable advice and encouragement during the course of this study. I am also grateful to A/P Uttam Surana and A/P Alan Munn for sharing some strains used in this study.

I would like to thank the past and present members in CMJ laboratory, for their helpful discussion, technique assistance, cooperation and friendship. Special thanks go to Dr. Guisheng Zeng, Dr. Yu Xianwen and Miss Suat Peng Neo for their help, advice, and sharing of experience. Desmond Dorairajoo and Jun Wang are thanked for the work with microscopy and other general technical assistance. Thanks also go to Dr. Guisheng Zeng, Dr. Chee Wai Fong and Miss Suat Peng Neo for their critical reading of my thesis.

Many thanks also to the past and present members in US laboratory, to Dr. Hong Hwa Lim, Miss Karen Crasta, Mr. Tao Zhang, Mr. Jenn Hui Khong and Mr. Saurabh Nirantar, for interesting discussions and help with the project.

I am also indebted to my former supervisor Dr. Sheng-Cai Lin for his help to begin my PH.D study and for the training of molecular biology techniques in his laboratory.

I cannot express in words my gratitude to my family: my wife Liqin Hu and my lovely little daughter Elim. Thanks for their love and encouragement over these years. I would like to thank my parents and parents-in-law too. Without their support and help, it would be impossible to finish my Ph.D. work.

# Table of contents

# List of Figures

**Figure:**

# List of Tables

**Table:**

# Abbreviations

| | |
|---|---|
| a.a. or aa | amino acid |
| AAK1 | adaptor-associated kinase 1 |
| ADF | actin depolymerizing factor |
| ADFH | actin depolymerizing factor homologous region |
| ADP | adenosine 5’-diphosphate |
| AP2 | adaptor protein 2 |
| ATP | adenosine 5'-triphosphate |
| BAR | BIN-amphiphysin-RVS domain |
| bp | base pair |
| BSA | bovine serum albumin |
| °C | degree Celsius |
| CAP | adenylyl cyclase-associated protein |
| CC | coiled coil |
| CDC | Cell Division Cycle |
| CDK | Cyclin-dependent kinase |
| CFP | cyan fluorescent protein |
| CFW | Calcofluor White |
| CIP | calf intestinal phosphatase |
| Cln | cyclin |
| C-terminal | carboxy-terminal |
| COPII | coated vesicle complex II |
| DAD | Diaphanous autoregulatory domain |
| DAPI | 4',6-diamidino-2-phenylindole |
| DID | Diaphanous inhibitory domain |
| DMSO | Dimethyl Sulfoxide |
| DNA | deoxyribonucleic acid |
| DPW | Asp-Pro-Trp motifs |

| | |
|---|---|
| DTT | dithiothreitol |
| ECL | enhanced chemiluminescence |
| *E. coli* | *Escherichia coli* |
| EDTA | ethylenediamine tetraacetic acid |
| EGFP | enhanced green fluorescent protein |
| EH | Eps15 homology |
| ENTH | Epsin amino-terminal homology |
| EVH | Ena/VASP homology |
| F-actin | filamentous actin |
| FCH | Fes/CIP4 homology domain |
| FH | formin homology domain |
| FRAP | fluorescence recovery after photo-bleaching |
| FUR | Fluoro Uracil Resistance |
| G-actin | actin monomer |
| GAP | GTPase-activating protein |
| GBD | GTPase binding domain |
| GDP | guanosine diphosphate |
| GED | GTPase effector domain |
| GEF | guanine-nucleotide exchange factor |
| GFP | green fluorescent protein |
| GST | glutathione *S*-transferase |
| GTP | guanosine triphosphate |
| GTPase | guanosine triphosphatase |
| hrs | hours |
| HA | haemagglutinin |
| HEPES | hydroxyethylpiperazine ethanesulfonic acid |
| HIP1 | Hungtingtin interacting protein-1 |
| HRP | horseradish peroxidase |
| HU | hydroxyurea |

| | |
|---|---|
| IgG | immunoglobulin G |
| IP | immunoprecipitation |
| IPTG | isopropyl-β-D-thiogalactoside |
| kb | kilobase(s) |
| kDa | kilodalton |
| Lat-A | Latrunculin-A |
| LB | Luria-Bertani medium |
| LY | Lucifer Yellow |
| M | molar |
| MAT | mating locus |
| min | minute |
| ml | milliliter |
| mM | millimolar |
| μg | microgram |
| μm | micrometer |
| nm | nanometer |
| N-terminal | amino-terminal |
| NPF | Asp-Pro-Phe motifs |
| NPFs | nucleation-promoting factors |
| N-WASP | neuronal Wiskott-Aldrich syndrome protein |
| OD | optical density |
| ORF | open reading frame |
| PAGE | polyacrylamide gel electrophoresis |
| PBS | phosphate-buffered saline |
| PCR | polymerase chain reaction |
| PEG | polyethylene glycol |
| PH | pleckstrin homology |
| $PIP_2$ | phosphatidylinositol-4,5-bisphosphate |
| PMSF | phenylmethylsulfonyl fluoride |

| | |
|---|---|
| PNPP | *p*-nitrophenylphosphate |
| poly-P | proline-rich region |
| PP2A | Protein Phosphatase 2A |
| PVDF | polyvinylidene difluoride |
| RBD | Rho-binding domain |
| RFP | red fluorescent protein |
| rpm | revolutions per minute |
| SBD | Spa2-binding domain |
| sec | second |
| SC | synthetic complete (medium) |
| SDS | Sodium dodecyl sulphate |
| SH2 | Src homology 2 |
| SH3 | Src homology 3 |
| SHD | Sla1 homology domain |
| SR | the C-terminal QxTG repeats of Sla1p |
| SYP | Suppressor of Yeast Profilin deletion |
| TAP | tandem-affinity purification |
| TCA | Trichloroacetic Acid |
| TE | Tris-EDTA buffer |
| TEMED | N,N,N',N'-tetramethylethylenediamine |
| Tris | Tris(hydroxymethyl)aminomethane |
| VASP | vacuolar protein sorting |
| VPS | vacuolar protein sorting |
| WA | WH2 domain and acidic motif |
| WASP | Wiskott-Aldrich syndrome protein |
| WAVE | WASP-family verprolin homologous protein |
| WH | WASP homology region |
| WIP | WASP interacting protein |
| WT | wild type |

| | |
|---|---|
| YEPD | yeast extract-peptone-dextrose (rich medium) |
| YFP | yellow fluorescent protein |

# Summary

Cell polarity is a fundamental property of cells. The budding yeast *Saccharomyces cerevisiae* is a model system for the study of cell polarity. Yeast cells first select a proper site to establish cell polarity. In this site, actin and septin cytoskeletons are organized to achieve polarized cell growth. Actin patches and actin cables are two essential organizations of actin cytoskeleton which are involved in the establishment and maintenance of polarized cell growth. Actin patches are required for endocytosis while actin cables are essential for the polarized vesicle transport. Upon internal and external signals, actin cytoskeleton undergoes a dramatic reorganization regulated by a large number of cytoskeleton-associated proteins, such as Pan1p, Sla1p and Bni1p. The functions of Pan1p and Sla1p are regulated by an important serine/throrine kinase Prk1p.

Septin cytoskeleton is required for cell morphogenesis and division in budding yeast. Septins form a heterooligomeric complex which localizes at the mother-daughter junction. Septin filaments also undergo assembly and disassembly in accordance with the progression of the cell cycle.

Syp1p was first identified as a multi-copy suppressor of profilin deletion mutant and its overexpression was found to cause an elongated bud phenotype. The functions of Syp1p in actin and septin cytoskeletons were investigated in depth in this study. Firstly, Syp1p is shown to be a novel substrate of Prk1p and its phosphorylation by Prk1p negatively regulates Syp1p's functions. Secondly, Syp1p overexpression suppresses the *bni1*Δ mutants at non-permissive temperature. Syp1p overexpression also partially rescues the depolarized localization of actin of the *bni1*Δ mutant. Thirdly, Syp1p is

found to colocalize with the actin cytoskeleton. The localization of Syp1p is dependent on the intact actin cytoskeleton. Fourthly, Syp1p is discovered to physically interact with the actin patch-associated protein Sla1p. These results indicate that Syp1p has functional relationships with both actin cables and actin patches.

In addition to its roles in the actin cytoskeleton, Syp1p is also discovered to be a new regulator of septin dynamics. Firstly, Syp1p is found to colocalize with septin throughout the cell cycle. Secondly, Syp1p is able to interact directly with the septin subunit Cdc10p. Thirdly, Syp1p overexpression disorganizes the septin structure and induces the Swe1p-dependent elongated bud phenotype. Fourthly, in the *syp1Δ* mutant, the formation of a complete septin ring at the incipient bud site and the disassembly of the septin ring at the end of cell division were both significantly delayed. These results suggest that Syp1p is involved in the regulation of cell cycle-dependent dynamics of the septin cytoskeleton in yeast.

In summary, Syp1p is a novel regulator of cell polarity through its regulation of both actin and septin cytoskeleton organization.

# Chapter 1 Introduction

The cytoskeleton filaments are fundamental structures to achieve polarized cell growth and directional cell division. The cytoskeleton is involved in the positioning of organelles or protein complexes, vesicle trafficking, cell shape maintenance and remodeling, and cell movement (Bretscher, 2003; Pruyne *et al.*, 2004b). There are basically three forms of cytoskeleton elements: actin cytoskeleton, intermediate filaments and microtubules. Recently, septin filament has been known as another type of cytoskeleton critical for cell polarity (Douglas *et al.*, 2005; Kinoshita, 2006; Spiliotis and Nelson, 2006). A central feature of the cytoskeleton is its ability to reorganize rapidly in response to internal and external stimuli to allow a cell to perform its function and to survive in a harsh environment (Moseley and Goode, 2006). This dynamic organization of the cytoskeleton has to be properly regulated. Therefore, it is critical to understand how different associated proteins regulate the reorganization of the cytoskeleton.

The yeast *Saccharomyces cerevisiae* is a powerful system to study the mechanisms of cell polarity and regulation of cytoskeleton. Many findings from yeast have been shown to be conserved in higher organisms such as vertebrates (Pruyne *et al.*, 2004b). In the following literature reviews, the cellular polarization and the role of actin/septin cytoskeletons in polarized cell growth in yeast will be discussed in detail.

## 1.1 Cell polarity and its mechanism in yeast

*S. cerevisiae* undergoes polarized growth during several stages of its life cycle (Fig.1.1) (Roemer *et al.*, 1996b). In the presence of rich nutrients, yeast grows by budding, and the position of bud growth is known as the cell division plane (Fig. 1.1 and Fig. 1.2).

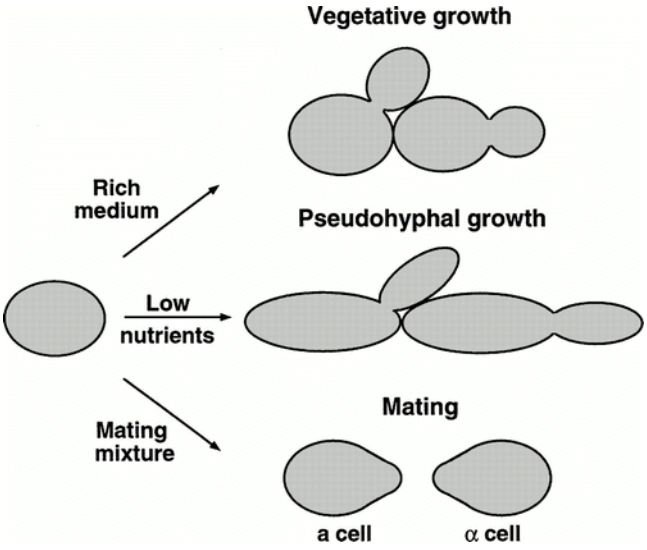


**Figure 1.1 Three forms of polarized cell growth in the *Saccharomyces cerevisiae* life cycle**. Cells grown in a rich medium are round or oval and have defined budding patterns. When exposed to a low-nutrient medium, cells elongate and bud from the distal end to form pseudohyphae. Haploid cells exposed to pheromone from cells of the opposite mating type arrest in G1 and extend a projection toward their mating partner. (Reproduced with permission from *Trends Cell Biol*.) (Roemer *et al.*, 1996b)

A second form of polarized growth in yeast is called pseudohyphal growth, which occurs when there is shortage of nutrients. Under these conditions, yeast cells elongate to form chains of cells (Fig. 1.1)(Gimeno *et al.*, 1992; Roberts and Fink, 1994).

A third form of polarized growth in yeast occurs during the mating response. Haploid yeast has two cell types, *MAT*a and *MAT*α. Upon exposure to pheromone from cells of the opposite mating type, the cells are arrested in late G1 and form an elongated mating projection (shmoo) (Fig. 1.1) (Cross *et al.*, 1988; Marsh *et al.*, 1991).

Although bud growth, pseudohyphal growth, and the mating response are different cellular processes, each process undergoes similar steps to achieve polarized growth (Madden and Snyder, 1998; Casamayor and Snyder, 2002). First, a proper site for polarized growth is selected and established upon internal or external signals. Next, cytoskeletons are organized and polarized to the chosen sites. The cytoskeleton then targets polarized secretion to that site. During these different stages of polarized growth, both actin and septin cytoskeletons play critical roles in establishment and maintenance of cell polarity.

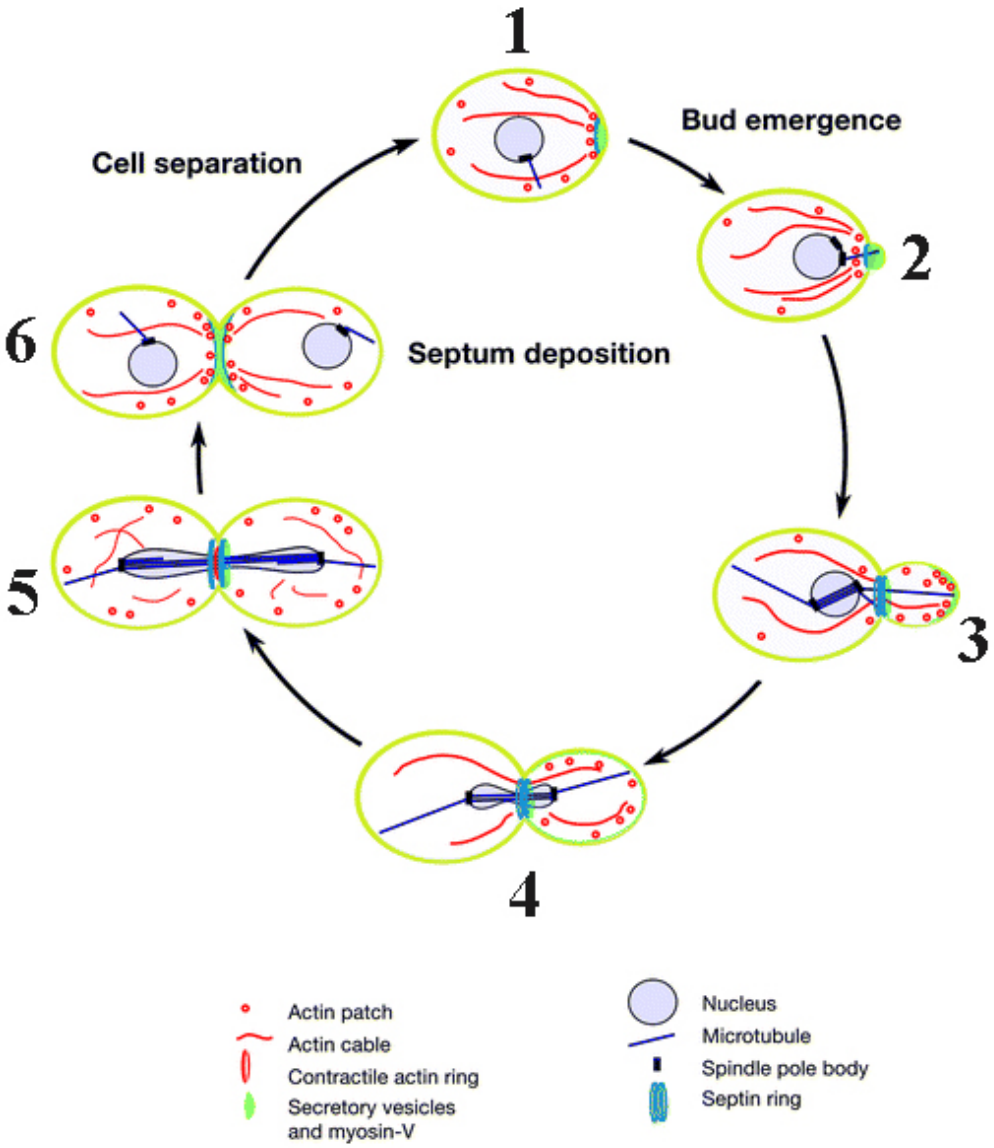


**Figure 1.2 Different stages of budding during the cell cycle. 1**) The cell first selects a defined site according to its ploidy for bud emergence during the late G1 stage of the cell cycle. **2**) The established site then organizes a cytoskeleton network, which is required for targeting secretion to that site for bud emergence. After bud emergence, cell growth is restricted first at the bud tip (apical growth) (**3**) and then throughout the bud (isotropic growth) (**4**). When the bud reaches certain sites, the cell undergoes mitosis (**5**) and cytokinesis (**6**), and secretion is directed to the bud neck for the synthesis of septum and actomyosin ring that separates the mother and daughter. (Modified with permission from *Annu Rev Cell Dev Biol*.) (Pruyne *et al.*, 2004b)

### 1.1.1 Bud site selection for polarized growth

Yeast cells choose a bud site according to its ploidy, with diploid cell budding from the poles of cells (bipolar pattern), and haploid budding from sites adjacent to their previous bud site (axial pattern) (Fig. 1.3) (Chant and Pringle, 1995; Roemer *et al.*, 1996b; Casamayor and Snyder, 2002). These budding patterns suggest that the polarization machinery recognizes the cortical cues that persist from the previous cell cycle. Initial insights into how this occurs came from a screen for mutants that altered the axial and bipolar budding patterns (Chant *et al.*, 1991; Chant and Herskowitz, 1991). Three classes of proteins have been identified to be important for bud site selection. One class is required for axial budding, but does not affect the bipolar pattern (Fig. 1.4, Gene set I) (Chant and Herskowitz, 1991). These proteins include Bud3p (Chant *et al.*, 1995), Bud4p (Sanders and Herskowitz, 1996), Axl2p/Bud10p (Halme *et al.*, 1996; Roemer *et al.*, 1996a) and Axl1p (Fujita *et al.*, 1994). Mutations of these genes result in bipolar budding in haploid cells. Another class is important for the bipolar budding pattern of diploid cells and not required for haploid axial budding (Fig. 1.4, Gene set II) (Zahner *et al.*, 1996), including Bud8p, Bud9p (Taheri *et al.*, 2000; Harkins *et al.*, 2001) and Rax2p (Chen *et al.*, 2000). The third class is required for both axial and bipolar budding which includes the Ras-related GTPase, Rsr1p/Bud1p, and its regulatory GTPase-activating protein (GAP) Bud2p and guanine-nucleotide exchange factor (GEF) Bud5p (Fig. 1.4, Gene set III) (Chant *et al.*, 1991; Bender, 1993; Park *et al.*, 1993). The Bud1p GTPase signaling module is thought to recruit bud formation components, such as Cdc42p, Cdc24p, and Bem1p (Fig. 1.4, Gene set IV), to the cortical region at the presumptive bud sites (Zheng *et al.*, 1995; Park *et al.*, 1997; Kozminski *et al.*, 2003).

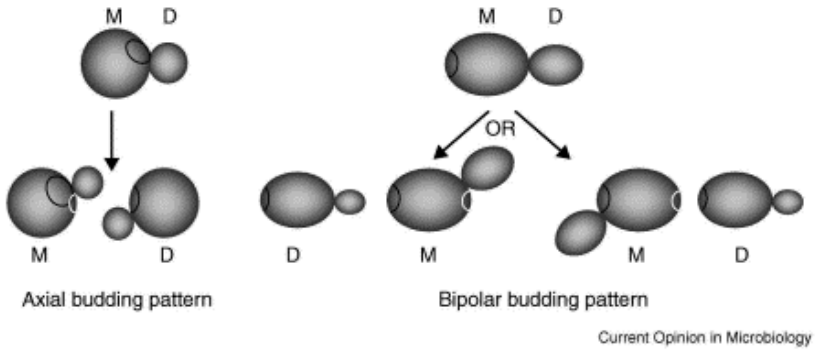


**Figure 1.3 Axial and bipolar budding patterns in yeast cells**. Staining with the calcofluor dye permits visualization of two types of scars on any yeast cell surface. The scar marking the place where the cell was initially attached to its mother (M) cell is called the birth scar, whereas smaller scars that originated by cytokinesis of the daughter (D) cells are named bud scars. Examination of the pattern of bud and/or birth scars reveals different budding patterns. The axial budding pattern is typically found in haploid *MAT*a and *MAT*α cells, and is characterized by adjacent budding to the birth scar in both mother and daughter cells. Diploid *MAT*a/*MAT*α cells follow a bipolar budding pattern in which daughter cells usually bud distally (that is, at the opposite pole to the birth scar), and the mother cell buds at either pole. The birth scar is represented by a curved black line, and subsequent bud scars are represented by curved white lines. (Reproduced with permission from *Curr Opin Microbiol.*) (Casamayor and Snyder, 2002).

## 1.1.2 Establishment of polarized growth by Cdc42p

Deletion of any one of the bud site selection genes is not lethal. However, some genes that are involved in bud formation are essential. Factors required for bud formation were identified in screens for temperature-sensitive mutants that were arrested as enlarged, round unbudded cells at the restrictive temperature. Two essential factors identified in this way are the Rho-family GTPase Cdc42p (Adams *et al.*, 1990; Johnson and Pringle, 1990) and its Rho-GEF Cdc24p (Sloat and Pringle, 1978; Zheng *et al.*, 1994). The third component Bem1p was identified as a scaffold protein that binds Cdc24p and Cdc42p (Zheng *et al.*, 1995; Bose *et al.*, 2001).

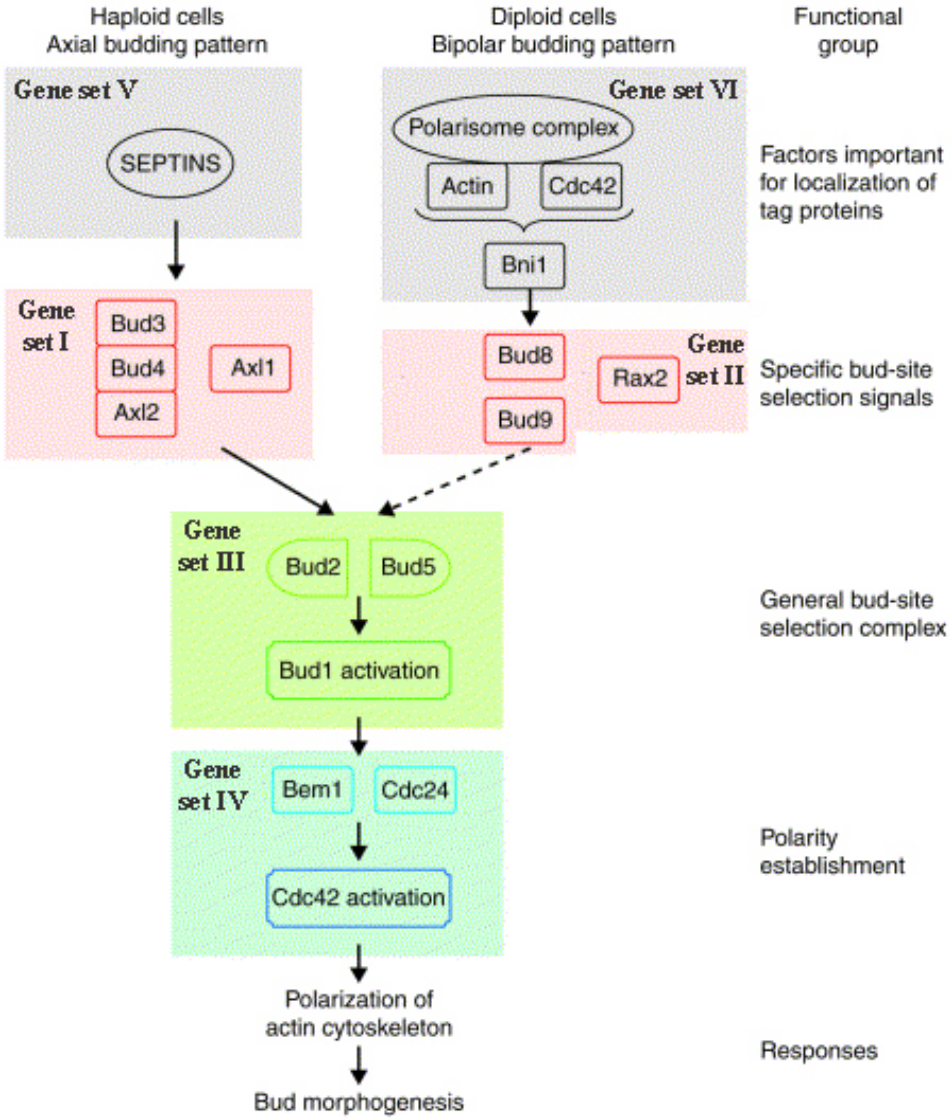


**Figure 1.4 Summary of signaling pathways that lead to the polarity establishment during bud formation.** Proteins belonging to the same functional group are framed in the same color (Gene sets I–VI). The dotted arrow represents hypothetic regulation of gene set II by the specific bud-site selection signals present in diploid cells. (Modified with permission from *Curr Opin Microbiol.*) (Casamayor and Snyder, 2002)

The polarity-establishing proteins are thought to promote the assembly of cytoskeleton components such as actins and septins to target the secretory vesicles to the bud site for bud formation (Fig. 1.4). The earliest events of polarized growth are the

depositions of the septin ring and assembly of polarized actin cytoskeleton (Li *et al.*, 1995; Gladfelter *et al.*, 2002).

## 1.2 Yeast actin cytoskeleton

### 1.2.1 Roles of yeast actin cytoskeleton in polarized growth

The Yeast actin cytoskeleton is required for cellular polarization at different stages of polarized growth. The actin cytoskeleton plays an important role in bipolar bud site selection and maintenance of polarized budding growth. The actin cytoskeleton is also required for maintaining the polarity of Cdc42p localization. In addition, the actin cytoskeleton is required for cell wall synthesis which is involved in polarity growth and morphogenesis.

#### 1.2.1.1 The role of actin cytoskeleton in bipolar bud site selection

Bipolar bud site selection requires the actin cytoskeleton and its associated proteins (Fig. 1.4, Gene set VI). Many *act1* mutations have been found to affect the bipolar budding pattern (Drubin *et al.*, 1993; Yang *et al.*, 1997). These mutations do not affect the budding pattern of daughter cells but instead cause mother cells to bud randomly. The amino acids important for bud site selection were all mapped to a specific domain of the actin protein (Wertman *et al.*, 1992; Yang *et al.*, 1997), suggesting that this region of Act1p may recognize bipolar-specific proteins or cues. Mutations in genes encoding some actin-associated proteins (e.g. Sac6p, Srv2p, Sla1p, Sla2p, Rvs161p, Rvs167p) also cause defects in bipolar budding similar to those of the *act1* mutations (Adams *et al.*, 1991; Crouzet *et al.*, 1991; Bauer *et al.*, 1993; Holtzman *et al.*, 1993; Amberg *et al.*,

1995; Freeman *et al.*, 1996; Yang *et al.*, 1997). In addition, the polarisome, a protein complex that regulates the assembly of actin filaments at the bud site (see section 1.2.4.3 for more detail), plays a role in bipolar bud site selection (Valtz and Herskowitz, 1996; Amberg *et al.*, 1997).

Several mechanisms are used by actin-associated proteins to participate in bipolar budding (Madden and Snyder, 1998). First, one or more of these proteins might interact with the Act1p domain required for bipolar budding. Second, the actin cytoskeleton at the incipient bud site and at the neck might help to target bud site selection components to their proper localization.

#### 1.2.1.2 The role of actin cytoskeleton in maintenance of the polarity of Cdc42p

The actin cytoskeleton is an important element for the maintenance of Cdc42p polarity through an actin-based positive feedback loop (Irazoqui *et al.*, 2005). Cdc42p can polarize in the absence of filamentous actin (Gulli *et al.*, 2000; Irazoqui *et al.*, 2003), which suggests that actin cytoskeleton is not required for initial polarized localization of Cdc42p. However, actin cytoskeleton is required for the maintenance of Cdc42p polarity in the unbudded cells (Irazoqui *et al.*, 2005). Firstly, Cdc42p disperses from the polarized site through actin patch-dependent endocytosis. Secondly, actin cables are required to counteract the dispersal and maintain the polarized localization of Cdc42p. These findings indicate an actin-based positive feedback loop for Cdc42p polarization.

#### 1.2.1.3 The role of actin cytoskeleton in polarized growth

In addition to its role in establishing polarity through regulation of bipolar bud site selection and Cdc42p polarized localization, the actin cytoskeleton is also required for polarized growth. Unlike animal cells, which primarily use microtubule-based transport to establish and maintain cell polarity (Small and Kaverina, 2003), yeast cells employ actin cable-based transport to direct polarized cell growth (Bretscher, 2003). The involvement of actin cytoskeleton in polarized growth was discovered through the *act1* mutants. Temperature-sensitive mutations in *ACT1* were found to exhibit polarity defects. At restrictive temperature, *act1* mutant cells were arrested as either large unbudded cells or small budded cells with an enlarged mother cell, accompanied by phenotypes including delocalized chitin staining, cell lysis, and sensitivity to high osmolarity (Novick and Botstein, 1985; Wertman *et al.*, 1992). Many of these phenotypes are probably caused by defects in polarized secretion which requires actin cables (Pruyne *et al.*, 2004b). Actin cables are assembled at the bud site in $G_1$ for targeting of growth and secretion to the future bud tip. During cytokinesis, actin cables are re-oriented to the bud neck and direct the secretion to the bud neck for septum formation. These cables function as polarized tracks for Type V myosin-dependent delivery of vesicles (Pruyne *et al.*, 1998; Karpova *et al.*, 2000).

### 1.2.2 Actin assembly and actin turnover

The actin cytoskeleton is a highly dynamic network composed of actin filaments and actin-associated proteins. Assembly of actin monomers into a filament involves an initial nucleation step, which has inherently slow efficiency due to instability of actin

dimers and trimers. The Arp2/3 complex and formins bypass the inefficient slow formation of actin dimers and trimers to nucleate actin polymerization (Welch and Mullins, 2002; Kovar, 2006). Actin assembly is highly directional and is known as treadmilling, a process by which the actin subunits are added at the barbed end and are dissociated at the pointed end (Wang, 1985). Addition of an ATP-actin subunit to the barbed end triggers hydrolysis of ATP bound to that subunit (Pollard *et al.*, 2000). ADP-actin subunits dissociate from the pointed ends and the resulting ADP-actin monomers undergo nucleotide exchange (ADP to ATP) for subsequent rounds of barbed-end addition. Actin turnover refers to the collective dynamic events of actin subunits assembling at the filament barbed ends, dissociating from filament pointed ends and recycling of actin monomers for new rounds of polymerization (Moseley and Goode, 2006).

All eukaryotic cells contain a core set of actin-binding proteins that regulate actin filament assembly and turnover. These factors cooperate to drive the remodeling of the actin cytoskeleton in response to internal and external stimuli.

## 1.2.3 Cortical actin patches

### 1.2.3.1 Dynamic localization of cortical actin patches

The actin cytoskeleton consists of three distinct structures: cortical patches, cables, and actomyosin ring (Fig. 1.2) (Adams and Pringle, 1984; Amberg, 1998). Both actin patches and actin cables are polarized toward regions of cell growth. Cortical actin patches undergo dynamic localization throughout the cell cycle (Kilmartin and Adams, 1984). In unbudded $G_1$ cells which grow isotropically, actin patches are distributed

randomly over the entire cell surface. During the budding period, the actin patches congregate first at the incipient bud site and later inside the bud with actin cables aligned toward them. During mitosis, actin patches are randomized within the mother and daughter cell, and at cytokinesis, they are polarized to the mother-bud neck again (Fig. 1.2).

#### 1.2.3.2 Assembly of actin filament by Arp2/3 complex and its NPFs

Arp2/3 complex is required for the assembly of cortical actin patches (Moreau *et al.*, 1996; Winter *et al.*, 1997; Winter *et al.*, 1999b). The Arp2/3 complex is composed of seven conserved subunits, including two *a*ctin-*r*elated *p*roteins (Arp2p and Arp3p) and five unique proteins (Arc40p/p40, Arc35p/p35, Arc19p/p20, Arc18p/p21, and Arc15p/p15). Deletion of any subunit except *ARC18* causes severe growth defects or lethality (Winter *et al.*, 1999b) accompanied by endocytosis defects and severe or complete loss of cortical actin patches. It has been proposed that the Arp2/3 complex promotes actin assembly by mimicing the barbed end of a filament (Pollard and Beltzner, 2002). The Arp2/3 complex can also bind to the sides of a preexisting (mother) actin filament and assemble a new (daughter) filament at a 70° angle, thus producing branched actin networks (Blanchoin *et al.*, 2000; Amann and Pollard, 2001; Higgs and Pollard, 2001). However, the Arp2/3 complex is a weak actin nucleator and requires nucleation-promoting factors (NPFs) to enhance its activity.

There are five NPFs of Arp2/3 complex in budding yeast: Las17p, Myo3p, Myo5p, Pan1p, and Abp1p (Moseley and Goode, 2006). Each NPF has an acidic motif that binds

to the Arp2/3 complex (Fig. 1.5). Binding to actin is critical for the NPF activity of Las17p, Pan1p, and Abp1p.

**(i) Las17p/WASp**

Las17p (also termed Bee1p) was the first NPF reported in yeast and was identified by its sequence homology with mammalian WASp (Li, 1997). Similar to Mammalian WASp, a homologous WA fragment (containing the WH2 domain and acidic motif) (Fig. 1.5) of Las17p can activate the Arp2/3 complex (Winter *et al.*, 1999a). The NPF activity of full-length Las17p is much stronger than that of its WA fragment *in vitro*. This could be due to its binding to F-actin and/or the Arp2/3 complex by N-terminal regions (Rodal *et al.*, 2003). The NPF activity of WASp can be inhibited by intra-molecular interaction or inter-molecular interaction (Bompard and Caron, 2004). In both mechanisms, Rho GTPase activity can relieve the inhibition. For example, Cdc42p binds

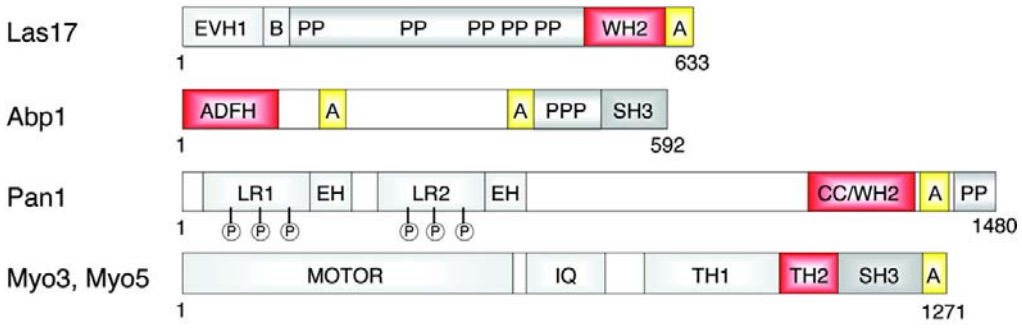


**Figure 1.5 Schematics of yeast NPFs**. Abbreviations: A, acidic; B, basic; CC, coiled-coil; EH, Eps15 homology; EVH1, Ena/VASP homology 1; IQ, IQ binding; LR, long repeat; PP or PPP, polyproline; SH3, Src homology 3; TH1/2, tail homology 1/2; WH1, WASp homology 1; WH2, WASp homology 2. The proposed actin-binding domain of each NPF is colored red; acidic domains are yellow. Pan1p contains many Ark1/Prk1 consensus phosphorylation sites in LR1 and LR2 (indicated by the circled P). (Reproduced with permission from *Microbiol Mol Biol Rev*.) (Moseley and Goode, 2006)

to the GTPase-binding domain (GBD) of N-WASp to relieve the auto-inhibition (Rohatgi *et al.*, 2000), and Rac1p binds to the transinhibitory complex of WAVE1 to activate WAVE1 (Eden *et al.*, 2002). Currently, it is not clear how Las17p activity is regulated. Las17p lacks a GBD domain and can not bind yeast Rho GTPases (Li, 1997). Purified full-length Las17p does not exhibit auto-inhibition and constitutively promotes Arp2/3 complex to nucleate actin (Rodal *et al.*, 2003)**.** However, two Las17p associated proteins, Sla1p and Bbc1p, can directly inhibit Las17p activity (Rodal *et al.*, 2003). Thus, transinhibition may be one mechanism to regulate Las17p activity. In addition, Las17p has many other binding proteins which may contribute to its activity regulation (Goode and Rodal, 2001).

**(ii) Pan1p**

Pan1p is required for actin organization and endocytosis (Tang and Cai, 1996; Duncan *et al.*, 2001). Pan1p can be recruited to patches through its interactions with End3p, Sla1p, and/or clathrin adaptors (Wendland and Emr, 1998; Tang *et al.*, 2000). The NPF activity of Pan1p requires its A motif and the WH2 domain (Fig. 1.5), which interacts directly with the Arp2/3 complex and F-actin respectively (Toshima *et al.*, 2005). Through these interactions, Pan1p may recruit the Arp2/3 complex to the cortical patches for actin nucleation. The NPF activity of Pan1p is strongly inhibited *in vitro* by Prk1p phosphorylation (Toshima *et al.*, 2005).

**(iii) Myo3p and Myo5p**

Like Las17p, type I myosins Myo3p and Myo5p are required for actin patch assembly in the permeabilized cell assay (Lechler *et al.*, 2000). Myo3p and Myo5p contain an N-terminal motor domain, a lipid-binding TH1 domain, an F-actin-binding

TH2 domain, an SH3 domain, and an Arp2/3 complex-binding A motif (Fig. 1.5). The TH2-SH3-A fragment of *S. pombe* myosin type I can activate the Arp2/3 complex *in vitro* (Lee *et al.*, 2000). Since the TH2-SH3-A fragment binds to F-actin weakly, the NPF activity of Myo3p and Myo5p was proposed to be enhanced by the interactions with other proteins such as Vrp1p and Las17p (Anderson *et al.*, 1998; Evangelista *et al.*, 2000; Lechler *et al.*, 2000). Indeed, Vrp1p was found to stimulate Arp2/3 complex activation by Myo5p *in vitro* (Sun *et al.*, 2006).

**(iv) Abp1p**

Abp1p comprises an N-terminal *ADF*/cofilin homology (ADFH) actin-binding domain (ABD), two A motifs, a polyproline region, and a C-terminal SH3 domain (Fig. 1.5). The NPF activity of Abp1p requires its A motifs and ADFH domain (Goode *et al.*, 2001). There are several reasons for Abp1p to be thought as a competitive antagonist of other NPFs during the patch development (Fig. 1.6). Firstly, Abp1p binds to the Arp2/3 complex with high affinity, but has significantly weaker NPF activity compared to full-length Las17p and Pan1p (Goode *et al.*, 2001). Secondly, Abp1p attenuates the NPF activity of Las17p *in vitro* (D'Agostino and Goode, 2005). Thirdly, Abp1p is recruited to patches later than other NPFs (Kaksonen *et al.*, 2003). The recruited Abp1p may target Ark1p and Prk1p kinases to the patches (Cope *et al.*, 1999), which will phosphorylate Pan1p to disrupt the Pan1p-Sla1p-End3p complex (Zeng *et al.*, 2001). Therefore, Abp1p is important for patch development.

### 1.2.3.3 Actin patches and endocytosis

Actin patches mediate endocytosis. The mutations in genes required for patch functions have endocytic defects. In addition, many proteins functioning in endocytosis were identified as patch components, including actin, Arc35p, Rvs167p, Sac6p, Sla2p, and Vrp1p (Kubler and Riezman, 1993; Munn *et al.*, 1995; Engqvist-Goldstein and Drubin, 2003). Actin patches may also function in exocytosis. A number of patch-associated protein mutants accumulate post-Golgi vesicles (Harsay and Bretscher, 1995; Mulholland *et al.*, 1999), indicating temporal and spatial links between endocytosis and exocytosis.

There are several steps for the actin patch development corresponding to the different stages of endocytosis (Fig. 1.6) (Kaksonen *et al.*, 2003; Kaksonen *et al.*, 2005; Newpher *et al.*, 2005). Endocytosis begins with the recruitment of early patch components by the cytosolic regions of membrane receptors (Fig. 1.6, Step 1) (Tan *et al.*, 1996; Howard *et al.*, 2002). At this stage, the patches are non-motile**.** These early patches contain Las17p, Sla1p and Pan1p, but no actin. Clathrin and its adaptors are also recruited to this early endocytic patches. Next, patches move slowly along the cortex (0.05 to 0.1 μm/s). This slow patch movement is thought to benefit the vesicle scission (Fig. 1.6, Step2-3) (Kaksonen *et al.*, 2003; Kaksonen *et al.*, 2005). Once patches/vesicles leave the cell cortex, they move rapidly inward along the actin cables (Fig. 1.6, Step 4) (Huckaba *et al.*, 2004). Slow patch movement in the cell cortex depends on an Arp2/3 complex-based actin polymerization whereas rapid inward movement of patches depends on transport on cables.

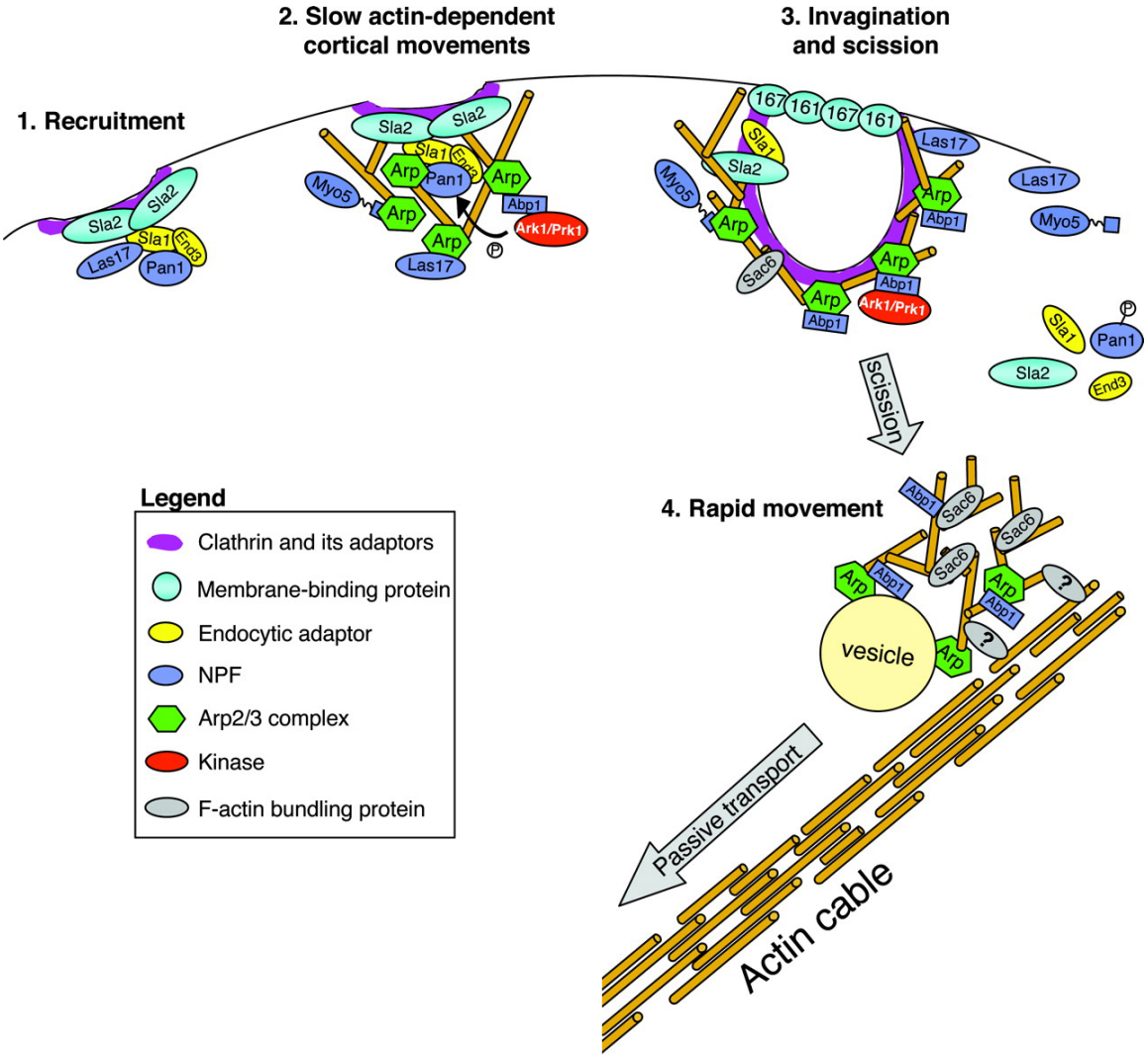


**Figure 1.6 Model for actin patch development**. (Step 1) Receptors recruit early patch components to the cell cortex to form a relatively immobile complex. (Step 2) Slow patch movement at the cortex. (Step 3) Pan1p phosphorylation and/or the activities of Rvs161p, Rvs167p, and the type I myosins Myo3p and Myo5p promote vesicle scission and internalization. (Step 4) Endocytic vesicles move passively alone actin cable. (Modified with permission from *Microbiol Mol Biol Rev*.) (Moseley and Goode, 2006)

### 1.2.3.4 Role of Pan1p and Sla1p in patch development

Pan1p is a central coordinator for early patch formation and development through its binding to multiple early endocytic proteins and promoting actin filament assembly by activating the Arp2/3 complex. The initial endocytic components recruited to patches include clathrin, clathrin adaptors and multiple scaffolds such as Yap1801p and Yap1802p (AP180 homologues) (Newpher *et al.*, 2005), Ent1p and Ent2p (epsin homologues) (Aguilar *et al.*, 2003) , Ede1p (Eps15R homologue) (Gagny *et al.*, 2000), Scd5p (Henry *et al.*, 2003), Sla1p, and Sla2p (Howard *et al.*, 2002) (Fig. 1.6, Step 1-2). Pan1p have been found to interact with most of these components. The EH domains of Pan1p can interact with the C-terminal regions of Yap1801p and Yap1802p which contain multiple Asparagine-Proline-Phenylalanine (NPF) tripeptide sequences (Wendland and Emr, 1998). Ent1p and Ent2p also interact with the EH domains of Pan1p through similar NPF motifs located in their C-terminal regions (Wendland *et al.*, 1999). In addition to the adaptors and epsins, Pan1p has also been found to interact with Sla1p and End3p (Tang *et al.*, 2000).

Sla1p can bind directly to receptors to promote their internalization (Howard *et al.*, 2002). In addition to its interaction with Pan1p and End3p, Sla1p also appears to be important for recruiting other factors to the patches, such as Las17p (Li, 1997) and Sla2p (Gourlay *et al.*, 2003). Sla2p is a multi-domain protein that has many functions in endocytosis (Peter *et al.*, 2004; Newpher *et al.*, 2005; Sun *et al.*, 2005). Firstly, Sla2p helps to localize clathrin to patches (Newpher *et al.*, 2005). Secondly, Sla2p may bind to and regulate Rvs167p, which promotes membrane curvature to facilitate vesicle budding (Peter *et al.*, 2004). Thirdly, Sla2p binds directly to F-actin via its talin-like domain

(McCann and Craig, 1997, 1999). This domain, along with the clathrin adaptors, is required for cell growth and endocytosis. Fourthly, Sla2p binds to phosphoinositide PI(4,5)P (PIP2) to facilitate the internalization step of receptor-mediated endocytosis (Sun *et al.*, 2005). Finally, Sla2p contributes to the regulation of Arp2/3 complex's activity through interactions with two NPFs, Pan1p and Las17p, (Ayscough *et al.*, 1999).

Pan1p and Las17p recruit and activate the Arp2/3 complex for actin assembly, leading to slow patch movement along the cortex (Kaksonen *et al.*, 2003; Kaksonen *et al.*, 2005). During this stage, two additional NPFs Abp1p and Myo3p/Myo5p are recruited. Abp1p in turn recruits the actin-regulating kinases Ark1p and Prk1p (Fig. 1.6, Step2), which regulate Pan1p functions through direct phosphorylation.

#### 1.2.3.5 Regulation of actin cytoskeleton and endocytosis by Prk1p

Prk1p, together with Ark1p and Akl1p, belong to the same family of serine/threonine kinases which also include a few homologous kinases from higher eukaryotic organisms (Smythe and Ayscough, 2003). One member of this family, AAK1, is important for the process of endocytosis in mammalian cells and phosphorylates subunit of the AP2 complexes with similar sequence specificity as Prk1p (Conner and Schmid, 2002; Ricotta *et al.*, 2002). It is therefore possible that the mechanism of endocytosis regulation by Prk1p-like kinases is highly conserved from yeast to mammalian cells.

Prk1p phosphorylates the threonine residue within the [L/I/V/M]XX[Q/N/T/S]XTG motif (Huang *et al.*, 2003). Loss-of-function mutations of *PRK1* suppressed the *pan1* and *end3* mutations and caused a delay in the actin polarization and bud formation at the early

stage of the cell cycle (Zeng and Cai, 1999). Overexpression of Prk1p led to cell death accompanied by gross actin abnormalities (Zeng and Cai, 1999). Prk1p is able to phosphorylate Pan1p and Sla1p *in vivo* and *in vitro* in a sequence-specific manner (Zeng and Cai, 1999; Zeng *et al.*, 2001). This phosphorylation affects many functions of Pan1p. Firstly, the phosphorylated N-terminus auto-inhibits the NPF activity of Pan1p C-terminus (Toshima *et al.*, 2005). Secondly, the F-actin binding activity of Pan1p was dramatically reduced upon phosphorylation (Toshima *et al.*, 2005). Thirdly, phosphorylation of Pan1p disassembles the Pan1p– Sla1p– End3p trimeric complex (Fig. 1.6, Step3) (Zeng *et al.*, 2001). In addition to Pan1p and Sla1p, some other proteins that associate with Pan1p in the early endocytic patches are also phosphorylated by Prk1p. These proteins include Ent1p/Ent2p (Watson *et al.*, 2001), Yap1801p/Yap1802p (Huang *et al.*, 2003) and possibly Sla2p. Their phosphorylation was suggested to further enhance disassembly of the early patch components, promoting the fast movement of vesicles. Therefore, Prk1p negatively regulates the activity of early endocytic proteins in stimulating actin assembly and plays a critical role in endocytic patch development.

The negative regulation through phosphorylation by Prk1p as in the case of Pan1p seems to be a rather general mode of function for Prk1p. Scd5p, another protein containing three LxxTxTG motifs and known to be important for endocytosis and actin organization, has been demonstrated to be negatively regulated by Prk1p through direct phosphorylation (Henry *et al.*, 2003; Huang *et al.*, 2003). In addition to Pan1p, Sla1p, Ent1p, Ent2p, and Scd5p, there are many other yeast proteins that contain the Prk1p phosphorylation motifs, indicating that they might be the potential substrates of Prk1p. These proteins include Sla2p, Yap1801p, Yap1802p, Las17p, Ede1p, Chc1p, Arp2/3p,

Aip1p, Sac6p, Bni1p, Bnr1p, Bud6p, Spa2p, Bud2p, Bud3p and Syp1p (Huang *et al.*, 2003). Interestingly, most of these candidates are involved in assembly of actin cytoskeleton or establishment of cell polarity. Some of these proteins also show either physical or genetic interactions. Like Pan1p-Sla1p-End3p complex, the interactions of these proteins may also be affected by Prk1p phosphorylation. Therefore, it is important to know whether these candidates are the true phosphorylation targets of Prk1p *in vivo*.

## 1.2.4 Actin cables

As discussed above, actin cables are utilized as transport track to direct polarized growth. Mutants of most factors required for cable assembly and stability have cell polarity defects. These factors include formins (Evangelista *et al.*, 1997; Evangelista *et al.*, 2002; Sagot *et al.*, 2002a), tropomyosin (Pruyne *et al.*, 1998), profilin (Pfy1p) (Haarer *et al.*, 1990; Wolven *et al.*, 2000), Bud6p (Amberg *et al.*, 1997), Sac6p/fimbrin (Adams *et al.*, 1989), capping proteins (Amatruda *et al.*, 1992), and Srv2p (Vojtek *et al.*, 1991).

### 1.2.4.1 Actin cable formation by Formins

Formins form a protein family with members found in fungi, plants, insects, nematodes, and vertebrates (Evangelista *et al.*, 2003; Wallar and Alberts, 2003). Budding yeast has two formins, Bni1p [Bud neck interactor (Zahner *et al.*, 1996)] and Bnr1p ([BNI1-related (Imamura *et al.*, 1997)], each with an N-terminal Rho GTPase-binding domain and C-terminal formin-homology FH1 and FH2 domains (Fig. 1.7). Formins promote actin cable assembly in an Arp2/3-independent manner. Deletion mutant of

either yeast formin is viable (Kohno *et al.*, 1996; Imamura *et al.*, 1997), but loss of both is lethal (Vallen *et al.*, 2000; Ozaki-Kuroda *et al.*, 2001). The conditional mutations of *BNI1* in a cell with *BNR1* deletion cause rapid loss of all cables upon shifting to the non-permissive temperature. These observations suggest that both formins in yeast are involved in cable formation. FH1/FH2 domains of formins are required for cable formation, with the FH2 alone providing the core activity (Evangelista *et al.*, 2002; Pruyne *et al.*, 2002; Sagot *et al.*, 2002b). Although formins alone can nucleate actin assembly, other proteins, such as profilin, are also important for the activity of formins in stimulating actin nucleation.

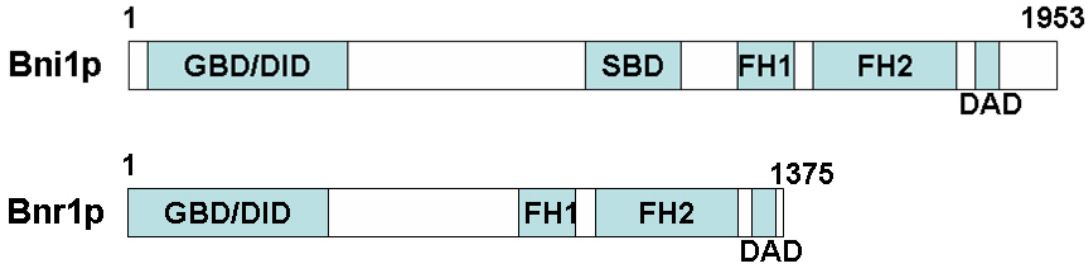


**Figure 1.7 Domain organization of budding yeast formins Bni1p and Bnr1p**. GBD, Rho-GTPase binding domain; DID, Diaphanous inhibitory domain; SBD, Spa2-binding domain; FH1/FH2, forming homology; DAD, Diaphanous autoregulatory domain.

### 1.2.4.2 Profilin promotes actin filament elongation

Profilin is a small (15kDa), abundant actin monomer-binding protein (Witke, 2004). In all organisms examined, mutation of profilin is lethal and/or causes severe defects in cell polarity and actin organization. There are four known functions of profilin in promoting actin turnover and assembly. Firstly, it accelerates actin turnover by promoting nucleotide exchange (ATP for ADP) on G-actin (Mockrin and Korn, 1980). Secondly, it suppresses spontaneous actin assembly by inhibiting the interactions

between actin monomers (Pollard *et al.*, 2000). Thirdly, it restricts actin monomer addition to filament barbed ends and blocks the addition to pointed ends (Pollard and Cooper, 1984). Fourthly, it can increase the rate of actin cable elongation mediated by formins, Bni1p and Bnr1p (Romero *et al.*, 2004; Kovar *et al.*, 2006).

Profilin can bind to the polyproline motifs in the FH1 domain of Bni1p and Bnr1p (Evangelista *et al.*, 1997; Imamura *et al.*, 1997). The FH1-FH2 domain of Bni1p assembles actin filaments equally well in the presence and absence of profilin. However, FH1-profilin binding is required for formins to assemble profilin-bound actin monomers (Sagot *et al.*, 2002b; Pring *et al.*, 2003). Thus, although the FH2 domain alone can assemble filaments using free actin monomers, the FH1 domain is required for filament assembly using profilin-bound actin monomers. Therefore, the FH1 domain is important for formin function *in vivo*, whereby profilin-bound actin monomers are the primary substrate available for actin assembly (Evangelista *et al.*, 2002; Pruyne *et al.*, 2002; Sagot *et al.*, 2002a; Moseley *et al.*, 2004). It has been proposed that profilin-FH1 interaction can increase the rate of filament elongation (Romero *et al.*, 2004).

### 1.2.4.3 Regulation of actin cable assembly by polarisome

Numerous polarity proteins localize primarily to the bud tip during bud emergence and growth. Just before the cell division, they are relocated to the bud neck, where they appear to promote cytokinesis. Some of these proteins, such as Spa2p, Pea2p, Bud6p, GTPase Cdc42p and two Cdc42p effectors, Bni1p and Gic2p may assemble into a functional complex termed the polarisome that helps to facilitate cable assembly (Fujiwara *et al.*, 1998; Sheu *et al.*, 1998; Jaquenoud and Peter, 2000). Bud6p and Cdc42p

are thought to regulate Bni1p directly to promote actin cable assembly (Evangelista *et al.*, 1997; Evangelista *et al.*, 2002; Moseley *et al.*, 2004), and Spa2p can directly interact with Bni1p and Pea2p (Fujiwara *et al.*, 1998; Sheu *et al.*, 1998). The localization of Bni1p requires Spa2p and Pea2p (Ozaki-Kuroda *et al.*, 2001). Gic2p, which binds to Cdc42p and Bud6p, is also required for the localization of Bni1p and Bud6p in early bud emergence (Jaquenoud and Peter, 2000).

#### 1.2.4.4 Regulation of actin cable assembly by Rho GTPases

Mammalian formins mDia1p and mDia2p are auto-inhibited by interactions between their N-terminal diaphanous inhibitory domain (DID) and their C-terminal diaphanous autoregulatory domain (DAD ) (Watanabe *et al.*, 1999; Alberts, 2001). This intra-molecular interaction abolishes actin nucleation activity of the FH2 domain (Li and Higgs, 2003). It has been shown that the auto-inhibition of mammalian formins can be overcome by direct binding of Rho GTPases to the N-terminal GTPase binding domain (GBD) (Watanabe *et al.*, 1999; Alberts, 2001). Overexpression of N- and C-terminal truncations of Bni1p and Bnr1p results in excess actin assembly *in vivo* (Evangelista *et al.*, 1997; Evangelista *et al.*, 2002; Sagot *et al.*, 2002a; Pruyne *et al.*, 2004a), indicating that Bni1p and Bnr1p may be auto-inhibited like mDia1p and mDia2p. However, the direct interactions between N and C termini have not been reported for either Bni1p or Bnr1p.

Rho GTPases play important roles in yeast formin regulation *in vivo*. There are six different Rho GTPases in budding yeast: Rho1p, Rho2p, Rho3p, Rho4p, Rho5p, and Cdc42p. Bni1p interacts with Cdc42p, Rho1p, and possibly Rho3p and Rho4p (Kohno *et*

*al.*, 1996; Evangelista *et al.*, 1997), while Bnr1p binds to Rho4p (Imamura *et al.*, 1997). Different Rho GTPases are required for regulation of formins in different cell cycle stages. Cdc42p is required for the control of formin-mediated actin assembly during bud emergence, Rho3p and Rho4p during bud growth, and Rho1p at cytokinesis (Tolliday *et al.*, 2002; Dong *et al.*, 2003). Rho1p is also required for formin regulation during the response to cell stress (Dong *et al.*, 2003).

### 1.2.5 Actin ring formation and cytokinesis

In addition to the role of polarized secretion, formins are required for actin ring formation during anaphase to achieve cytokinesis in budding yeast. Actin ring is assembled at the mother-bud neck and the position is determined by the site of bud emergence initiated in early $G_1$ (Pruyne *et al.*, 2004b). Many components important for cytokinesis are recruited to the bud neck , such as Myo1p, formins Bni1p and Bnr1p, two myosin light chains (Mlc1p and Mlc2p), Hof1p/Cyk2p, IQGAP (Iqg1p/Cyk1p), and Cyk3p (Balasubramanian *et al.*, 2004). During anaphase, actin ring forms and constricts in a Myo1p-dependent manner to close the neck to finish cytokinesis (Bi *et al.*, 1998; Lippincott and Li, 1998b). Both Bni1p and Bnr1p are required for ring formation and function. It has been demonstrated that the actin ring can still be formed in either *bni1* or *bnr1* single mutants (Vallen *et al.*, 2000). However, a temperature-sensitive formin mutant strain (*bni1*$^{ts}$ *bni1*) fails to assemble the ring (Tolliday *et al.*, 2002). Other factors which regulate actin cable formation, such as profilin and tropomyosin, are also required for actin ring assembly (Tolliday *et al.*, 2002). Therefore, the mechanism of ring formation is highly similar to that of cable assembly.

## 1.3 Septin cytoskeleton

In addition to the actin ring, the septum is also required for cytokinesis. Septins are important structures to coordinate the septum formation and actin ring contraction. Septins were first identified in yeast *Saccharomyces cerevisiae* as a set of *cdc* mutants defective in cytokinesis and were subsequently found to be present in many other eukaryotic species including human (Hartwell, 1971; Longtine *et al.*, 1996). Their primary functions are structural in nature, which is to polymerize into microfilaments that participate in diverse cellular processes. Recently, emerging data have implicated septins in pathogenesis of diverse diseases including neoplasia, neurodegeneration and infections in mammals (Kartmann and Roth, 2001; Hall and Russell, 2004; Martinez and Ware, 2004; Spiliotis and Nelson, 2006). In budding yeast, septins play an essential role in many cell processes. In addition to their role in cytokinesis, septins are necessary for bud site selection. Septins also play at least two other important roles during bud growth, namely chitin deposition and morphogenesis checkpoint control (Lew, 2003).

### 1.3.1 The role of septins in cell division and polarized growth

#### 1.3.1.1 Role of septins in cytokinesis

Septins are important for coordinating the septum formation and actin ring contraction. Septins serve as a molecular scaffold for bud neck localization of the molecular machinery that assembles the actomyosin contractile ring and the septum (Longtine and Bi, 2003). Formation of the actomyosin ring depends on septin integrity

(Bi *et al.*, 1998; Lippincott and Li, 1998b). Septins also recruit enzymes, such as chitin synthase II, which are required for septum formation (Bi, 2001).

In addition to being a molecular scaffold, septins also serve as a diffusion barrier to maintain asymmetric distribution and compartmentalization proteins. Septins split into two separate rings prior to cytokinesis (Longtine *et al.*, 1996), and the separated rings compartmentalize and restrict factors such as Spa2p and Chs2p at the bud neck (Dobbelaere and Barral, 2004). In wild-type cells, Spa2p diffuses freely within this small zone between the splitted septin rings. However, in *cdc12-6* mutants, Spa2p and Chs2p rapidly diffuse away from the bud neck at non-permissive temperature (Dobbelaere and Barral, 2004). Therefore, septins serve as both scaffolds and compartments to localize cytokinetic machinery to the bud neck.

#### 1.3.1.2 Role of septins in axial bud site selection

Many proteins that localize to the bud neck are required for the axial budding pattern. Septins are one of the important complexes critical for axial bud site selection. Recognition of this complex by other bud site selection components such as Bud3p and Bud4p would establish polarized growth at proximal sites, resulting in the axial budding pattern (Fig. 1.3, Gene set V) (Chant & Stowers 1995, Flescher et al. 1993).

#### 1.3.1.3 Role of septins in cell wall synthesis

Septins are important for chitin deposition during cell wall synthesis. The cell wall is the extracellular matrix of the yeast cell and plays a critical role in cell polarity and morphogenesis (Cid *et al.*, 1995). Chitin staining is prominent at the incipient bud

site, at the bud neck, and in the primary septum (i.e. bud scar) at the division site of the mother cells (Moore and Campbell, 1973; Shaw *et al.*, 1991; Cid *et al.*, 1995). The chitin ring at the neck is assembled by chitin synthase III (Chs3p) (Cid *et al.*, 1995; Santos and Snyder, 1997). The localization of Chs3p to the bud neck is dependent on Chs4p (DeMarini *et al.*, 1997; Trilla *et al.*, 1997). Chs4p interacts with Bni4p, whose localization requires septins. A second chitin synthase, Chs2p, which is required for assembly of the primary septum, also depends on septins to polarize at the neck region (Cid *et al.*, 1995).

#### 1.3.1.4 Morphogenesis checkpoint

Cell growth is tightly coordinated with every phase of the cell cycle. Damage or stress to either DNA itself or the DNA replication machinery will block nuclear division and cytokinesis. The mechanisms that monitor DNA replication to initiate the cell cycle arrest are known as checkpoints (Hartwell and Weinert, 1989). A series of checkpoints also monitor the assembly of the mitotic spindle and nuclear division (Kops *et al.*, 2005). Recently, a pathway that regulates the activity of Swe1p, the fission yeast Weelp homolog in budding yeast, has been identified as a morphogenesis checkpoint that coordinates the process of bud formation and mitosis by monitoring septin disorganization and actin perturbation (Fig. 1.8) (Lew, 2003; Keaton and Lew, 2006).

Many environmental stresses (including mild heat shock and osmotic shock) and mutations of the actin-associated proteins result in actin depolarization, accompanied by delay in bud formation and the nuclear cycle. Subsequent studies demonstrated that the cell cycle delay is due to the inhibitory effect of Swe1p on Cdc28p-G2/M cyclin kinases

which is required for entry to mitosis (Sia *et al.*, 1996; McMillan *et al.*, 1998; Alexander *et al.*, 2001). Swe1p inhibits the Cdc28p-G2/M cyclin kinases by phosphorylating a

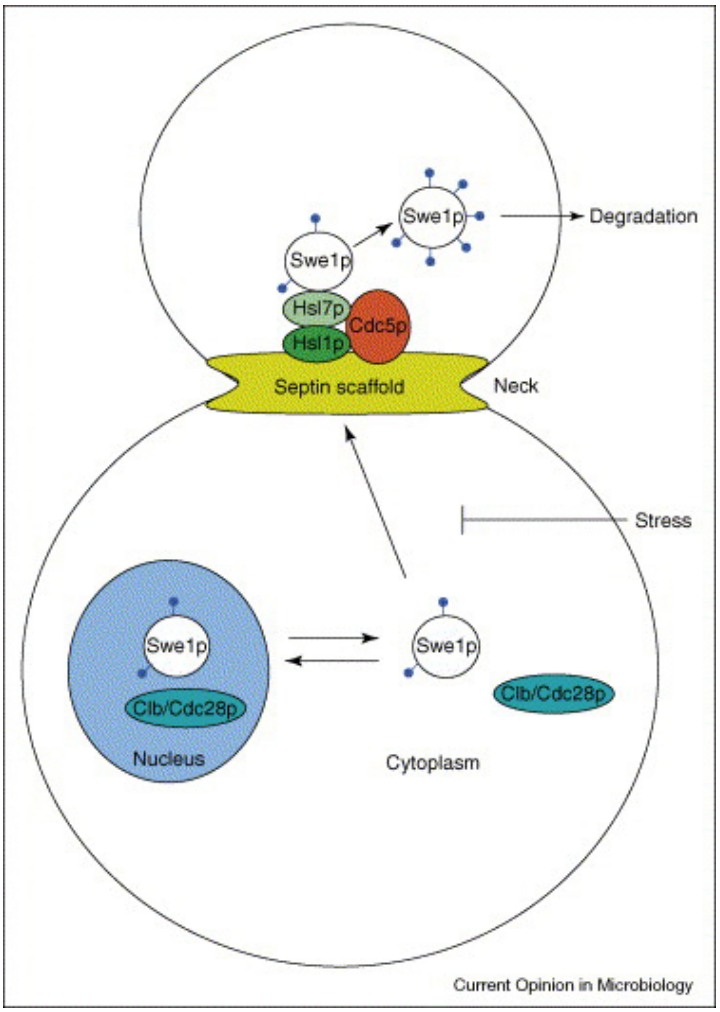


**Figure 1.8 Swe1p localization and degradation in yeast**. Swe1p first accumulates in the nucleus of unbudded cells. Following bud emergence, Hsl1p becomes activated at the septin cortex. This enables Hsl1p to recruit Hsl7p, which in turn recruits Swe1p and Cdc5p (Polo) to the septin collar. Swe1p phosphorylated by Cdc28p (CDK) is primed for subsequent phosphorylation by Cdc5p (Polo) at the neck, leading to Swe1p degradation. Stresses that delay bud emergence prevent activation of Hsl1p, precluding neck targeting and/or degradation of Swe1p and enabling Swe1p to return to the nucleus. (Reproduced with permission from *Curr Opin Microbiol.*) (Keaton and Lew, 2006)

conserved tyrosine on Cdc28p (Booher *et al.*, 1993). Swe1p accumulates during late $G_1$ and S phase, and is degraded by the time of nuclear division. However, upon depolarization of the actin cytoskeleton and delay in budding, Swe1p becomes stabilized and in turn inhibits the Cdc28p-G2/M cyclins kinase. These findings indicate that a morphogenesis checkpoint is able to inhibit Swe1p degradation.

Swe1p degradation requires the formation of the Hsl1p-Hsl7p-Swe1p complex on the septins in the bud neck (Fig. 1.8)(Lew, 2003). Hsl1p can bind to septin directly and its bud neck localization and activation require the proper organization of septins (Theesfeld *et al.*, 2003). Hsl1p at the bud neck then recruits an adaptor protein, Hsl7p, which in turn recruits Swe1p and Cdc5p to the septin collar (McMillan *et al.*, 1999; Asano *et al.*, 2005). Swe1p degradation requires the phosphorylation of Swe1p by Cdc5p and Cdc28p (Sia *et al.*, 1998; Sakchaisri *et al.*, 2004; Asano *et al.*, 2005; Harvey *et al.*, 2005; Watanabe *et al.*, 2005). Therefore, the morphogenesis checkpoint begins with the septin cytoskeleton. Successful bud formation and the proper septin structure at the bud neck will result in Swe1p degradation, whereas stresses that delay bud formation or cause disorganization of the septin structure will block Swe1p degradation.

Although it is known that septin disorganization and bud formation trigger the morphogenesis checkpoint, it remains unclear how actin perturbation promotes Swe1p-dependent arrest. Unlike septin disorganization which mislocalizes Hsl1p and Hsl7p from the bud neck, actin perturbation does not change the localization of Hsl1p and Hsl7p in the bud neck (Longtine *et al.*, 2000; Theesfeld *et al.*, 2003). However, Swe1p still moves from the bud neck upon actin perturbation (Longtine *et al.*, 2000). Therefore, there are other factors responsible for the localization of Swe1p during actin perturbation. It is

necessary to investigate how the signal of actin perturbation is transmitted to the septin-dependent Swe1p degradation pathway. It is required to identify more actin/septin associated proteins and to understand how these proteins regulate actin/septin organization.

## 1.3.2 Organization and dynamic localization of Septins

Yeast cells produce seven septins, of which five (Cdc3p, Cdc10p, Cdc11p, Cdc12p, and Shs1/Sep7p) are engaged in the assembly of the ring-like septin filaments at the mother-bud junction during vegetative growth, and the other two (Spr3p and Spr28p) are expressed only during sporulation (Versele and Thorner, 2005). The yeast septins contain a GTPase domain that is flanked by a short basic amino acid region at the N-terminal side and by a conserved septin-unique domain at the C-terminal side (Fig. 1.9A). The region of basic amino acids is thought to bind phosphoinositide and is required for membrane attachment. Most *S. cerevisiae* septins, except Cdc10p, contain a C-terminal coiled-coil domain which is required for protein-protein interaction (Fig. 1.9) (Frazier *et al.*, 1998; Mendoza *et al.*, 2002; Casamayor and Snyder, 2003; Versele *et al.*, 2004; Farkasovsky *et al.*, 2005). All five yeast septins (Cdc3p, Cdc10p, Cdc11p, Cdc12p and Shs1p) associate (Fig. 1.9B) to form the septin ring at the bud neck which marks the division site. The septin ring remains at the neck throughout most of the cell cycle and is the most important filament structure at the bud neck (Haarer and Pringle, 1987; Kim *et al.*, 1991; Frazier *et al.*, 1998; Longtine and Bi, 2003). Various proteins are recruited to the septin rings to serve different functions such as cytokinesis and bud morphogenesis.

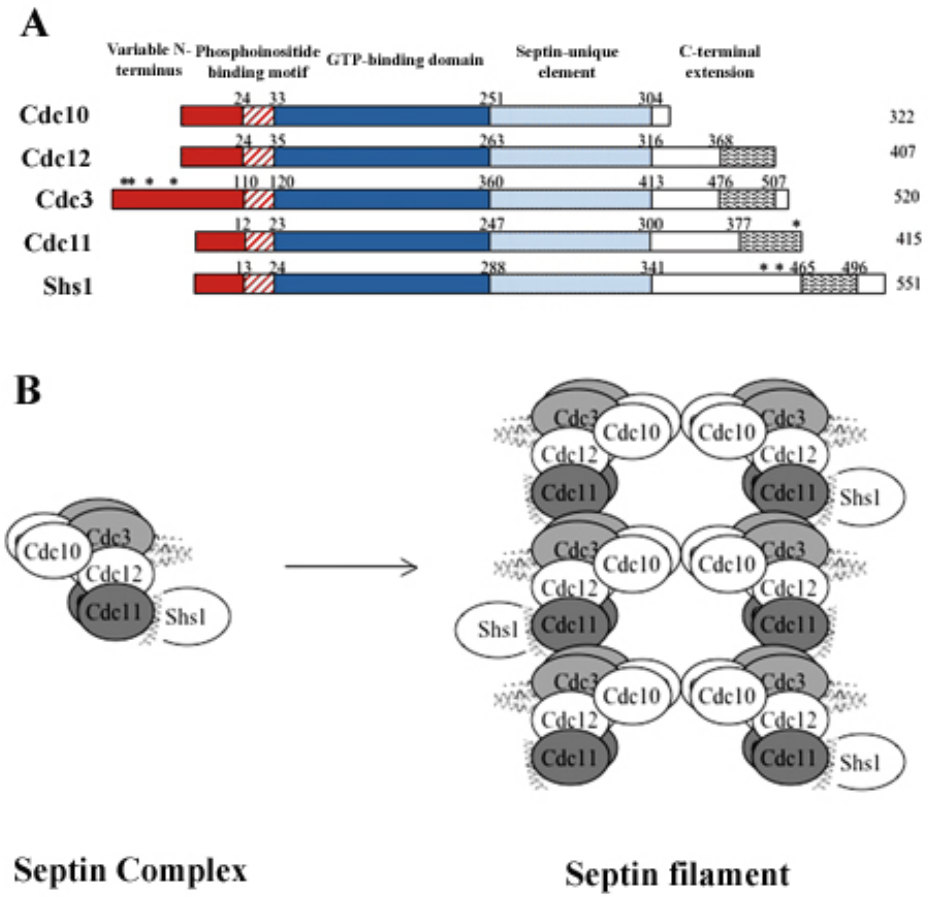


**Figure 1.9 Primary structure and organization of *S. cerevisiae* mitotic septins**. (A) Schematic depiction of the domain structure of yeast septins. Red box, N termini of variable length; hatched box, phosphoinositide binding motif; light blue box, GTPase domain; white box, the variable C-terminal extensions containing, where indicated, a predicted coiled coil segment (wavy box). Asterisks denote known sites of covalent attachment of Smt3 (yeast SUMO). (B) Model for septin heteropentamer organization and assembly into filaments. Septin heteropentamers are assembled with the inter-septin contacts indicated and filaments are formed by the end-to-end polymerization of Cdc3–Cdc12–Cdc11 complexes, with Cdc10 serving as a bridge to bundle the polymers into paired filaments. (Reproduced with permission from *Mol Biol Cell.*) (Versele *et al.*, 2004)

The septin cytoskeleton in yeast undergoes structure reorganization during the different cell cycle stages. Yeast septins localize to the incipient bud site several minutes before bud emergence where they quickly organize into a ring. During bud growth, the

ring expands into an hourglass-like collar spanning the mother-bud neck. At the onset of cytokinesis, the septin collar splits into two septin rings with one each at the mother and daughter sides. After completion of cell division, the old septins normally disintegrate before the new septin structures are formed for the next cell cycle (Cid *et al.*, 2001; Lippincott *et al.*, 2001; Versele and Thorner, 2004; Iwase *et al.*, 2006). The septin filament reorganization during cell cycle correlates with the dynamic properties of septin subunits as detected by FRAP (Fluorescence Recovery After Photobleaching) experiments (Dobbelaere *et al.*, 2003). At the early or late cell cycle stages, when septins are in the process of assembly or disassembly, the subunits of the septin filaments are replaceable. However, during the S, G2 and M phases, where the septins are in the state of a stable ring, the septin subunits are "frozen" (Dobbelaere *et al.*, 2003). The septin dynamics in budding yeast has made *S. cerevisiae* a good model to study the cell-cycle regulation of septin assembly and disassembly.

### 1.3.3 Regulation of septin organization

Various proteins have been found to regulate septin organization at different cell cycle stages. The small GTPase Cdc42p and its guanine nucleotide exchange factor Cdc24p are required for assembly of the early septin ring at the bud site (Gladfelter *et al.*, 2002; Caviston *et al.*, 2003; Iwase *et al.*, 2006). The cycles of GTP loading and hydrolysis of Cdc42p were thought to promote septin ring assembly. Such cycles involve the proper functions of three Cdc42p-directed GTPase-activating proteins (GAPs) (Rga1p, Rga2p, and Bem3p). The kinases Cla4p and Ste20p, two effectors of Cdc42p,

also play an important role in the initial septin organization (Cvrckova *et al.*, 1995; Weiss *et al.*, 2000; Dobbelaere *et al.*, 2003; Kadota *et al.*, 2004; Versele and Thorner, 2004).

During bud growth, when the septin ring converts to the stable hourglass structure, the proteins Gin4p, Nap1p and Elm1p appear to play an important regulatory role (Bouquin *et al.*, 2000; Mortensen *et al.*, 2002; Okuzaki *et al.*, 2003; Gladfelter *et al.*, 2004). Septin phosphorylation by Gin4p is thought to play a direct role in stabilizing septin filaments since septins in *gin4*Δ cells are found to be in fluid state (Dobbelaere *et al.*, 2003). The *gin4*Δ cells form a series of septin bars across the bud neck which is parallel to the mother-daughter axis. Interestingly, similar bars are observed at the neck of shmoo projection (Longtine *et al.*, 1998). Recently, it has been reported that septins are organized as filaments aligned along the mother-daughter axis in the yeast bud neck (Vrabioiu and Mitchison, 2006). Cdc5p, Yck2p protein kinases and Bni5p (a protein with no known catalytic activity) have also been found to regulate septin ring organization (Robinson *et al.*, 1999; Song and Lee, 2001; Lee *et al.*, 2002). The mechanisms of how these proteins regulate septin organization are not clear.

Several proteins have been identified as regulators for septin ring disassembly at the end of the cell cycle. Late-G1 cyclin-CDK has been found to be required for the disassembly of the old septin rings (Moffat and Andrews, 2004). Phosphorylation of Cdc3p by Cln-activated Cdc28p cyclin-dependent kinase in G1 phase is thought to be necessary for septin disassembly (Tang and Reed, 2002). On the other hand, the dephosphorylation of septins by PP2A phosphatase also appears to be involved in proper septin disassembly (Mitchell and Sprague, 2001; Dobbelaere *et al.*, 2003). Despite all the

findings, the regulation of septin dynamics in yeast cell cycle still leaves much to be elucidated.

## 1.4 Objectives and significances of the study

Although many factors were identified as actin or septin cytoskeleton regulators that help to achieve cell polarity through regulating the assembly and dynamics of cytoskeletons, little is known about how the actin and septin cytoskeletons are coordinated during cellular processes. It is therefore necessary to identify components that can associate with both cytoskeletons. The yeast protein Syp1p is a candidate that might regulate both cytoskeletons. Although little is known about Syp1p's function, limited studies so far suggest that Syp1p may have functional interactions with both the actin cytoskeleton and septins. Syp1p was first identified as a multi-copy suppressor of a profilin deletion mutant (Marcoux *et al.*, 2000), thus suggesting its function in the regulation of the actin cytoskeleton. Additionally, Syp1p localizes to the bud neck and its overexpression can induce an elongated bud phenotype (Marcoux *et al.*, 2000), similar to those proteins that are involved in the organization of septins (DeMarini *et al.*, 1997; Lippincott and Li, 1998a; Kikyo *et al.*, 1999). Interestingly, Syp1p contains two potential phosphorylation motifs of Prk1p kinase which is an important regulator of the actin cytoskeleton. Thus, it is also important to find out whether Syp1p is a substrate of Prk1p.

The objective of this thesis is to study: 1) whether Syp1p is a substrate of Prk1p; 2) the function of Syp1p in the actin cytoskeleton; 3) the function of Syp1p in septins. From this study, the functions of Syp1p in the actin and septin cytoskeletons would be more clearly understood.

# Chapter 2

# Materials and Methods

## 2.1 Materials

### 2.1.1 Reagents and Antibodies

Reagents used in this study and their sources are listed below unless otherwise stated:

| Description | Source |
|---|---|
| Chemicals and reagents | BDH Laboratory Supplies (UK)<br>Sigma-Aldrich Chemical Company (USA) |
| Media components | Difco Laboratories (USA)<br>Sigma-Aldrich Chemical Company (USA) |
| Restriction enzymes and modifying enzymes for DNA recombination | New England Biolabs (USA)<br>Amersham (UK)<br>Boehringer Mannheim (Germany). |
| Latrunculin-A (LAT-A) | Molecular Probes (USA) |
| Alpha Factor (α-factor) | Biotechnology Centre (Singapore) |
| Calcofluor | Sigma-Aldrich Chemical Company (USA) |

The antibodies used for protein analysis in this study were obtained from the following sources.

| Antibodies | Source |
|---|---|
| Rabbit polyclonal anti-HA Y-11 | Santa Cruz Biotechnology (USA) |
| Mouse monoclonal anti-Myc 9E10 | Santa Cruz Biotechnology (USA) |
| Mouse monoclonal anti-HA 12CA5 | Boehringer Mannheim (Germany) |
| HRP-conjugated sheep anti-mouse IgG | Amersham (UK) |

### 2.1.2 Strains

**Table 1**. Yeast strains used in this Study

| Strains | Genotype |
|---|---|
| W303-1A | *MAT***a** *ade2-1 trp1-1 can1-100 leu2-3,112 his3-11,15 ura3-1* |
| SFY526 | *MAT***a** *ura3-52 his3-200 ade2-101 lys2-801 trp1-901 leu2-3,112 canr gal4-542 gal80-538 URA3:: GAL1-lacZ* |
| YMC515 | *MAT***a** *ade2-1 trp1-1 can1-100 leu2-3,112 his3-11,15 ura3-1 syp1Δ::HIS3* |
| YMC517 | *MAT***a** *ade2-1 trp1-1 can1-100 leu2-3,112 his3-11,15 ura3-1 cdc12::CDC12-GFP-LEU2* |
| YMC516 | *MAT***a** *ade2-1 trp1-1 can1-100 leu2-3,112 his3-11,15 ura3-1 syp1Δ::HIS3* |

| | |
|---|---|
| | *cdc12::CDC12-GFP-LEU2* |
| YMC518 | *MAT***a** *ade2-1 trp1-1 can1-100 leu2-3,112 his3-11,15 ura3-1 cdc12::CDC12-GFP-LEU2*p314 |
| YMC519 | *MAT***a** *ade2-1 trp1-1 can1-100 leu2-3,112 his3-11,15 ura3-1 cdc12::CDC12-GFP-LEU2*pGAL-SYP1-HA-314 |
| YMC520 | *MAT***a** *ade2-1 trp1-1 can1-100 leu2-3,112 his3-11,15 ura3-1 ::GAL-HA-URA* |
| YMC521 | *MAT***a** *ade2-1 trp1-1 can1-100 leu2-3,112 his3-11,15 ura3-1 ::GAL-SYP1-HA-URA* |
| US810 | *MAT*α *ade2-1 trp1-1 can1-100 leu2-3,112 his3-11,15 ura3-1 swe1Δ::HIS3* |
| YMC522 | *MAT*α *ade2-1 trp1-1 can1-100 leu2-3,112 his3-11,15 ura3-1 swe1Δ::HIS3::GAL-HA-URA* |
| YMC523 | *MAT*α *ade2-1 trp1-1 can1-100 leu2-3,112 his3-11,15 ura3-1 swe1Δ::HIS3::GAL-SYP1-HA-URA* |
| YMC524 | *MAT*α *ade2-1 trp1-1 can1-100 leu2-3,112 his3-11,15 ura3-1 swe1Δ::HIS3::GAL-SYP1-Myc-URA*p314 |
| YMC525 | *MAT*α *ade2-1 trp1-1 can1-100 leu2-3,112 his3-11,15 ura3-1 swe1Δ::HIS3::GAL-SYP1-Myc-URA*pSWE1-HA-314 |
| YMC526 | *MAT***a** *ade2-1 trp1-1 can1-100 leu2-3,112 his3-11,15 ura3-1 cdc10::CDC10-GFP-LEU2::GAL-HA-URA* |
| YMC527 | *MAT***a** *ade2-1 trp1-1 can1-100 leu2-3,112 his3-11,15 ura3-1 cdc10::CDC10-GFP-LEU2::GAL-SYP1-HA-URA* |
| YEF473-1619 | *MAT*α *his3 leu2 lys2 ura3 trp1cdc10-1* |
| YMC528 | *MAT*α *his3 leu2 lys2 ura3 trp1cdc10-1::cdc12::CDC12-GFP-LEU::GAL-HA-URA* |
| YMC529 | *MAT*α *his3 leu2 lys2 ura3 trp1cdc10-1::cdc12::CDC12-GFP-LEU::GAL-SYP1-HA-URA* |
| YMC530 | *MAT***a** *ade2-1 trp1-1 can1-100 leu2-3,112 his3-11,15 ura3-1 cdc12::CDC12-YFP-LEU syp1::SYP1-CFP-URA* |
| YMC531 | *MAT*α *his3 leu2 lys2 ura3 trp1cdc10-1 cdc12::CDC12-GFP-LEU syp1::SYP1-CFP-URA* |
| YMC532 | *MAT***a** *ade2-1 trp1-1 can1-100 leu2-3,112 his3-11,15 ura3-1 syp1::SYP1-HA-URA* |
| YMC533 | *MAT***a** *ade2-1 trp1-1 can1-100 leu2-3,112 his3-11,15 ura3-1 syp1::SYP1-GFP-LEU* |
| YMC534 | *MATa ade2-1 trp1-1 can1-100 leu2-3,112 his3-11,15 ura3-1 syp1::SYP1-CFP-URA* |
| YMC535 | *MAT□ his3 leu2 lys2 ura3 trp1cdc10-1 cdc12::SYP1-CFP-URA* |
| YWJ97 | *MAT***a** *ade2-1 trp1-1 can1-100 leu2-3,112 his3-11,15 ura3-11 prk1Δ::HIS3 syp1::SYP1-HA-URA* |
| DDY335 | *MAT***a** *his3D200 leu2-3,112 ura3-52 tub2-201act1-3(act1-1)* |
| YWJ33 | *MAT***a** *his3D200 leu2-3,112 ura3-52 tub2-201act1-3(act1-1) syp1::SYP1-GFP-LEU* |
| YWJ40 | *MAT***a** *ade2-1 trp1-1 can1-100 leu2-3,112 his3-11,15 ura3-1 syp1Δ::HIS3* pSYP1-GFP-314 |

| | |
|---|---|
| YWJ63 | *MAT***a** *ade2-1 trp1-1 can1-100 leu2-3,112 his3-11,15 ura3-1* p316 |
| YWJ67 | *MAT***a** *ade2-1 trp1-1 can1-100 leu2-3,112 his3-11,15 ura3-1 syp1Δ::HIS3* p316 |
| YWJ68 | *MAT***a** *ade2-1 trp1-1 can1-100 leu2-3,112 his3-11,15 ura3-1 syp1Δ::HIS3* pGal-SYP1-GFP-316 |
| YWJ69 | *MAT***a** *ade2-1 trp1-1 can1-100 leu2-3,112 his3-11,15 ura3-1 syp1Δ::HIS3* pGal-SYP1$^{AA}$-GFP-316 |
| YWJ70 | *MAT***a** *ade2-1 trp1-1 can1-100 leu2-3,112 his3-11,15 ura3-1 syp1Δ::HIS3* pGal-SYP1$^{EE}$-GFP-316 |
| YWJ89 | *MAT***a** *ade2-1 trp1-1 can1-100 leu2-3,112 his3-11,15 ura3-1* pGal-SYP1-HA-316 |
| YWJ99 | *MAT***a** *ade2-1 trp1-1 can1-100 leu2-3,112 his3-11,15 ura3-1pan1-4* p314 pFUR4-316 |
| YWJ100 | *MAT***a** *ade2-1 trp1-1 can1-100 leu2-3,112 his3-11,15 ura3-1* p314 pFUR4-316 |
| YWJ101 | *MAT***a** *ade2-1 trp1-1 can1-100 leu2-3,112 his3-11,15 ura3-1 syp1Δ::HIS3* p314 pFUR4-316 |
| YWJ107 | *MAT***a** *ade2-1 trp1-1 can1-100 leu2-3,112 his3-11,15 ura3-1* pSYP1-GFP-314 |
| YWJ128 | *MAT***a** *ade2-1 trp1-1 can1-100 leu2-3,112 his3-11,15 ura3-1 pfy1Δ::LEU2* p424 |
| YWJ129 | *MAT***a** *ade2-1 trp1-1 can1-100 leu2-3,112 his3-11,15 ura3-1 pfy1Δ::LEU2* p SYP1-GFP-424 |
| YWJ130 | *MAT***a** *ade2-1 trp1-1 can1-100 leu2-3,112 his3-11,15 ura3-1 pfy1Δ::LEU2* pGal-SYP1$^{AA}$-GFP-424 |
| YWJ131 | *MAT***a** *ade2-1 trp1-1 can1-100 leu2-3,112 his3-11,15 ura3-1 pfy1Δ::LEU2* pGal-SYP1$^{EE}$-GFP-424 |
| YWJ137 | *MAT***a** *ade2-1 trp1-1 can1-100 leu2-3,112 his3-11,15 ura3-1 pfy1Δ::LEU2 syp1::SYP1-GFP-URA* |
| YWJ184 | *MAT***a** *ade2-1 trp1-1 can1-100 leu2-3,112 his3-11,15 ura3-1 sla1::SLA1-CFP-TRP syp1::SYP1-YFP-URA* |
| YWJ186 | *MAT***a** *ade2-1 trp1-1 can1-100 leu2-3,112 his3-11,15 ura3-1 sla1::SLA1-GFP-LEU* |
| YWJ189 | *MAT***a** *ade2-1 trp1-1 can1-100 leu2-3,112 his3-11,15 ura3-1 syp1Δ::HIS sla1::SLA1-GFP-LEU* |
| YGS36 | *MAT***a** *ade2-1 trp1-1 can1-100 leu2-3,112 his3-11,15 ura3-1 bni1Δ::LEU* |
| YWJ202 | *MAT***a** *ade2-1 trp1-1 can1-100 leu2-3,112 his3-11,15 ura3-1 sla1::SLA1-GFP-LEU* p314 |
| YWJ203 | *MAT***a** *ade2-1 trp1-1 can1-100 leu2-3,112 his3-11,15 ura3-1 sla1::SLA1-GFP-LEU* pGAL-SYP1-HA-314 |
| YWJ207 | *MAT***a** *ade2-1 trp1-1 can1-100 leu2-3,112 his3-11,15 ura3-1 bni1Δ::LEU* pSYP1-GFP-314 |
| YWJ209 | *MAT***a** *ade2-1 trp1-1 can1-100 leu2-3,112 his3-11,15 ura3-1 sla1Δ::TRP* pSYP1-GFP-314 |
| YWJ211 | *MAT***a** *ade2-1 trp1-1 can1-100 leu2-3,112 his3-11,15 ura3-1 sla1Δ::TRP* p316 |
| YWJ212 | *MAT***a** *ade2-1 trp1-1 can1-100 leu2-3,112 his3-11,15 ura3-1 sla1Δ::TRP* pGAL-SYP1-HA-316 |

| | |
|---|---|
| YWJ213 | *MAT***a** *ade2-1 trp1-1 can1-100 leu2-3,112 his3-11,15 ura3-1 bni1Δ::LEU* p316 |
| YWJ214 | *MAT***a** *ade2-1 trp1-1 can1-100 leu2-3,112 his3-11,15 ura3-1 bni1Δ::LEU* pGAL-SYP1-HA-316 |
| YWJ217 | *MAT***a** *ade2-1 trp1-1 can1-100 leu2-3,112 his3-11,15 ura3-1 syp1::SYP1-GFP-LEU* p313 |
| YWJ218 | *MAT***a** *ade2-1 trp1-1 can1-100 leu2-3,112 his3-11,15 ura3-1 syp1::SYP1-GFP-LEU* pGAL-HA-SLA1-313 |
| YWJ219 | *MAT***a** *ade2-1 trp1-1 can1-100 leu2-3,112 his3-11,15 ura3-1* pGAL-HA-SLA1-313 p316 |
| YWJ220 | *MAT***a** *ade2-1 trp1-1 can1-100 leu2-3,112 his3-11,15 ura3-1* p313 pGAL-SYP1-MYC-316 |
| YWJ221 | *MAT***a** *ade2-1 trp1-1 can1-100 leu2-3,112 his3-11,15 ura3-1* pGAL-HA-SLA1-313 pGAL-SYP1-MYC-316 |
| YWJ288 | *MAT***a** *ade2-1 trp1-1 can1-100 leu2-3,112 his3-11,15 ura3-1 pfy1Δ::LEU2* |
| YGS223 | *MAT***a** *ade2-1 trp1-1 can1-100 leu2-3,112 his3-11,15 ura3-1 bni1Δ::URA* |
| YWJ720 | *MAT***a** *ade2-1 trp1-1 can1-100 leu2-3,112 his3-11,15 ura3-1* p424 |
| YWJ721 | *MAT***a** *ade2-1 trp1-1 can1-100 leu2-3,112 his3-11,15 ura3-1* pSYP1-HA-424 |
| YWJ722 | *MAT***a** *ade2-1 trp1-1 can1-100 leu2-3,112 his3-11,15 ura3-1 bni1Δ::URA* p424 |
| YWJ723 | *MAT***a** *ade2-1 trp1-1 can1-100 leu2-3,112 his3-11,15 ura3-1 bni1Δ::URA* pSYP1-HA-424 |
| YWJ724 | *MAT***a** *ade2-1 trp1-1 can1-100 leu2-3,112 his3-11,15 ura3-1 bni1Δ::URA* pBNI1-HA-314 |

### 2.1.3 Constructs

**Table 2**. Plasmids used in this study

| Construct | Description |
|---|---|
| pRS304 | Integration vector containing *TRP1*. (Sikorski and Hieter, 1989) |
| pRS305 | Integration vector containing *LEU2*. (Sikorski and Hieter, 1989) |
| pRS306 | Integration vector containing *URA3*. (Sikorski and Hieter, 1989) |
| pRS313 | *CEN6 HIS3* vector. (Sikorski and Hieter, 1989) |
| pRS314 | *CEN6 TRP1* vector. (Sikorski and Hieter, 1989) |
| pRS315 | *CEN6 LEU2* vector. (Sikorski and Hieter, 1989) |
| pRS316 | *CEN6 URA3* vector. (Sikorski and Hieter, 1989) |
| pRS424 | High copy 2μ vector. (Sikorski and Hieter, 1989) |
| pGBKT7 | *2μ TRP1*, *GAL4* DNA binding domain (1-147 a.a.). (CLONTECH Laboratories, Inc. Cat. No. #K1612-1. (Louvet *et al.*, 1997) |
| pGADT7 | *2μ LEU2*, *GAL4* activation domain (768-881 a.a.). (CLONTECH Laboratories, Inc. Cat. No. #K1612-1.(Chien *et al.*, 1991) |
| pFA6a- | Plasmid contains the ORF of the green fluorescent protein variant S65T |

| | |
|---|---|
| GFPS65T-HIS3MX6 | (Yeast Resource Center, University of Washington) |
| pYAM1 | pYep352-*FUR4*; *FUR4* gene in multi-copy plasmid pYep352 with *URA3* marker, a gift from Dr. Alan Munn. |
| pBKS (+) | Vector pBluescript SK (+), CMJ lab collection. |
| pBKS-SYP1 | The SYP1 construct used for sub-cloning; the DNA coding region for Syp1p (1-870 a.a.) was generated by PCR and cloned into pBKS. |
| pBKS-SYP1-SalI/XbaI | The DNA fragment encoding SYP1( SalI site / XbaI site) was cloned into pBKS; the construct was used to do site-directed mutagenesis. |
| pGEX-LR2 | DNA fragment encoding Pan1p (384-846 aa) was cloned into pGEX-4T-1 (Zeng and Cai, 1999). |
| pGEX-SLA1-SH3 | GST-SH3; the DNA coding region for Sla1p (2-440 a.a.) was generated by PCR and cloned in frame into pGEX-4T-1 (Tang *et al.*, 2000). |
| pGEX-SLA1-RP | GST-SR; the DNA coding region for Sla1p (856-1244 a.a.) was generated by PCR and cloned in frame into pGEX-4T-1 (Tang *et al.*, 2000). |
| pGEX-SLA1-NT | GST-NT; The DNA coding region for Sla1p (1-854 a.a.) was generated by PCR and cloned in frame into pGEX-4T-1. |
| pGEX-SYP1-CT-WT | DNA fragment encoding Syp1p (561-870 aa) was cloned into pGEX-4T-1. |
| pGEX-SYP1-CT-T577A | DNA fragment encoding Syp1p (561-870 aa) was cloned into pGEX-4T-1, The Threonine at position 577 in Syp1p was mutated to Alanine. |
| pGEX-SYP1-CT-T588A | DNA fragment encoding Syp1p (561-870 aa) was cloned into pGEX-4T-1, The Threonine at position 588 in Syp1p was mutated to Alanine. |
| pGEX-SYP1-CT-TATA | DNA fragment encoding Syp1p (561-870 aa) was cloned into pGEX-4T-1, The Threonines at position 577 and 588 in Syp1p were mutated to Alanines. |
| pGEX-CDC3 | DNA fragment encoding Cdc3p (1-520 aa) was cloned into pGEX-4T-1. |
| pGEX-CDC10 | DNA fragment encoding Cdc10p (1-322 aa) was cloned into pGEX-4T-1. |
| pGEX-CDC11 | DNA fragment encoding Cdc11p (1-415 aa) was cloned into pGEX-4T-1. |
| pGEX-CDC12 | DNA fragment encoding Cdc12p (1-407 aa) was cloned into pGEX-4T-1. |
| pGADT7-SLA1 | *SLA1* (2-1244) in pGADT7. The DNA coding region of Sla1p (aa 2-1244) was generated by PCR and cloned into pGADT7 (Zeng *et al.*, 2001). |
| pGADT7-SLA1-NT | The DNA coding region for Sla1p (1-854 a.a.) was generated by PCR and cloned in frame into pGADT7 (Zeng *et al.*, 2001). |
| pGADT7-SLA1-SR(RP) | The DNA coding region for Sla1p (856-1244 a.a.) was generated by PCR and cloned in frame into pGADT7 (Zeng *et al.*, 2001). |
| pGADT7-SLA1-SH3 | The DNA coding region for Sla1p (2-440 a.a.) was generated by PCR and cloned in frame into pGADT7 (Zeng *et al.*, 2001). |
| pGBKT7-SYP1 | The DNA coding region for Syp1p (1-870 a.a.) was generated by PCR and cloned in frame into pGBKT7. |
| pMC67 | Vector with LEU marker, CMJ lab collection. |
| pBKS-PFY1 | PFY1 coding region with its upstream promoter was generated by PCR and cloned to pBKS vector. |
| pBKS-PFY1- | The plasmid used to create *PFY1* deletion mutant. The fragment from PvuI |

| | |
|---|---|
| LEU | site to Sal1I site of PFY1 in pBKS-PFY1 was replaced by the expressing region of LEU from pMC67. |
| pSLA1c-CFP-304 | *SLA1c-CFP in TRP1,* integration plasmid pRS304, *SLA1*(1105-1244 a.a.) Tagged with GFP at its COOH-terminus in pRS304, can be linearized by SacI site within *SLA1* sequence for integration. |
| pSLA1c-GFP-305 | *SLA1c-GFP in LEU2,* integration plasmid pRS305, *SLA1*(1105-1244 a.a.) Tagged with GFP at its COOH-terminus in pRS305, can be linearized by SacI site within *SLA1* sequence for integration (Zeng *et al.*, 2001). |
| pCDC12-GFP-305 | DNA fragment encoding Cdc12p (1-407 aa) was cloned in frame with a C-terminal GFP epitope followed by the ADH1 terminator in pRS305. |
| pCDC10-GFP-305 | DNA fragment encoding Cdc10p (1-322 aa) was cloned in frame with a C-terminal GFP epitope followed by the ADH1 terminator in pRS305. |
| pSYP1-GFP-306 | DNA fragment encoding Syp1p (1-870 aa) was cloned in frame with a C-terminal GFP epitope followed by the ADH1 terminator in pRS306. |
| pSYP1-CFP-306 | DNA fragment encoding Syp1p (1-870 aa) was cloned in frame with a C-terminal CFP epitope followed by the ADH1 terminator in pRS306. |
| pSYP1-YFP-306 | DNA fragment encoding Syp1p (1-870 aa) was cloned in frame with a C-terminal YFP epitope followed by the ADH1 terminator in pRS306. |
| pSYP1-HA-306 | DNA fragment encoding Syp1p (1-870 aa) was cloned in frame with a C-terminal HA epitope followed by the *ADH1* terminator in pRS306. |
| pGAL-SYP1-HA-306 | DNA fragment encoding Syp1p (1-870 aa) was cloned in frame with a C-terminal HA epitope followed by the ADH1 terminator and placed under GAL1 promoter control in pRS306. |
| pGAL-SYP1-Myc-306 | DNA fragment encoding Syp1p (1-870 aa) was cloned in frame with a C-terminal Myc epitope followed by the ADH1 terminator and placed under GAL1 promoter control in pRS306. |
| pSWE1-HA-314 | DNA fragment encoding Swe1p (1-819 aa) was cloned in frame with a C-terminal HA epitope followed by the ADH1 terminator and placed under SWE1 promoter control in pRS314. |
| pBNI1-HA-314 | BNI1 full length with HA tag in p314, a gift from Wang Junxiao. |
| pSYP1-HA-314 | DNA fragment encoding Syp1p (1-870 aa) was cloned in frame with a C-terminal HA epitope followed by the ADH1 terminator and placed under SYP1 own promoter control in pRS314. |
| pSYP1$^{AA}$-HA-314 | DNA fragment encoding Syp1p (1-870 aa) was cloned in frame with a C-terminal HA epitope followed by the ADH1 terminator and placed under SYP1 own promoter control in pRS314. The Threonines at position 577 and 588 in Syp1p were mutated to Alanines. |
| pSYP1-GFP-314 | DNA fragment encoding Syp1p (1-870 aa) was cloned in frame with a C-terminal GFP epitope followed by the ADH1 terminator and placed under SYP1 own promoter control in pRS314. |
| pSYP1$^{N320}$-GFP-314 | DNA fragment encoding Syp1p (1-320 aa) was cloned in frame with a C-terminal GFP epitope followed by the ADH1 terminator and placed under SYP1 own promoter control in pRS314. |
| pSYP1$^{N475}$-GFP-314 | DNA fragment encoding Syp1p (1-475 aa) was cloned in frame with a C-terminal GFP epitope followed by the ADH1 terminator and placed under SYP1 own promoter control in pRS314. |

| | |
|---|---|
| pSYP1$^{N600}$-GFP-314 | DNA fragment encoding Syp1p (1-600 aa) was cloned in frame with a C-terminal GFP epitope followed by the ADH1 terminator and placed under SYP1 own promoter control in pRS314. |
| pSYP1$^{N683}$-GFP-314 | DNA fragment encoding Syp1p (1-683 aa) was cloned in frame with a C-terminal GFP epitope followed by the ADH1 terminator and placed under SYP1 own promoter control in pRS314. |
| pSYP1$^{N731}$-GFP-314 | DNA fragment encoding Syp1p (1-731 aa) was cloned in frame with a C-terminal GFP epitope followed by the ADH1 terminator and placed under SYP1 own promoter control in pRS314. |
| pSYP1$^{N830}$-GFP-314 | DNA fragment encoding Syp1p (1-830 aa) was cloned in frame with a C-terminal GFP epitope followed by the ADH1 terminator and placed under SYP1 own promoter control in pRS314. |
| pSYP1$^{C473}$-GFP-314 | DNA fragment encoding Syp1p (473-870 aa) was cloned in frame with a C-terminal GFP epitope followed by the ADH1 terminator and placed under SYP1 own promoter control in pRS314. |
| pSYP1$^{C600}$-GFP-314 | DNA fragment encoding Syp1p (600-870 aa) was cloned in frame with a C-terminal GFP epitope followed by the ADH1 terminator and placed under SYP1 own promoter control in pRS314. |
| pSYP1$^{C731}$-GFP-314 | DNA fragment encoding Syp1p (731-870 aa) was cloned in frame with a C-terminal GFP epitope followed by the ADH1 terminator and placed under SYP1 own promoter control in pRS314. |
| pSYP1$^{C473-820}$-GFP-314 | DNA fragment encoding Syp1p (473-820 aa) was cloned in frame with a C-terminal GFP epitope followed by the ADH1 terminator and placed under SYP1 own promoter control in pRS314. |
| pSYP1$^{M320-600}$-GFP-314 | DNA fragment encoding Syp1p (320-600 aa) was cloned in frame with a C-terminal GFP epitope followed by the ADH1 terminator and placed under SYP1 own promoter control in pRS314. |
| pGAL-HA-SLA1-313 | The N-terminal of Sla1p (aa 2-1244) was tagged with HA and placed under GAL1 promoter control in pRS313. |
| pGAL-SYP1-HA-314 | DNA fragment encoding Syp1p (1-870 aa) was cloned in frame with a C-terminal HA epitope followed by the ADH1 terminator and placed under GAL1 promoter control in pRS314. |
| pGAL-PRK1-315 | PRK1 coding region was generated by PCR and placed under GAL1 promoter control in vector derived from pRS315 (Zeng and Cai, 1999). |
| pGAL-PRK1$^{D158Y}$-315 | PRK1D158Y under GAL1 promoter control in pRS315; generated by replacing the SmaI/SpeI fragment of pGAL-PRK1 with the SmaI/SpeI fragment of pPRK1D158Y (Zeng and Cai, 1999). |
| pGAL-HA-PRK1-316 | The PRK1 coding region was generated by PCR, cloned in frame with the HA epitope, and placed under GAL1 promoter control in pRS316 (Zeng and Cai, 1999). |
| pGAL-SYP1-HA-316 | DNA fragment encoding Syp1p (1-870 aa) was cloned in frame with a C-terminal HA epitope followed by the ADH1 terminator and placed under GAL1 promoter control in pRS316. |
| pGAL-SYP1$^{N320}$-HA-316 | DNA fragment encoding Syp1p (1-320 aa) was cloned in frame with a C-terminal HA epitope followed by the ADH1 terminator and placed under GAL1 promoter control in pRS316. |

| | |
|---|---|
| pGAL-SYP1$^{N600}$-HA-316 | DNA fragment encoding Syp1p (1-600 aa) was cloned in frame with a C-terminal HA epitope followed by the ADH1 terminator and placed under GAL1 promoter control in pRS316. |
| pGAL-SYP1$^{C600}$-HA-316 | DNA fragment encoding Syp1p (600-870 aa) was cloned in frame with a C-terminal HA epitope followed by the ADH1 terminator and placed under GAL1 promoter control in pRS316. |
| pGAL-SYP1$^{M320-600}$-HA-316 | DNA fragment encoding Syp1p (320-600 aa) was cloned in frame with a C-terminal HA epitope followed by the ADH1 terminator and placed under GAL1 promoter control in pRS316. |
| pGAL-SYP1-MYC-316 | DNA fragment encoding Syp1p (1-870 aa) was cloned in frame with a C-terminal MYC epitope followed by the ADH1 terminator and placed under GAL1 promoter control in pRS316. |
| pGAL-SYP1-GFP-316 | DNA fragment encoding Syp1p (1-870 aa) was cloned in frame with a C-terminal GFP epitope followed by the ADH1 terminator and placed under GAL promoter control in pRS316. |
| pGAL-SYP1$^{AA}$-GFP-316 | DNA fragment encoding Syp1p (1-870 aa) was cloned in frame with a C-terminal GFP epitope followed by the ADH1 terminator and placed under GAL promoter control in pRS316. The Threonines at position 577 and 588 in Syp1p were mutated to Alanines. |
| pGAL-SYP1$^{EE}$-GFP-316 | DNA fragment encoding Syp1p (1-870 aa) was cloned in frame with a C-terminal GFP epitope followed by the ADH1 terminator and placed under GAL promoter control in pRS316. The Threonines at position 577 and 588 in Syp1p were mutated to Glutamis Acids. |
| pSYP1-HA-424 | DNA fragment encoding Syp1p (1-870 aa) was cloned in frame with a C-terminal HA epitope followed by the ADH1 terminator and placed under SYP1 own promoter control in pRS424. |
| pSYP1-GFP-424 | DNA fragment encoding Syp1p (1-870 aa) was cloned in frame with a C-terminal GFP epitope followed by the ADH1 terminator and placed under SYP1 own promoter control in pRS424. |
| pSYP1$^{AA}$-GFP-424 | DNA fragment encoding Syp1p (1-870 aa) was cloned in frame with a C-terminal GFP epitope followed by the ADH1 terminator and placed under SYP1 own promoter control in pRS424. The Threonines at position 577 and 588 in Syp1p were mutated to Alanines. |
| pSYP1$^{EE}$-GFP-424 | DNA fragment encoding Syp1p (1-870 aa) was cloned in frame with a C-terminal GFP epitope followed by the ADH1 terminator and placed under SYP1 own promoter control in pRS424. The Threonines at position 577 and 588 in Syp1p were mutated to Glutamis Acids. |
| pSYP1$^{N475}$-GFP-424 | DNA fragment encoding Syp1p (1-475 aa) was cloned in frame with a C-terminal GFP epitope followed by the ADH1 terminator and placed under SYP1 own promoter control in Prs424. |
| pSYP1$^{N600}$-GFP-424 | DNA fragment encoding Syp1p (1-600 aa) was cloned in frame with a C-terminal GFP epitope followed by the ADH1 terminator and placed under SYP1 own promoter control in pRS424. |
| pSYP1$^{C473}$-GFP-424 | DNA fragment encoding Syp1p (473-870 aa) was cloned in frame with a C-terminal GFP epitope followed by the ADH1 terminator and placed |

| | |
|---|---|
| | under SYP1 own promoter control in pRS424. |
| pSYP1$^{C600}$-GFP-424 | DNA fragment encoding Syp1p (600-870 aa) was cloned in frame with a C-terminal GFP epitope followed by the ADH1 terminator and placed under SYP1 own promoter control in pRS424. |

## 2.2 Methods

### 2.2.1 Strains and culture conditions

The *E. coli* strain DH5α (GIBCO BRL, USA) was used as the host strain in this study for DNA recombination and plasmid amplification. The *E. coli* cells were cultured at 37$^{o}$C in LB broth (1% bacto-tryptone, 0.5% bacto-yeast extract, 1% NaCl, pH 7.0) or on LB agar plates (LB containing 2% bacto-agar). 100 μg/ml Ampicilin (Sigma) or 25 μg/ml Kanamycin (Sigma) was added to the media to select for cells carrying recombinant plasmids.

All yeast strains (see Table 1) used in this study were derived from the wild type strain W303, except for the strain SFY526, which was used in the two-hybrid assay. Gene deletion in YMC515 was created by integrating a *S. pombe HIS5* selection cassette to replace the *SYP1* chromosomal locus. Gene deletion in YWJ288 was created by integrating a *LEU2* selection cassette to replace the *PFY1* chromosomal locus. YMC517, YMC520, YMC521, YMC532, YMC533, YWJ184 and YWJ186 were generated by integrating linearized pCDC12-GFP-305, pGAL-HA-306, pGAL-SYP1-HA-306, pSYP1-HA-306, pSYP1-GFP-305, pSLA1c-CFP-304/pSYP1-YFP-306 and pSLA1c-GFP-305 into wild-type cells, respectively. The same strategy was used for the integration of pGAL-SYP1-Myc-306, pCDC10-GFP-305, pSYP1-CFP-306 and pSYP1-GFP-306 into respective strains. Yeast cells were grown in standard yeast extract-peptone-dextrose

(YEPD; 1.1% yeast extract, 2.2% peptone, 0.006% adenine and 2% glucose) or synthetic complete (SC; 0.67% yeast nitrogen base without amino acids, 2% D-glucose and 0.2% amino-acids mix) medium lacking appropriate amino acids for plasmid maintenance. In experiments requiring the expression of genes under the *GAL1* promoter, raffinose instead of dextrose was used as the carbon source and galactose was later added for *GAL1* induction. Hydroxyurea (HU, Sigma) was added to a final concentration of 15 mg/ml where required.

For the examination of mating projection formation, overnight yeast cultures were diluted and refreshed at appropriate temperature for 2 hours, and α-factor was added to the culture to a final concentration of 6 μg/ml. Cells were further incubated at indicated temperatures for another 2 hours.

### 2.2.2 Recombinant DNA methods

General recombinant DNA methods were performed essentially as described previously (Sambrook, 1989). Polymerase chain reaction (PCR) was carried out with Vent DNA polymerase. Restriction enzyme digestion was performed using the appropriate buffers supplied by the manufacturers. Blunt ending of DNA fragments was carried out using Klenow DNA polymerase. Dephosphorylation of cloning vectors was done using calf intestinal phosphatase (CIP). T4 DNA ligase was used for the ligation of DNA fragments.

#### 2.2.2.1 DNA Transformation of *E. coli* cells

For heat shock transformation, DNA from ligation mix (7.5 μl) or plasmid DNA (less than 0.1 μg) was mixed with 50 μl KCM buffer (100 mM KCl, 30 mM $CaCl_2$, 50 mM $MgCl_2$), and 100 μl of competent cells. After incubation on ice for 30-45 min, the cells were heat shocked in a 43$^{o}$C water bath for 50 seconds. The transformed cells were quickly chilled on ice for at least 1 min before being plated out on the LB agar plates with appropriate antibiotics according to the selection marker of individual plasmid. For electroporation transformation, DNA was added to 50 μl of the competent cells and incubated on ice for 10 min. This was followed by a high-voltage electroporation using the Gene Pulser (Bio-Rad, USA) according to the manufacturer's instructions. The cells were then mixed with 950 μl of prewarmed LB broth and incubated at 37°C for 1 hour before being plated onto antibiotic-containing LB plates.

#### 2.2.2.2 Plasmid DNA preparation

Overnight bacterial culture (2.0 ml) was pelleted by centrifugation at full speed in a table-top centrifuge for 30 sec. The resulting pellet was resuspended in 250 μl of STET buffer (8% sucrose, 0.5% Triton X-100, 50 mM Tris-HCI pH8.0, 50 mM EDTA, 1 mg/ml freshly prepared lysozyme). The mixture was boiled in a 100$^{o}$C water bath for 2 min and subsequently centrifuged at full speed for 5 min. After removal of the bacterial debris using a toothpick, 250 μl of isopropanol was added to the supernatant, and the mixture was mixed by vortex before being centrifuged at full speed (13,000 rpm) for 10 min. The DNA pellet was washed with 70% ethanol and then dissolved in 50 μl of TE buffer (10 mM Tris-HCl, 1 mM EDTA, [pH8.0]) containing 0.1 μg/μl RNAase.

#### 2.2.2.3 Site-directed mutagenesis

*In vitro* site-directed mutagenesis was performed using the QuickChange™ Site-Directed Mutagenesis Kit from STRATAGENE (USA). The plasmid pBKS-SYP1-SalI/XbaI (Table 2) was used as the template to generate the *SYP1* mutations. PCR reaction was performed using *Pfu* DNA polymerase, and primers SYP1-T577A-5': 5'-CTCTCCTCTCAGATTGCTGGCGAGCTAAGAGAAC-3' and SYP1-T577A-3': 5'-CTCTTAGCTCGCCAGCAATCTGAGAGGAGAGTGTGG-3' to generate a mutated DNA containing the *SYP1*$^{T577A}$ mutation. The resulting PCR product was further treated with *Dpn*I to remove the parental DNA template and to select for the mutation-containing synthesized DNA. The DNA that had incorporated the desired mutation was then transformed into *E. coli* for amplification. The *SYP1*$^{T577E}$, *SYP1*$^{T588A}$ and *SYP1*$^{T588E}$ mutations were performed in the same way by using different sets of primers. All the mutations were confirmed by DNA sequencing.

#### 2.2.2.4 Plasmid constructions

For the generation of plasmids used in this study, please refer to the "Description" in **Table 2**.

### 2.2.3 Yeast manipulations

Yeast genetic techniques were performed according to standard methods described previously (Rose, 1990).

#### 2.2.3.1 Yeast transformation

The host cells were grown in appropriate medium to the log phase and harvested by centrifugation at 3000 rpm for 5 min. For each transformation, about 50 μl of the cell pellet was washed once in Li-TE buffer (0.1 M lithium acetate, 10 mM Tris-HCl pH 7.5, 1 mM EDTA), and resuspended in 100 μl of yeast transformation mix (2 M LiAc : 50% PEG 8000 : 1 M DTT = 1:8:1). The cell suspension was then mixed with the plasmid DNA and 10 μl of salmon sperm carrier DNA (9.5 μg/μl salmon testes DNA, Sigma) followed by incubation at 45°C for 30 min. The cells were collected by centrifugation at low speed and resuspended in 1 ml of $H_2O$. The cell suspension was spread onto selective plates and incubated at the appropriate temperature for 3 to 4 days.

#### 2.2.3.2 Two-hybrid assays

The MATCHMAKER system (Clontech Laboratories, USA) was used in two-hybrid analysis. DNA fragments of *SLA1* and the components of septins (*CDC3*, *CDC10*, *CDC11* and *CDC12*) were fused in frame to the *GAL4* activation domain on pGADT7 (Table 2). DNA fragments of *SYP1* were fused in frame to the DNA binding domain of *GAL4* on pGBT7 as indicated in Table 2. Plasmids were cotransformed into the yeast strain SFY526 and the expression of each fusion protein was verified by Western blotting using either anti-HA or anti-Myc antibodies. The β-galactosidase activities were measured on at least three different isolates of each co-transformation as described in the product protocol.

#### 2.2.3.3 Uracil uptake assay

The uracil uptake assay was carried out as described by Volland *et al* (Volland *et al.*, 1994). Each testing strain was transformed with pYep352-*FUR4 (*pYAM1, Table 2)

to increase the production of uracil permease. The transformants were grown at 30°C or 37°C to $OD_{600}$ of 0.2-0.3, followed by the addition of 100 μg/ml Cycloheximide (Sigma). Samples were taken at 30 min interval to measure uracil uptake. The assay was performed by incubating 1 ml of yeast culture with 5 μM [$^{14}$C]uracil (NEN) for 20 sec at 30°C or 37$^{o}$C followed by quick filtration through a Whatman GF/C filter. The filter was washed twice with ice-cold water and then counted for the retained radioactivity. Data were compiled from at least two independent experiments.

#### 2.2.3.4 Lucifer yellow uptake

The lucifer yellow (LY) uptake assay was performed as described previously (Dulic *et al.*, 1991) with minor modifications. Cells were grown at 25°C in YEPD to early log phase, and cultures were kept at 25°C or preshifted to 37°C for 15 min before addition of lucifer yellow (Sigma-Aldrich) to 5 mg/ml. After incubation for 2 h at 25°C or 37°C, cells were collected and washed five times with PBS containing 10 mM sodium azide and 50 mM sodium fluoride, followed by suspension in Vectashield mounting medium (Vector Laboratories, Burlingame, CA) and observation by fluorescein isothiocyanate and Nomarski optics with a Leica DMAXA microscope equipped with a Hamamatsu C4742–98 digital camera.

### 2.2.4 Fluorescence microscopy studies

#### 2.2.4.1 Staining of F-actin and chitin

The actin cytoskeleton was stained with rhodamine-conjugated phalloidin as described previously (Adams and Pringle, 1991) with minor modifications. Cells were

grown in appropriate media as mentioned in figure legends to a concentration of 4-8 X $10^6$ cells/ml. Cells were collected and fixed by 3.7% formaldehyde, 100 mM $KH_2PO_4$, 100 mM $K_2HPO_4$ at 24°C for 1 hour. The fixation time can be decreased to 15 min for those cells containing GFP-tagged proteins which need to be observed together with actin structures. Cells were then washed two times with PBS and incubated with PBS containing 0.1% Triton X-100 for 15 min. After washing again with PBS for two times, cells were incubated with PBS containing rhodamine-phalloidin (1:100) at 25°C for 30 min. Cells were finally washed with PBS for four times and suspended in the Vectashield mounting medium before visualization. For chitin staining, cells were fixed with 3.7% formaldehyde and stained with calcofluor (Sigma) as described by Pringle (Pringle *et al.*, 1989). The samples stained with actin or chitin were examined under a Leica DMAXA microscope equipped with a Hamamatsu C4742 digital camera. The analyses of actin organization and the budding scar patterns followed previous studies (Drubin *et al.*, 1993; Chant and Pringle, 1995). Actin depolarization was scored only in budded cells with small- and medium-sized buds. In cases where quantitation was required, at least 200 cells were counted for each sample.

#### 2.2.4.2 Real time imaging of proteins with fluorescent tags

For the time-lapse experiments, microscopy was performed with a Zeiss Axiovert 200M microscope equipped with a Coolsnap HQ camera (Roper Scientific, Tucson, AZ). To visualize septin dynamics, the CS U22 Laser power supply and Cascade 512B camera were used. Yeast cells expressing GFP and/or CFP tagged proteins were allowed to grow to early log phase at 30°C. Cells were harvested, resuspended in fresh media, and

adhered to the surface of an agarose (2 %) coated glass slide, covered with a cover slip and sealed with Vaseline. All the imaging procedures were performed within a closed chamber at 30°C. Images were acquired at the intervals of 1 min for Cdc12p-GFP and 2 min for Syp1p-GFP or Syp1p-CFP/Cdc12p-GFP dual fluorescence with motorized GFP and CFP filters. At each time point, 7 images (at a speed of 100 ms/image for septins or 400 ms for Syp1p) were acquired at 0.5 μm increments, deconvolved, and reconstructed into 3D images.

## 2.3 Protein Analysis

### 2.3.1 Preparation of crude protein extracts using acid-washed glass beads

Preparation of yeast extracts followed previous procedures (Zeng *et al.*, 2001). Yeast strains were grown in appropriate conditions to mid-log phase ($OD_{600}$ = 0.9 to 1.2). Cells were harvested, washed once with the Stop mix (0.9% NaCl, 1 mM $NaN_3$, 10 mM EDTA, 50 mM NaF) and resuspended in ice-cold lysis buffer (1% Triton X-100, 0.1% SDS, 100 mM NaCl, 50 mM Tris-HCl [pH7.2], 1 mM PMSF, 20 μg/ml leupeptin, 40 μg/ml aprotinin, 0.1 mM Na-orthovanadate, 15 mM p-nitrophenyl phosphate (PNPP) ). 200 μl of acid-washed 500-μm-diameter glass beads (Sigma) were added to the cell suspension and the cells were lysed by vortexing vigorously at 4°C. After two rounds of high speed centrifugation to pellet out the cellular debris, the supernatant was collected, snap-frozen in liquid nitrogen and stored at -80°C. Protein concentration was determined using the Coomassie Plus-200 Protein Assay Reagent (PIERCE, U.S.A). Crude protein extraction prepared by this method can be used for immunoprecipitation.

### 2.3.2 Preparation of total protein extracts using TCA precipitation

Cells equivalent to $OD_{600}$=4 were harvested by centrifugation and resuspended in 300 μl ice-cold water. Then, 150 μl of YEX lysis buffer (1.85 M NaOH, 7.5% β-mercaptoethanol) was added and the suspension was kept on ice for 10 min. Subsequently, 150 μl of 50% ice-cold TCA was added to the suspension which was further kept on ice for another 10 min. The precipitate was collected by centrifugation at 4°C for 5 min and then resuspended in a solution containing 100 μl of SDS-loading buffer (100 mM dithiothreitol, 50 mM Tris-HCl [pH 6.8], 2% SDS, 0.1% bromophenol blue, 10% glycerol) and 15 μl 1 M Tris buffer [pH 8.0]. The preparation is ready for SDS-PAGE after boiling for 10 min.

### 2.3.3 *In vitro* kinase assay and GST-fusion protein binding assay

Expression and purification of the fusion proteins were performed according to Zeng and Cai (Zeng and Cai, 1999). The GST-fusion protein expressing plasmids (pGEXs, Table 2) were transformed into *E. coli* strain DH5α. Transformants were grown to OD600 = 0.5, and induced with 1 mM isopropyl-β-D-thiogalactoside (IPTG) (Life Technologies, Inc.) at 37°C for 4 h to express the fusion proteins. Cells were collected by centrifugation and suspended in cold PBS. The suspensions were sonicated on ice to lyse the cells and the lysates were centrifuged at 10,000 rpm for 10 min in a Sorvall SS-34 rotor. The supernatants were incubated with glutathione-Sepharose 4B beads (Pharmacia) for 30 min at room temperature, and then transferred to disposable columns (Pharmacia).

The beads were washed with PBS three times and the fusion proteins were eluted from the beads by elution buffer (10 mM glutathione, 50 mM Tris-HCl, pH 8.0).

For *in vitro* kinase assays, the polyclonal rabbit anti-HA antibody was used to precipitate HA-tagged Prk1p. The beads were first washed with the RIPA buffer (50 mM Tris-HCl, pH 7.2, 1% Triton X-100, 1% sodium deoxycholate, 0.1% SDS, 150 mM NaCl) for five times, then three times with 25 mM MOPS (pH 7.2) and resuspended in 6 µl of HBII buffer (60 mM β-glycerophosphate, 25 mM MOPS, pH 7.2, 15 mM p-nitrophenylphosphate, 15 mM MgCl2, 5 mM EGTA, 1 mM dithiothreitol, 1 mM phenylmethylsulfonyl fluoride, 20 µg leupeptin/ml, and 0.1 mM sodium orthovanadate). The kinase assay was performed by incubating the beads with 5 µg of GST-fusion proteins, 0.5 µl of 1 mM ATP, 0.5 µl of [γ-32P] ATP (10 mCi/ml; New England Nuclear Inc.), 1 µl of 250 mM MOPS in a total volume of 20 µl at 25°C for 15 min, followed by addition of 3× loading buffer and 10% SDS-PAGE. The gels were first stained with Coomassie blue to visualize the protein bands. After pictures were taken, the gels were fixed, dried, and exposed to x-ray films.

To analyze the gel mobility change of Syp1p upon *PRK1* overexpression, yeast strain (YWJ97) containing various plasmids (pRS315, pGAL-PRK1, and pGAL-PRK1$^{D158Y}$) were grown at 30°C to log phase followed by addition of galactose to 2%. After incubation for 5 h, cells were collected for immunoprecipitation (IP) of Syp1p-HA as described previously (Tang *et al.*, 1997). To treat the immunoprecipitates with calf intestinal alkaline phosphatase (CIP), the protein A-Sepharose beads were washed with RIPA buffer, followed by incubation at 37°C with 1 µl of 10 U/µl CIP (Biolabs, Inc.) for 30 min and boiling in the sample buffer.

For GST-fusion protein binding experiments, yeast lysates containing Syp1p-HA was incubated with GST-fusion protein-coupled beads for 2 h at 4°C. The beads containing bound proteins were washed five times with RIPA buffer before eluted into SDS-PAGE sample buffer.

### 2.3.4 Immunoprecipitation and Western blotting

Immunoprecipitation (IP) of Syp1p-HA was performed as described previously (Tang *et al.*, 1997). About 800 μl of crude yeast cell lysate was incubated with either rabbit polyclonal anti-HA antibody Y-11 (1:100 dilution) or mouse monoclonal anti-Myc antibody 9E10 (1:80 dilution) to precipitate HA-tagged and Myc-tagged proteins. The mixture was incubated on ice for 1 hour and followed by incubation with Protein A/G PLUS-Agrose beads (SC-2003, Lot#A2004, Santa Cruz Biotechnology, pre-equilibrated in lysis buffer with protease inhibitors) for another 1 hour in the cold room with gentle agitation. The beads were then washed 4 times with RIPA buffer containing protease inhibitors. Proteins bound to immuno-complexes were released by boiling with SDS-loading buffer for 10 min and then subjected to SDS-PAGE.

SDS-PAGE was performed according to standard protocols (Sambrook *et al*., 1989) using the Mini-PROTEIN II electrophoresis cell (Bio-Rad, USA). The separation gel contained 8% to 12% of acrylamide mix (acrylamide:bisacrylamide, 29:1), 375 mM Tris-HCI [pH8.8] and 0.1% SDS. The stacking gel contained 5% acrylamide mix, 125 mM Tris-HCl [pH6.8] and 0.1% SDS. Polymerization was induced by the addition of TEMED and freshly prepared ammonium persulfate (10%). Protein samples in SDS-loading buffer were boiled for 8 min, and loaded onto the gel. Electrophoresis was carried out in Tris-glycine buffer (25 mM Tris, 250 mM glycine, 0.1% SDS). The rainbow

coloured high molecular weight protein marker (Amersham) or the prestained broad range protein marker (New England Biolabs) was used to estimate the size of proteins.

After electrophoresis, the separated proteins were electro-transferred onto Immobilon PVDF membranes (Millipore, USA) using the liquid transfer cell (Bio-Rad, USA). The transfer buffer contained 3.30 g/L Tris and 14.4 g/L glycine. For immunodetection (Western blot), the membrane was incubated overnight at 4°C with blocking solution (PBS containing 0.05% Tween-20 and 5% skimmed milk). The membrane was then incubated with the primary antibody followed by the HRP-conjugated secondary antibody. Each incubation lasted for 1 h at 25°C, followed by extensive wash with PBS containing 0.05% Tween-20. The antibody-antigen complexes were visualized with the Enhanced Chemiluminescence (ECL) system (Amersham, UK).

# Chapter 3

# Syp1p, a new phosphorylation target of Prk1p

## 3.1 Introduction

This project was started with the objective of identifying new substrates of Prk1p. Prk1p is a serine/threonine protein kinase involved in endocytosis by regulating actin patch assembly in *Saccharomyces cerevisiae* (Smythe and Ayscough, 2003; Zeng and Cai, 2005). The threonine within [L/I/V/M]xx[Q/N/T/S]xTG motifs of Pan1p can be phosphorylated by Prk1p (Zeng and Cai, 1999). Many other actin patch proteins, such as Sla1p, Ent1p, Ent2p and Scd5p, also contain these motifs and may be regulated by Prk1p phosphorylation (Watson *et al.*, 2001; Zeng *et al.*, 2001; Huang *et al.*, 2003). To advance our understanding in the regulation of actin dynamics in yeast, it is important to identify additional regulatory targets of Prk1p.

SYP1 was first identified as a multicopy suppressor of the yeast profilin deletion mutant (Marcoux *et al.*, 2000), suggesting that it might play a role in actin cytoskeleton. However, the cellular and biochemical functions of Syp1p are still unknown. Syp1p contains two adjacent LxxQxTG motifs, which could be recognized by Prk1p. Therefore, it would be interesting to find out whether Syp1p is a phosphorylation target of Prk1p and how Prk1p regulates the function of Syp1p.

## 3.2 Results

### 3.2.1 Phosphorylation of Syp1p by Prk1p *in vitro* and *in vivo*

To answer the question of whether Syp1p is a substrate of Prk1p, a truncated Syp1-GST fusion protein containing the potential Prk1p phosphorylation motifs and three other mutants which had either one or both T mutated to A (Fig. 3.1A). Using these GST fusion proteins and GST alone as the negative control, *in vitro* kinase assays

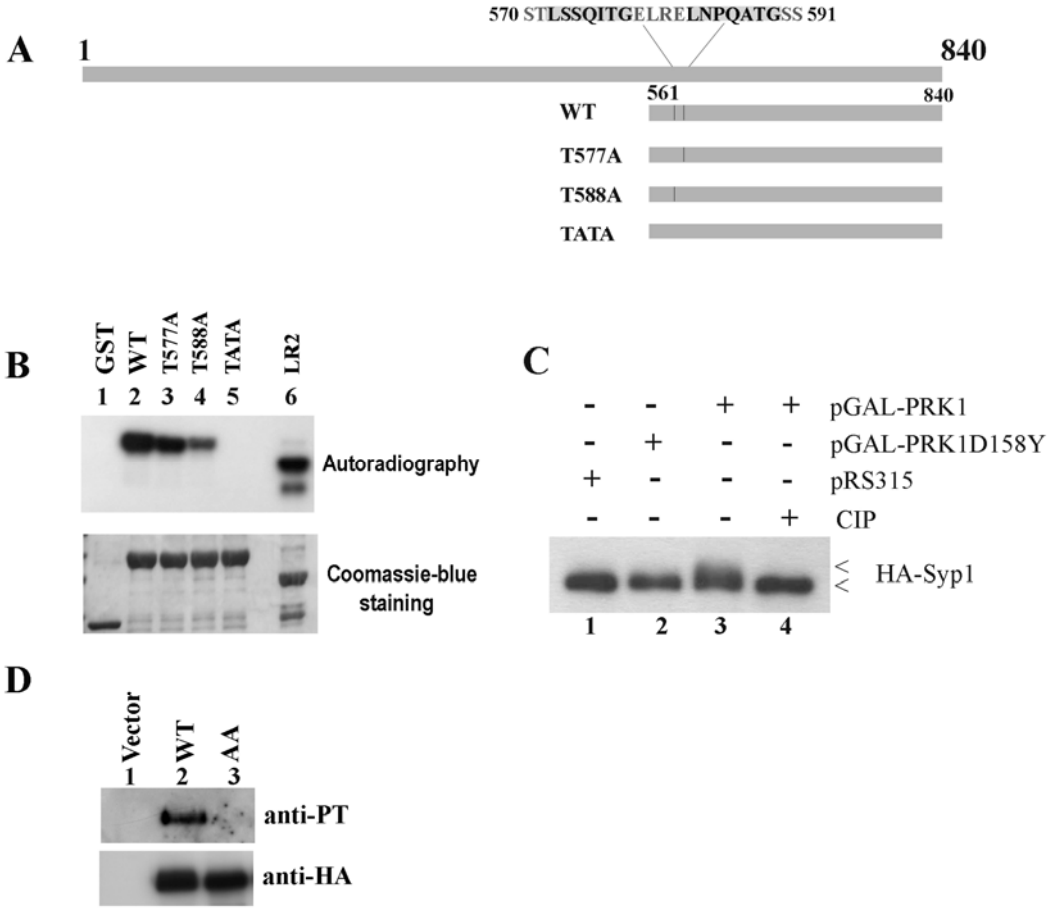


**Figure 3.1 Identification of Syp1p as a new phosphorylation target of Prk1p.** (A) Schematic diagram of Syp1p showing the locations of two LxxQxTG motifs. The bars below the diagram represent the regions used for GST-fusion protein expression. (B) *In vitro* phosphorylation of Syp1p by Prk1p. Phosphorylation results are shown in the upper panel as autoradiography and the input substrates visualized by the Coomassie blue staining of the same gel are shown in the lower panel. Immunoprecipitated HA-tagged Prk1p was added in lanes 1-6 as the kinase. Substrates used in lanes 1-5 were GST, GST-WT, GST-T577A, GST-588A and GST-TATA respectively. Substrate in lane 6 was GST-LR2 fragment of Pan1p as a positive control. (C) Phosphorylation of Syp1p by Prk1p *in vivo*. YWJ97 (*prk1*Δ*::SYP1-HA*) was transformed with vector pRS315, pGAL-PRK1 or pGAL-PRK1$^{D158Y}$. Syp1p from cells containing different plasmids was immuno-precipitated by HA antibody and analyzed by SDS-PAGE and immunoblotting. The immunoprecipitates in lane 4 were incubated with 1 μl of CIP for 30 min at 37°C prior to loading. (D) *In vivo* phosphorylation of Syp1p. Strain YMC515 (*syp1*Δ) was transformed with vector pRS314, pSYP1-HA-314 or pSYP1$^{AA}$-HA-314. Syp1-HA from cells containing different plasmids was immunoprecipitated and subsequently immunoblotted with anti-HA and anti-PThr antibodies.

Were carried out and the results are shown in Fig. 3.1B. Indeed, Syp1p can be phosphorylated by Prk1p *in vitro* (Fig. 3.1B, lane 2) and this phosphorylation was abolished when the two phosphorylation sites (T) were mutated to Alanine (A) (Fig. 3.1B, lane 5). The proteins which contained only a single mutation can still be phosphorylated by Prk1p (Fig. 3.1B, lane 3, 4), indicating that each of the motifs can be recognized by Prk1p *in vitro*. Although these two phosphorylation sites contain the same conserved amino acids L, Q and G in the LxxQxxTG motif (Fig. 3.1 A), the phosphorylation intensity of T577A (Fig. 3.1B, Lane 3) is much higher than that of T588A (Fig. 3.1 B, lane 4). This result suggests that the T588 site is more efficiently phosphorylated by Prk1p than the T577 site.

To further confirm that Syp1p is a new substrate of Prk1p, *in vivo* experiments were performed in a host that overproduced the kinase. Syp1p (tagged with HA) was immunoprecipitated (IP) from cell lysates and resuspended in loading buffer for SDS-PAGE analysis. As shown in Figure 1C, in the absence of Prk1p overexpression, Syp1p-HA migrated as a single band on the gel (Fig. 3.1C, lane 1). In contrast, the band of Syp1p extracted from cells with Prk1p overexpression exhibited a mobility shift and became smeared (Fig. 3.1C, lane 3). This phenomenon was not observed when the IP sample was treated with calf intestine phosphatase (CIP) before loading (Fig. 3.1C, lane 4). The retarded band was also not observed in Syp1p-HA precipitated from cells overexpressing the kinase-dead mutant of *PRK1* (Fig. 3.1C, lane 2). These results indicate that the gel-mobility change observed in Syp1p-HA extracted from Prk1p-overproducing cells was likely due to its phosphorylation by Prk1p.

To answer whether Syp1p can be phosphorylated by endogenous Prk1p, an *in vivo* kinase assay was carried out using anti-phospho-Threonine antibody. Syp1p or its AA mutant (tagged with HA) was expressed in *syp1*Δ cells and directly precipitated from cell lysates by TCA to preserve its maximum phosphorylated states for SDS-PAGE analysis. As shown in Fig. 3.1D, the wild type Syp1p could be detected by the anti-phospho-Threonine antibody (lane2), whereas Syp1$^{AA}$p was not (lane 3). These results demonstrated that Syp1p can be phosphorylated by Prk1p *in vitro* and possibly *in vivo*.

### 3.2.2 Effect of Prk1p phosphorylation on Syp1p

The functions of Prk1p substrates identified so far were negatively regulated by Prk1p phosphorylation. For example, Pan1p or Ent1p phosphorylation by Prk1p negatively regulates the formation and activity of Pan1p-End3p-Sla1p or Pan1p-Ent1p complex (Watson *et al.*, 2001; Zeng *et al.*, 2001). As a novel substrate of Prk1p, the Prk1p phosphorylation effect on Syp1p was next investigated. Syp1p was first identified as a multicopy suppressor of the *pfy1*Δ mutant. The two threonine phosphorylation sites of Syp1p were mutated to either glutamine or alanine to mimic constitutively phosphorylated or dephosphorylated Syp1p, respectively. Serial dilutions of cells transformed with either empty vector or with 2μ *SYP1* and its mutant plasmids were spotted onto rich medium and grown at 25°C and 37°C for 2 days. The results are shown in Fig. 3.2, *pfy1*Δ cells were viable but sensitive to 37°C treatment (Fig. 3.2A, row 2). At non-permissive temperature, cells transformed with high copy *SYP1* (Fig. 3.2A, row 3) grew better than those with the vector, but still weaker than the wild type cells (Fig. 3.2A, row 1). These findings indicate that high copy *SYP1* is able to partially suppress the temperature sensitivity (ts) of *pfy1*Δ cells. The other two mutated *SYP1* could also

partially suppress the ts of *pfy1*Δ (Fig. 3.2A, row 4, 5). However, the suppression activity of Syp1p$^{EE}$ was weaker compared with the wild-type Syp1p and the Syp1p$^{AA}$ mutant. These results indicate that phosphorylation of Syp1p by Prk1p may negatively regulate the ability of Syp1p on *pfy1*Δ suppression.

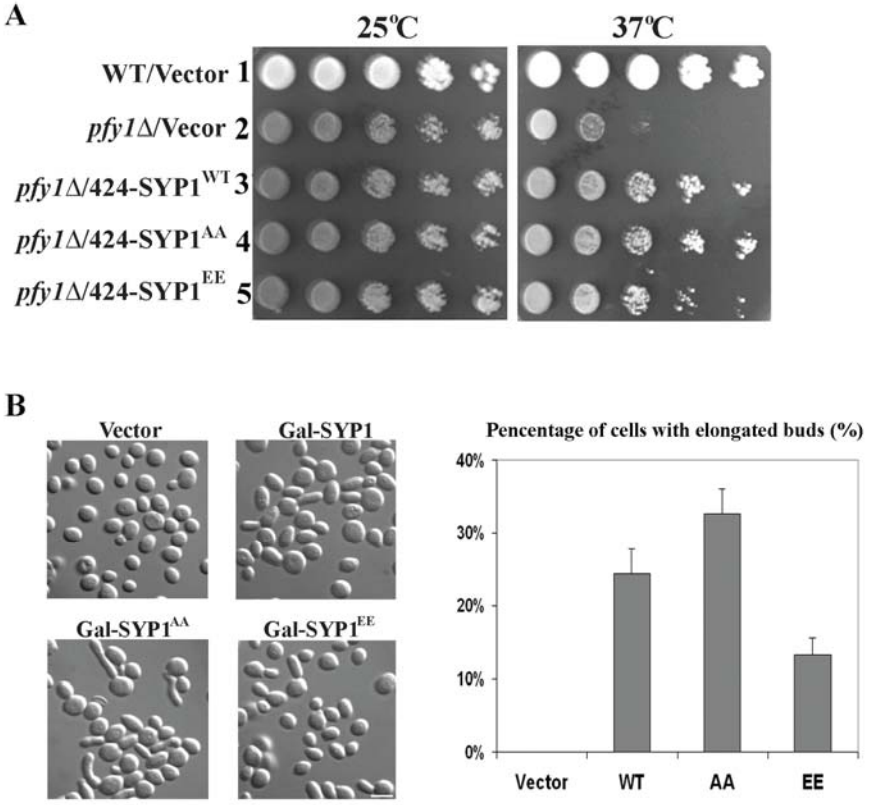


**Fig. 3.2 Effect of Syp1p phosphorylation by Prk1p on *pfy1*Δ suppression (A) and bud morphogenesis (B).** (A) Strain YWJ288 (*pfy1*Δ) was transformed with high copy vector p424, pSYP1-GFP-424, pSYP1$^{AA}$-GFP-424, or pSYP1$^{EE}$-GFP-424 to get trains YWJ128, YWJ129, YWJ130 and YWJ131 respectively. These strains were cultured in rich medium overnight at 25°C. Serial dilutions of overnight cultures were spotted onto rich medium and grown at 25°C and 37°C for 2 d. (B) Strain YMC515 (*syp1*Δ) was transformed with vector p316, pGal-SYP1-GFP, pGal-SYP1$^{AA}$-GFP or pGal-SYP1$^{EE}$-GFP. The resulting strains, YWJ67 (vector), YWJ68 (pGal-SYP1), YWJ69 (pGal-SYP1$^{AA}$) and YWJ70 (pGal-SYP1$^{EE}$), were cultured in raffinose at 30°C to log phase followed by addition of galactose to 2% to induce Syp1p expression. After 7 h, samples were taken, sonicated and prepared for microscopy. The quantitative data of cell morphology are shown in the right panel. Bar, 5 μm.

The effect of SYP1p$^{AA}$ and SYP1p$^{EE}$ overexpression on elongated bud induction was also studied. In the cells overexpressing Syp1p$^{AA}$, some of the elongated buds were much longer than the ones induced by wild-type Syp1p (Fig. 2B). The percentage of elongated buds found in cells overexpressing Syp1p$^{AA}$ was also higher (34%) than in cells overexpressing wild-type Syp1p (24%). However, in the cells overexpressing Syp1p$^{EE}$, the percentage of cells with elongated buds was only about 10%. These results suggest that the phosphorylation of Syp1p by Prk1p inhibits the function of Syp1p in the formation of elongated buds.

## 3.3 Discussion

### 3.3.1 Syp1p is a new regulatory target of Prk1p

Based on the presence of recognition sequence of Prk1p in Syp1p and its possible function in actin cytoskeleton, Syp1p was chosen for study of its functional relationship with Prk1p. Indeed, the results showed that Syp1p can be phosphorylated by Prk1p *in vitro* and possibly *in vivo* as well. The functions of Syp1p in suppression of *pfy1*Δ mutant and elongated bud induction also appear to be affected by phosphorylation. These findings suggest that Syp1p is a novel regulatory target of Prk1p.

Prk1p is known to be involved in the regulation of cell polarity. Firstly, many proteins such as Bni1p, Bnr1p, Bud6p, Spa2p, Bud2p and Bud3p, which contain canonical phosphorylation motifs of Prk1p play a role in polarity establishment, but not endocytosis (Huang *et al.*, 2003). Bni1p and Bnr1p are formins in yeast which are required for actin cable formation so as to establish polarized secretion (Evangelista *et al.*, 2002; Sagot *et al.*, 2002a). Both Bud6p and Spa2p are components of the polarisome

which is important for regulating the activity of formins and other cell polarity functions (Fujiwara *et al.*, 1998; Moseley and Goode, 2005). Bud2p and bud3p, together with septins, are necessary for bud site selection (Chant, 1999). It is possible that Prk1p plays a role in cell polarity through regulating the functions or interactions of these proteins. Secondly, overexpressing Prk1p or Ark1p resulted in cells with elongated buds or other abnormally shaped buds (Cope *et al.*, 1999). These phenotypes are similar to the mutants with disorganized septins. This observation suggests that Prk1p kinase family has a role in cell polarity. Therefore, it would be interesting to study whether Syp1p has functional relationships with these Prk1p potential targets.

To understand the mechanisms of how Prk1p regulates the functions of Syp1p, it is necessary to study the molecular functions of Syp1p and identify the interaction partners of Syp1p. In the following chapters, the findings of Syp1p functions in actin cytoskeleton (chapter 4) and septins (chapter 5) will be presented.

# Chapter 4

# Functional Relationship between Syp1p and actin cytoskeleton

## 4.1 Introduction

Limited studies so far suggest that Syp1p may play a role in actin cytoskeleton in relation to cell polarity. Overexpressing Syp1p restores the actin polarity in the profilin-deleted cell (Marcoux *et al.*, 2000). Profilin-deficient cells have depolarized actin patches but no actin cable, which result in large, rounded cells that undergo cell lysis at high temperature. These phenotypes are consistent with the molecular function of profilin in promoting formin-nucleated actin cable assembly (Sagot *et al.*, 2002b; Moseley *et al.*, 2004). Therefore, the function of Syp1p in cell polarity might be related to actin cable formation. In addition to its possible role in actin cables, Syp1p may play a role in the organization or regulation of actin patches. Firstly, similar to cortical actin patches, Syp1p is localized to the sites of cell growth, such as incipient bud site, bud neck and bud tip (Marcoux *et al.*, 2000). Secondly, using the tandem-affinity purification (TAP) and mass spectrometry in a large-scale approach, Syp1p was found in the Las17p complex (Gavin *et al.*, 2002). Las17p is an important NPF of Arp2/3p complex required for actin patches formation (Li, 1997). The Las17p complex also includes Sla1p and Sla2p; both of which are regulators of actin patches. These findings indicate that Syp1 may also have a role in the function or regulation of actin patches. Indeed, Syp1p was found to associate with Sla1p physically in this study (see section 4.2.3). Therefore, three perspectives on the functions of Syp1p in actin cytoskeleton were investigated: 1) its functional relationship with profilin (Pfy1p) and Bni1p; 2) the localization interdependence between Syp1p and actin cytoskeleton; 3) its functional relationship with Sla1p.

## 4.2 Results

### 4.2.1 Functional relationship between Syp1p and Pfy1p/Bni1p

#### 4.2.1.1 Syp1p overexpression partially suppresses the phenotypes of *pfy1*Δ mutant

As demonstrated in chapter 3, Syp1p overexpression partially suppressed ts of *pfy1*Δ cells. To test whether high copy of *SYP1* can suppress other phenotypes of *pfy1*Δ mutant, the sensitivity to Calcofluor White (CFW) was examined. Calcofluor White amplifies the effect of cell wall defects, causing the mutant cells to stop growing at low concentrations of CFW (Ram *et al.*, 1994). *pfy1*Δ cells have cell wall defects and abnormal chitin deposition (Haarer *et al.*, 1990). *pfy1*Δ cells are sensitive to growth on CFW-containing medium at 25°C (Fig. 4.1A, row 2). However, high copy of *SYP1* could not suppress the growth sensitivity of *pfy1*Δ cells on the Calcofluor White medium (Fig. 4.1A, row 3). Consistently, chitin deposition was still abnormal in these cells with Syp1p overexpression (Fig. 4.1B, frame c). To investigate whether overexpressing Syp1p restores actin polarity to *pfy1Δ* cells, the actin cytoskeleton in *pfy1*Δ cells overexpressing Syp1p was studied in detail. In *pfy1*Δ cells overexpressing Syp1p, actin patches are more concentrated in the small bud and the mother-daughter necks compared to cells with control vector (Fig. 4.1C, frame c, arrows). However, numerous actin patches were still observed in the mother site of the small-budded cells with Syp1p overexpression whereas there were only few actin patches observed in the mother cells in the wild-type control (Fig. 4.1C). Additionally, there was no actin cable visible in *pfy1*Δ cells transformed with either vector or high copy of *SYP1* (Fig. 4.1C, frame b-c). These results indicate that overexpressing Syp1p partially suppresses the actin cytoskeleton defect of *pfy1*Δ cells.

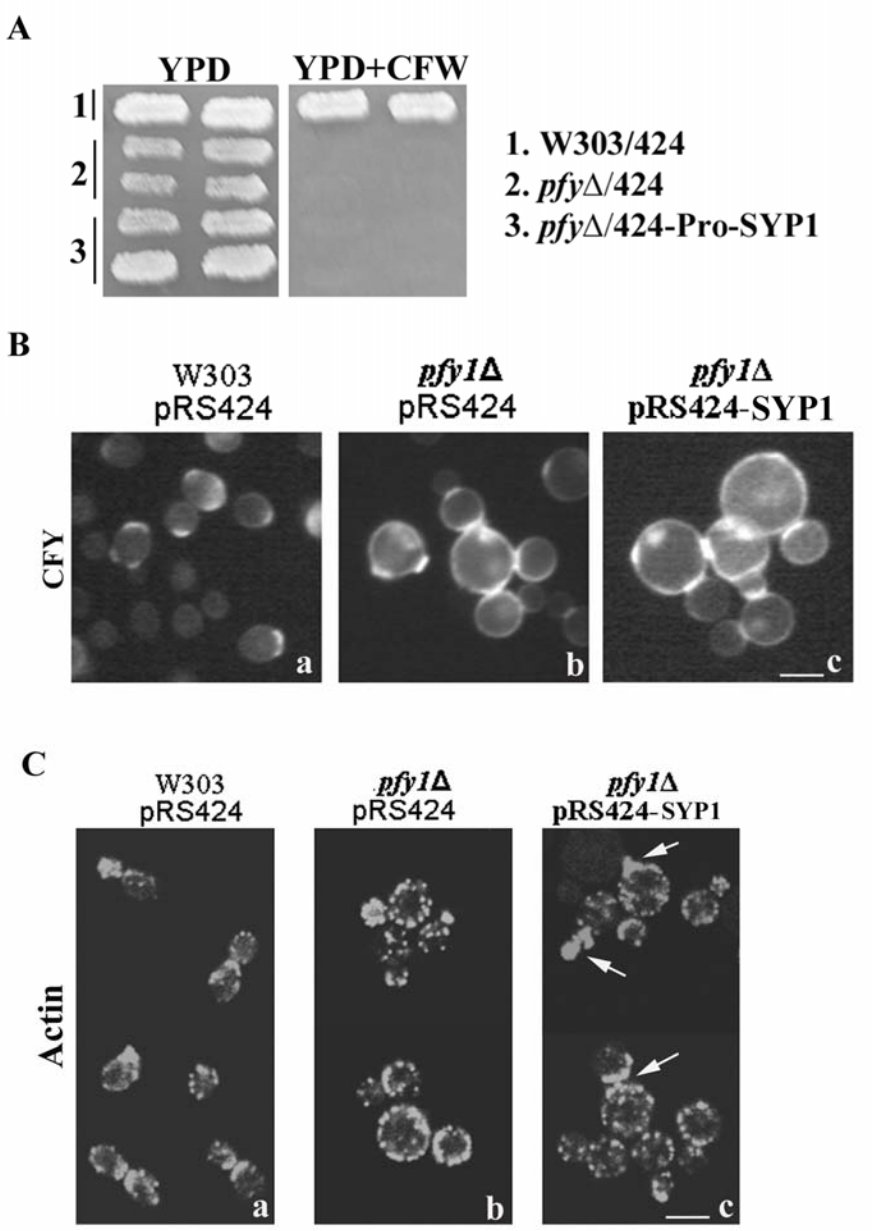


**Figure 4.1 Syp1p overexpression partially suppressed phenotypes of *pfy1Δ* mutant**. The strains YWJ128 (*pfy1Δ*/vector) and YWJ129 (*pfy1Δ*/424-*SYP1*) were used in these experiments. W303 transformed with empty vector was used as a positive control. (A) The strains were grown on YEPD plate, replica-plated onto YEPD plate containing 1 mg/ml Calcofluor White (CFW), and incubated at 25°C for 1 day before being photographed. (B-C) The strains were grown at 25°C to log phase and fixed for Calcofluor White staining (B) and actin staining using phalloidin (C). The arrows show the polarized actin in Syp1p overexpressing cells. Bars, 5 μm.

#### 4.2.1.2 Syp1p overexpression suppresses the phenotypes of *bni1*Δ mutant

Profilin is an important stimulator of Bni1p-dependent actin cable formation (Sagot *et al.*, 2002b). The *bni1 bnr1* mutant has similar cell polarity defects as the *pfy1*Δ mutant, such as defective morphogenesis and depolarized actin patches (Imamura *et al.*, 1997). To understand the molecular mechanism behind the suppression of profilin deletion mutant by high copy *SYP1*, the functional relationship between Syp1p and Bni1p was investigated. First, suppression of the temperature sensitivity of *bni1*Δ mutant by Syp1p overexpression was tested. Indeed, the temperature sensitivity of *bni1*Δ cells could be suppressed by Syp1p overexpression (Fig. 4.2A). *bni1*Δ cells expressing high copy *SYP1* still grew at 38$^{o}$C whereas the mutant cells with control vector were inviable (Fig. 4.2A).

To investigate whether overexpressing Syp1p could also suppress the actin defect of *bni1*Δ cells, the mutant cells transformed with control vector, one copy of *BNI,* or high copy of *SYP1* were grew overnight at 37°C before actin staining. *bni1*Δ cells showed severe defects: the cell morphology was abnormal with large round cells attached together indicative of cytokinesis defect; no actin cable was visible and the actin patches lost the polarity and distributed randomly in the cell cytosol (Fig. 4.2B, middle). One copy of *BNI1* could restore the normal morphology and actin cable formation to the *bni1*Δ cells (Fig. 4.2B, left). High copy *SYP1* also suppressed some of the deficient phenotypes of *bni1*Δ mutant. In the *bni1*Δ cells overexpressing Syp1p, the cell size became normal although cytokinesis defect still existed. Additionally, actin patches localized to the cell membrane periphery instead of diffusing to the cytoplasm as in the

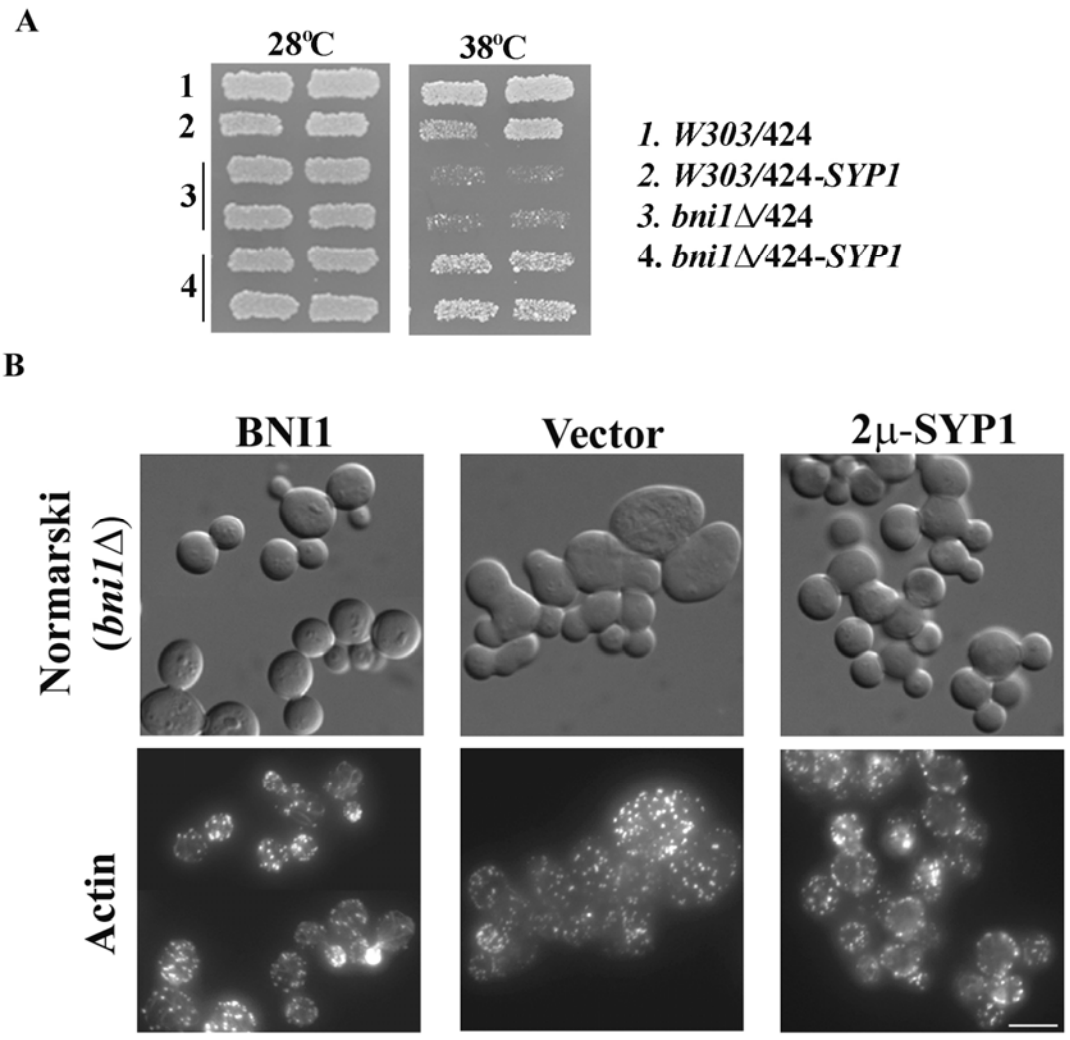


**Figure 4.2 Syp1p overexpression partially suppressed phenotypes of *bni1*Δ mutant**. (A). W303 and *bni1*Δ (YGS223) cells were transformed with vector p424 or pSYP1-HA-424 to get the trains YWJ720 (W303/424), YWJ721 (W303/424-SYP1), YWJ722 (*bni1*Δ/424) and YWJ723 (*bni1*Δ/424-SYP1). These strains were grown at 28°C on YPD plate. The plate was replica-plated onto two YPD plates. These replica plates were incubated at 28°C and 37°C for 2 days respectively. (B) The strains, YWJ724 (*bni1*Δ/314-BNI1), YWJ722 (*bni1*Δ/424) and YWJ723 (*bni1*Δ/424-SYP1) were grown at 25°C to log phase. The temperature was then shifted to 37°C and the cells grew another 16 hours at this temperature. The samples were fixed and stained with phalloidin. Bar, 5 μm.

*bni1*Δ cells. However, actin patches still lost their polarity and no cables were visible in these cells (Fig. 4.2B, right). These results indicate that overexpressing Syp1p partially suppresses the deficient phenotypes of *bni1*Δ cells.

#### 4.2.1.3 Polarized localization and function of Syp1p depend on profilin and Bni1p

To study whether Pfy1p and Bni1p were required for the Syp1p localization, *SYP1-GFP* was integrated into both the *pfy1*Δ and *bni1*Δ mutants to observe its localization. At 25°C, the localization of Syp1-GFP was normal in *pfy1*Δ cells. However, at 30°C, Syp1p-GFP was diffused to the cell membrane periphery (Fig. 4.3A). In addition, *pfy1*Δ cell was observed to have cytoplasmic Syp1p-GFP (Fig. 4.3A, arrow heads), which was not seen in wild-type cells. These findings suggest that the polarized localization of Syp1p is dependent on profilin. The diffusion of Syp1p is more severe in *bni1*Δ cells than in *pfy1*Δ cells at the same temperature. Syp1p was depolarized even at 25°C in *bni1*Δ cells (Fig. 4.3B). Syp1p could no longer concentrate to the small bud in *bni1*Δ cells (Fig. 4.3B) whereas this localization pattern was still observed in some *pfy1*Δ cells (Fig. 4.3A). These results indicate that both Pfy1p and Bni1p are required for the polarized localization of Syp1p. Since actin cytoskeleton loses its polarity in both *pfy1*Δ and *bni1*Δ mutants, the depolarization of Syp1p in these mutants could be due to the actin cytoskeleton defect.

In addition to the depolarization of Syp1p, *BNI1* deletion also abolished the elongation bud phenotype caused by Syp1p overexpression (Fig. 4.4). Overexpressing Syp1p in wild-type cells results in hyper-polarized cells with elongated buds as previously reported (Fig. 4.4, top) (Marcoux *et al.*, 2000). However, there was no

elongated bud observed in *bni1*Δ cells with Syp1p overexpression (Fig. 4.4, bottom). Similar result was also observed in *pfy1*Δ cells (data not shown). These findings suggest that the hyperpolarized growth induced by Syp1p overexpression is dependent on Bni1p and profilin.

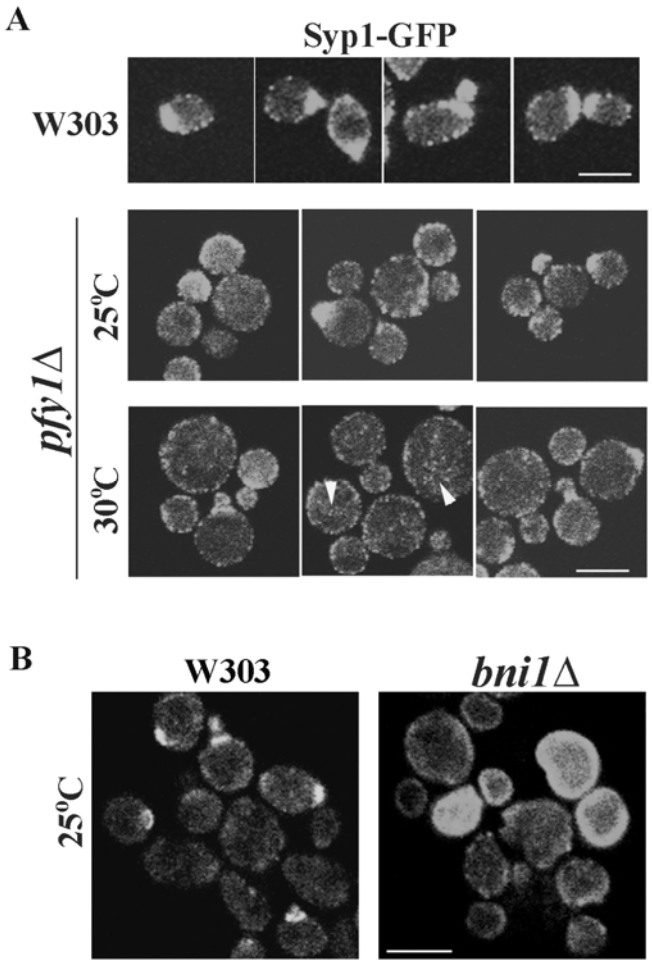


**Figure 4.3 Depolarization of Syp1p localization in *pfy1* and *bni1* mutants**. (A) W303 and *pfy1Δ* mutant integrated with *SYP1-GFP* (strains YMC533 and YWJ137 respectively) were grown to mid-log phase in YEPD at 25°C and then shifted to 37°C for 1 h. Syp1p-GFP of different samples was visualized. Arrow heads show Syp1p-GFP in the cytoplasm. (B) W303 and *bni1Δ* mutant transformed with pSYP1-GFP-314 (strains YWJ107 and YWJ207 respectively) were grown to mid-log phase in YEPD at 25°C and examined for the Syp1p-GFP localization. Bars, 5 μm.

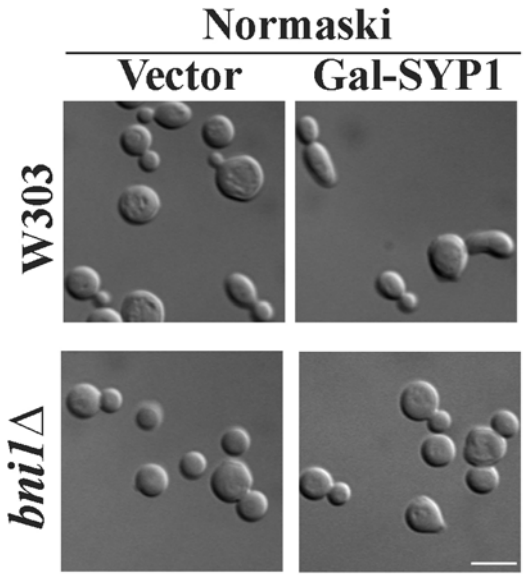


**Figure 4.4 *BNI1* deletion abolished the elongated bud induced by Syp1p overexpression**. YWJ63 (W303/vector), YWJ89 (W303/pGal-SYP1-HA), YWJ213 (*bni1Δ*/vector), YWJ214 (*bni1Δ*/pGal-SYP1-HA) were induced for Syp1p overexpression for 7 h as stated above. The samples were taken and examined for morphology. Bar, 5 μm.

### 4.2.2 Localization interdependency between Syp1p and actin cytoskeleton

#### 4.2.2.1 Dependency of Syp1p polarized localization on actin cytoskeleton

To further investigate the functional relationship between Syp1p and actin cytoskeleton, the localization pattern of Syp1p and that of actin cytoskeleton were compared. Syp1p-GFP was found to colocalize with actin cortical patches in different cell cycle stages (Fig. 4.5). For example, both Syp1p and actin patches concentrated to the incipient bud site in unbudded cells (Fig. 4.5, frame 1-2), localized to the tip and/or membrane periphery of small buds (Fig. 4.5, frame 3-5), formed two large patches with one each at the mother and daughter sides of the neck in large budded cells (Fig. 4.5, frame 6-7). However, Syp1p-GFP do not colocalized with actin cables as shown in Figure 4.5, frame 2, 3, 6. Also, when the bud was growing, some fraction of Syp1p-GFP was observed to remain concentrated at the mother-daughter neck while most of the actin patches already localized to the buds (Fig. 4.5, frame 4-5). These results indicate that the

cellular localization of Syp1p is tightly linked to actin patches at the active growth sites and Syp1p may play additional roles in the bud neck.

The cellular localization of Syp1p was also found to be strictly dependent on actin cytoskeleton. Upon treatment with Lat A, a drug that disassembles the actin filaments (Ayscough, 1998), Syp1p-GFP was diffused to the whole cell membrane periphery (Fig. 4.6A). Before Lat A treatment, both Syp1p-GFP and actin polarized to the bud or bud neck (Fig. 4.6A, left). However, after 15 minutes of Lat A treatment, the actin filaments disassembled and were diffused to all over the cytoplasm; similarly, Syp1p lost its polarized localization (Fig. 4.6A, right), but was still able to localize to the membrane periphery. In the control cells which were treated with DMSO, both Syp1p and actin cytoskeleton remained polarized (Fig. 4.6A).

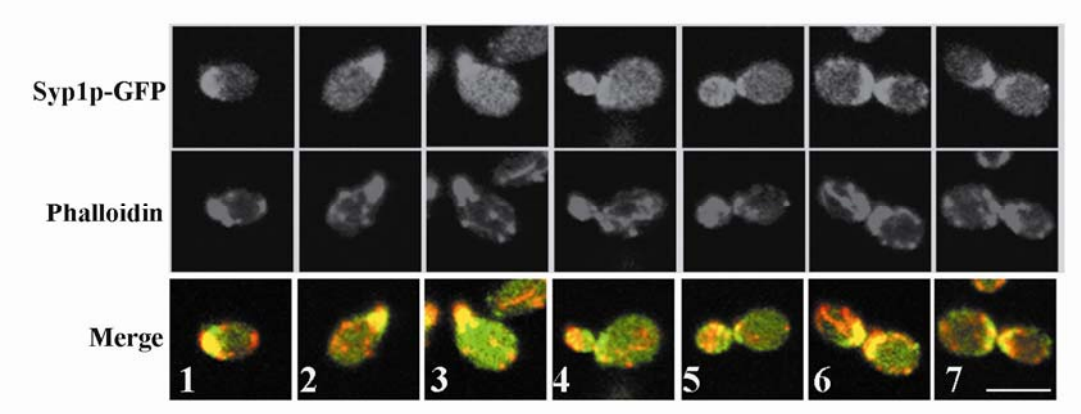


**Figure 4.5 Colocalization between Syp1p and actin cytoskeleton.** W303 strain integrated with SYP1-GFP (YMC533) was cultured to mid-log phase in YEPD at 30°C and stained with phalloidin. The sample was examined for Syp1p-GFP and actin cytoskeleton. The frames show the different cell cycle stages. The images of Syp1p-GFP and actin are merged into yellow. Bar, 5 μm.

To further study the dependency of Syp1p polarized localization on actin cytoskeleton, the *act1-1* ts mutant was used to examine the localization of Syp1p at non-permissive temperature. At the permissive temperature, the *act1-1* mutant grew well. Under this condition, both Syp1p-GFP and actin cytoskeleton displayed a normal pattern of localization similar to the wild-type strain (Fig. 4.6B, upper). However, at the non-permissive temperature of 37°C, actin patches depolarized to all over the cell membrane periphery (Fig. 4.6B, lower). Similarly, Syp1p lost its polarity and diffused to cell membrane as well (Fig. 4.6B, lower). These results further indicate that the polarity of Syp1p localization is dependent on the intact actin cytoskeleton.

#### 4.2.2.2 Polarity defects of actin patches in cells overexpressing Syp1p

Although the localization of actin cytoskeleton is normal in *syp1*Δ cells (Marcoux *et al.*, 2000), it was found that Syp1p overexpression resulted in the depolarization of actin patches. As shown in Fig. 4.7A, overexpressing Syp1p induced elongated buds (Fig. 4.7A, arrows, also see chapter 5 for more details). The organization of actin patches in a fraction of the cells was abnormal. Numerous patches were observed in the mother site in 42% of budded cells (small- and medium-sized buds) although actin patches also localized in the elongated bud (Fig. 4.7A). In comparison, only about 19% of the budded cells displayed depolarized actin patches in the vector control (Fig. 4.7A). These results suggest that Syp1p overexpression depolarizes the actin patches in yeast. These observations also suggest that the actin patches in cells overexpressing Syp1p have two types of distribution: one is localized in the elongated bud to support the hyperpolarized growth; the other is depolarized in the mother site.

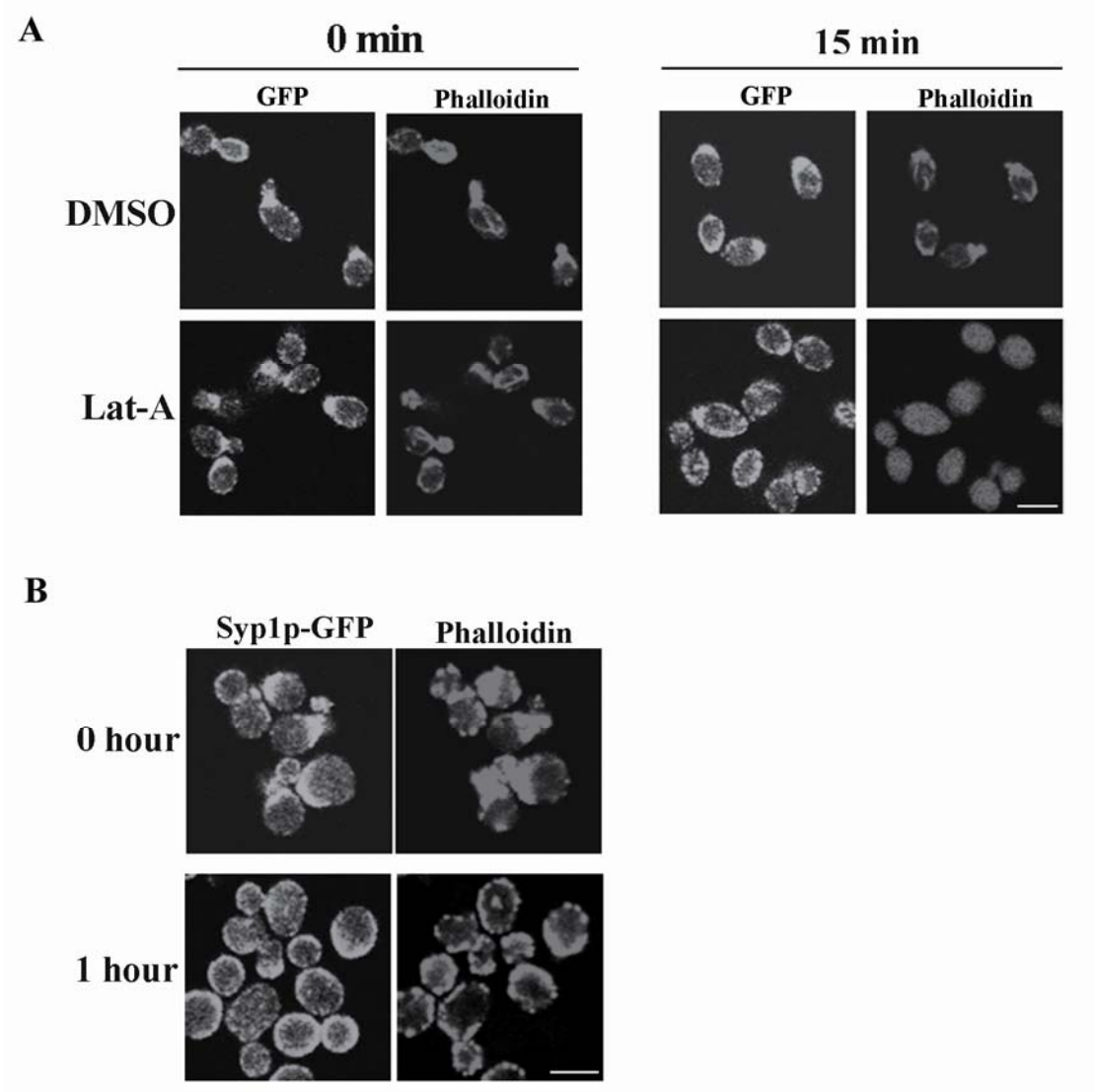


**Figure 4.6 The dependence of Syp1p polarized localization on actin cytoskeleton.** (A) Actin-dependent manner of Syp1p polarity. The strain YMC533 (W303::*SYP1-GFP*) was cultured to mid-log phase in YEPD at 30°C and then treated with Lat A or DMSO for 15 min. The samples were stained with phalloidin and examined for Syp1p-GFP and actin cytoskeleton. The images of Syp1p-GFP and actin are merged into yellow. (B). Depolarization of Syp1p localization in actin mutant. The *act1-1* mutant (DDY335) integrated with *SYP1-GFP* (YWJ33) was grown to mid-log phase in YEPD at 25°C and then shifted to 37°C for 1 h. The samples were fixed and stained with phalloidin. Bars, 5 μm.

It is known that defects of actin cytoskeleton organization are often accompanied by random bud site selection (Yang *et al.*, 1997). Wild-type haploid yeast cells normally form the new bud from a position proximal to the previous division site, and this is referred to as the axial budding pattern (Chant and Pringle, 1991; Casamayor and Snyder, 2002). Budding patterns can be examined and scored by staining cells with Calcofluor which labels chitin deposited on the cell wall of bud sites. To gather additional evidence of the actin cytoskeleton defect in cells overexpressing Syp1p, the budding pattern of the cells with Syp1p overexpression was examined. The wild-type strain used in this study, W303, has been shown to contain a *bud4* mutation and therefore exhibits a higher ratio of bipolar budding pattern (Voth *et al.*, 2005). Consistently, most of cells expressing the empty vector displayed the axial or bipolar budding pattern (Fig. 4.7B, upper), whereas for cells with Syp1p overexpression, 30% of cells displayed random budding pattern, which is 15% more than the cells expressing the control vector (Fig. 4.7, bottom) (about 200 cells with more than 3 bud scars were scored). This random bud site selection was chosen by cells regardless of whether the cell is in a normal morphology or with an elongated bud (Fig. 4.7B, bottom). This shows that cells overexpressing Syp1p were defective in bud site selection. The results also confirmed the finding that Syp1p overexpression results in the depolarization of actin patches.

### 4.2.3 Association of Syp1p with Sla1p

#### 4.2.3.1 Interaction between Syp1p and Sla1p *in vitro* and *in vivo*

The interdependence of localization of Syp1 and actin cytoskeleton suggests that Syp1p may interact with actin or actin-associated proteins. There is no actin binding

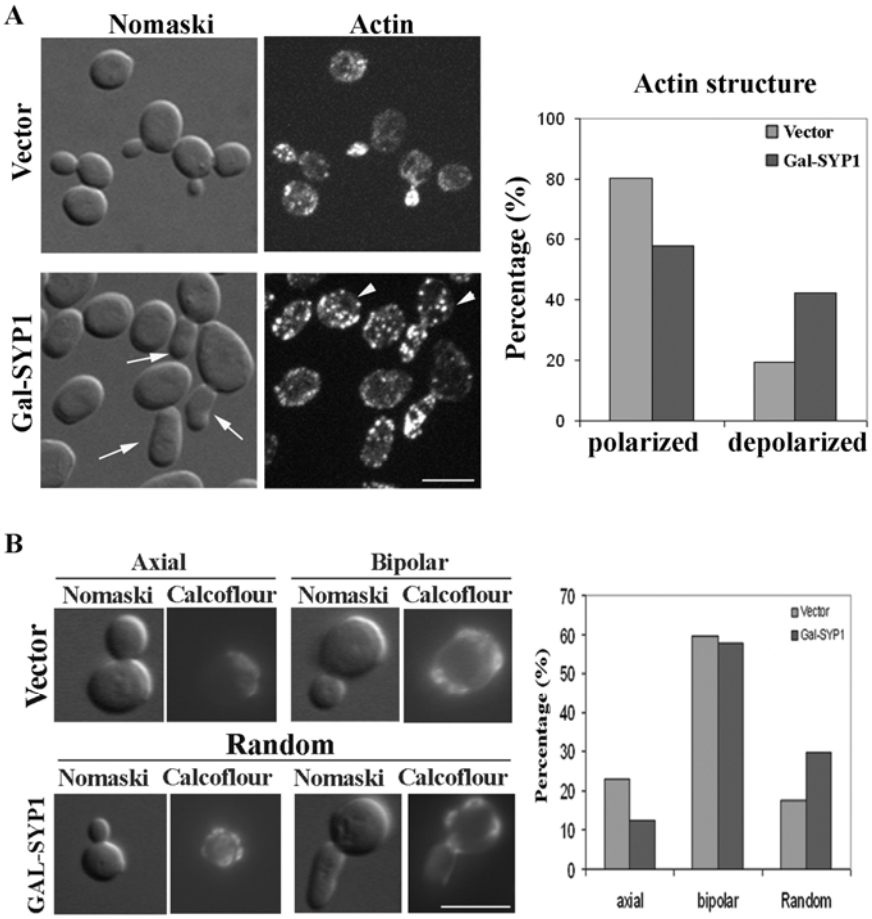


**Figure 4.7 Syp1p overexpression depolarized actin cytoskeleton and chitin deposition**. The strains, YWJ63 (vector) and YWJ89 (Gal-SYP1-GFP) were grown at 30°C to log phase and added 2% galactose to induce Syp1p overexpression for 7 hours. The samples were fixed for actin cytoskeleton staining using phalloidin (A) and bud scar staining using calcofluor white (B). The statistical data of actin depolarization and budding patterns are shown in the right panels. Arrows show the elongated buds and arrow heads indicate the depolarized actin patches. Bars, 5 μm.

motif in the Syp1p sequence and the interaction between Syp1p and actin was not observed by the yeast two-hybrid assay (data not shown). Therefore, it is unlikely that Syp1p can bind directly to actin. It has been reported that Syp1p is found in the complex of Las17p (Gavin *et al.*, 2002), which also includes End3p, Bzz1p, Sla1p and Sla2p that

are regulators of actin patches. To investigate which proteins in the Las17p complex can directly interact with Syp1p, Sla1p was first chosen as a potential interaction partner of Syp1p. Firstly, the localization patterns of Syp1-YFP and Sla1-CFP were examined using cells that contained both tagged proteins. Syp1-YFP was found to colocalize with Sla1-CFP during various cell cycle stages (Fig. 4.8A). However, during bud growth, some fraction of Syp1-YFP remained at the mother-daughter neck while most of Sla1-CFP localized to the buds (Fig. 4.8A, frame 3, arrow). These results indicate that the cellular localization of Syp1p is linked to Sla1p at the active growth sites especially at the early and late cell cycle stages.

To study whether the localizations of Sla1p and Syp1p are inter-dependent, the localization of Syp1-GFP in *sla1*Δ cells and that of Sla1-GFP in *syp1*Δ cells were examined. No defect in Sla1-GFP localization was observed, indicating that Syp1p is not required for Sla1p to localize properly (Fig. 4.8B, bottom). The cellular localization of Syp1p, however, was found to be dependent on Sla1p. At 25$^{o}$C, Syp1-GFP was diffused to the whole cell membrane periphery in *sla1*Δ cells (Fig. 4.8B, upper).

The overexpression effects on the localizations of both proteins were also examined using wild-type cells transformed with either *SYP1* or *SLA1* under *GAL1* promoter. Overexpressing Sla1p induced depolarization of Syp1p (Fig. 4.8C, left). The Syp1-GFP was diffused to the cytoplasm. On the other hand, overexpression of Syp1p also caused depolarization of Sla1p (Fig. 4.8C, right). In cells overexpressing Syp1p, the cortical patches of Sla1p depolarized to the whole cell membrane periphery. These results indicate that the polarized localization of Syp1p is dependent on Sla1p.

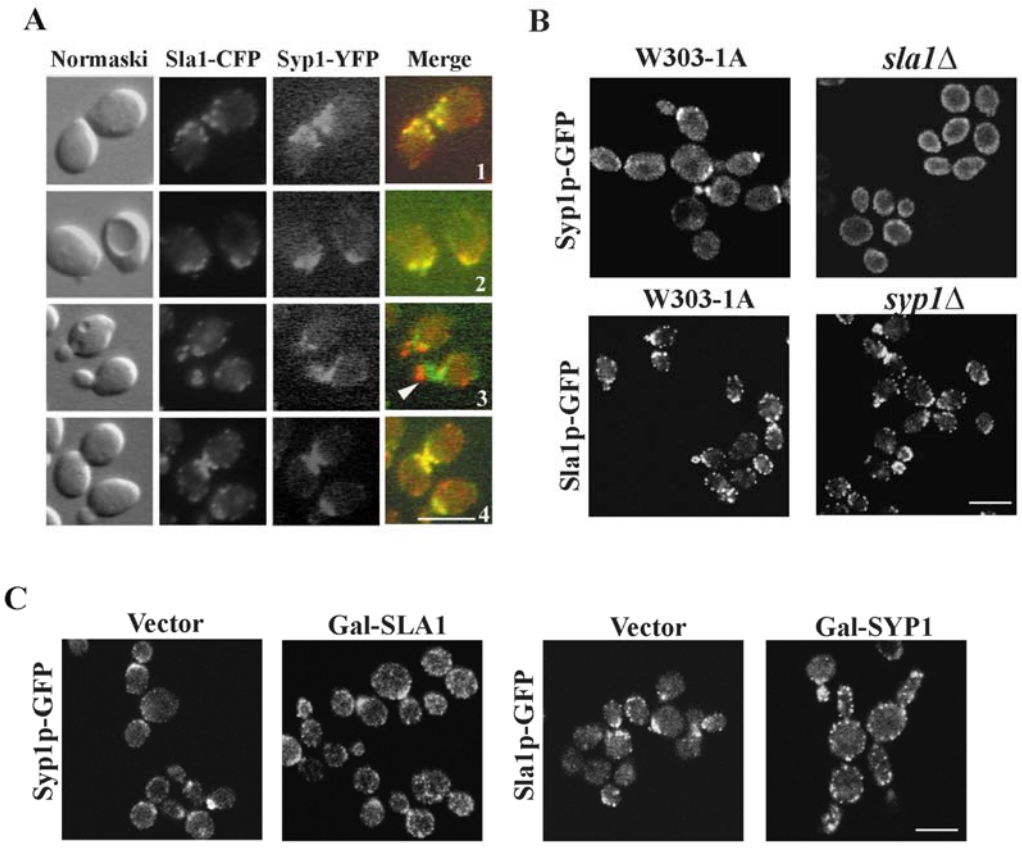


**Figure 4.8 Sla1p is required for the polarized localization of Syp1p**. (A) Colocalization of Syp1p and Sla1p. W303-1A integrated with *SYP1-YFP* and *SLA1-CFP* (YWJ184) was cultured to mid-log phase in YEPD at 30°C and fixed for visualization of DIC, Syp1-YFP and Sla1-CFP. The images of Syp1-YFP and Sla1-CFP are merged into yellow. (B) Depolarization of Syp1p localization in *sla1* mutant. The strains YWJ40 (*syp1*Δ/pSYP1-GFP), YWJ209 (*sla1*Δ/pSYP1-GFP), YWJ186 (W303::*SLA1-GFP*) and YWJ189 (*syp1*Δ::*SLA1-GFP*) were grown to mid-log phase in YEPD at 25°C. The samples were fixed for visualization of Syp1-GFP or Sla1-GFP. (C) Overexpression effect on the localization of Syp1p or Sla1p. The strains, YWJ217 (W303::*SYP1-GFP/*vector), YWJ218 (W303::*SYP1-GFP/*pGal-SLA1) , YWJ202 (W303::*SLA1-GFP/*vector) and YWJ203 (*W303*::*SLA1-GFP/*pGal-SYP1) were grown at 30°C to log phase and added 2% galactose to induce Sla1p or Syp1p overexpression for 7 hours. The samples were examined for Syp1-GFP or Sla1-GFP localization. Bars, 5 μm.

To investigate the possibility that Syp1p may physically associate with Sla1p *in vivo*, the two hybrid assay was carried out. As shown in Figure 4.9A upper panel, the full length Sla1p and different Sla1p truncations were used to test the interaction with full length Syp1p. Indeed, Syp1p demonstrated binding activity with full length Sla1p and its N-terminus (Fig. 4.9A). To further ascertain the interaction, two GST-SLA1 truncation fusion proteins, the N-terminus containing SH3 domains (SH3) and the C-terminus containing Sla1 repeat (RP), were used to precipitate Syp1-HA from the yeast cell lysates. As shown in Figure 7B, Sla1p N-terminus was able to pull down Syp1p readily (Figure 7B, lane 3) whereas the Sla1p C-terminal region was not. These results suggest that Syp1p may bind to Sla1p SH3 domains.

The interaction between Syp1p and Sla1p was further confirmed using the co-immuno-precipitation (CO-IP) assay. Wild-type cells were transformed with pGal-SLA1-HA and/or pGal- SYP1-Myc. The extracts from cell lysates were subjected to immuno-precipitation by the anti-HA and anti-Myc antibody respectively. As shown in the Fig. 4.10 lane 5, a weak Syp1-Myc band was detected. However, the Syp1-Myc was not detected in the control samples (Fig. 4.10, lane2 and 8). These results indicate that Sla1p can pull down Syp1p *in vivo*. When using anti-Myc to IP Syp1-Myc, Sla1-HA was detected in the Syp1-Myc complex (Fig. 4.10, lane 6). The Sla1-HA band was not detected in the control samples (Fig. 4.10, lane 3 and 9). These findings suggest that Syp1p and Sla1p indeed associate with each other *in vivo*.

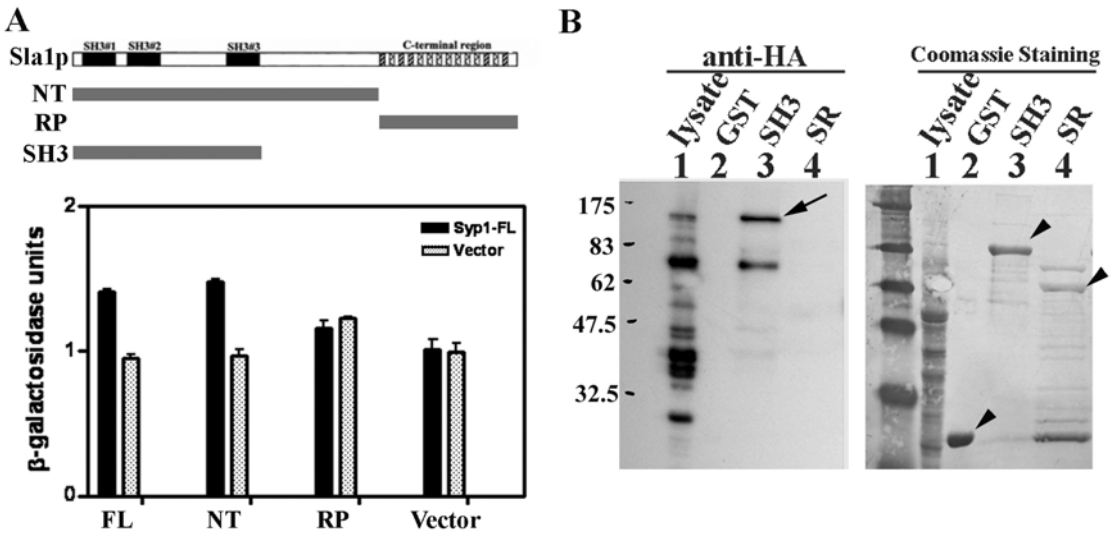


**Figure 4.9 Physical interaction between Syp1p and Sla1p**. (A) Two-hybrid interaction between pGBKT7-SYP1 and pGADT7-SLA1 full length or N-terminal/ C-terminal truncations was shown as the β-galactosidase activities. The schematic structures of Sla1p and its truncations NT, RP, SH3 are showed in the upper panel. (B) SH3 domains of Sla1p were required for Syp1p interaction by GST fusion proteins binding assay. Different Sla1p truncations (SH3 and RP as shown in A) were expressed as GST-fusion proteins and purified from bacteria. The yeast lysate was extracted from cells integrated with *SYP1-HA* (strain YMJ532). The GST-fusion proteins were incubated with yeast lysate. The precipitates were separated by gel electrophoresis, transferred to membrane, and immunoblotted with anti-HA antibody to detect Syp1p (left). After that, the membrane was stained with Coomassie blue to detect GST and GST-Sla1p fusion proteins (right). The arrow indicates the Syp1p protein pulled down by Sla1p SH3 domains. The arrow heads show the GST or GST fusion proteins.

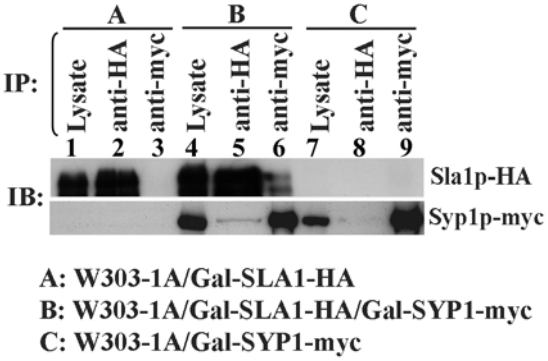


**Figure 4.10 Co-immunoprecipitation between Syp1p and Sla1p.** Equal amounts of protein extracts prepared from W303 containing *GAL1-SYP1-Myc* (YWJ221, C), *SLA1-HA* (YWJ219, A), or both (YWJ220, B), were subjected to anti-HA or anti-Myc immunoprecipitation (IP) and followed by SDS-PAGE and immunoblotting (IB).

### 4.2.3.2 Mapping binding regions on Syp1p for Sla1p

The above results showed that Syp1p is able to interact with Sla1p N-terminal region which contains three SH3 domains. Since the motifs for SH3 interaction usually contain poly-prolines (Sparks *et al.*, 1996; Mayer, 2001) , the poly-proline region in the primary sequence of Syp1p was possibly the domain to bind Sla1p. The poly-proline region is found to be located in the central region of Syp1p including residues 410-570 (Fig. 4.11A). The secondary structure of Syp1p was also analyzed by DNASTAR software. The alpha helix distribution and the hydrophilic plot were shown in Fig. 4.11B. Based on the above analyzed results, a series of Syp1p truncations tagged with HA were made for the GST-Sla1 SH3 fusion protein binding assay (Fig. 4.11C). The N-terminal region (residues 1-600) was further truncated into two parts, one containing the analyzed-alpha-helix region (residues 1-320) and the other containing the poly prolines (residues 320-600). As shown in Fig. 4.11D, the N-terminal region (residues 1-600, lane 2) could associate with Sla1p SH3 domains as strongly as full length Syp1p (lane 1) whereas the C-terminal region ( residues 600-870, lane 3) could not be precipitated by Sla1p. Further mapping of the N-terminal region showed that the residues 320-600 (Fig. 4.11E, lane 5) containing the poly prolines can interact with Sla1p very strongly whereas the residues 1-320 (Fig. 4.11E, lane 4) showed very weak binding activity. These results indicate that Syp1p possibly utilizes its poly-proline region to physically interact with Sla1p SH3 domains.

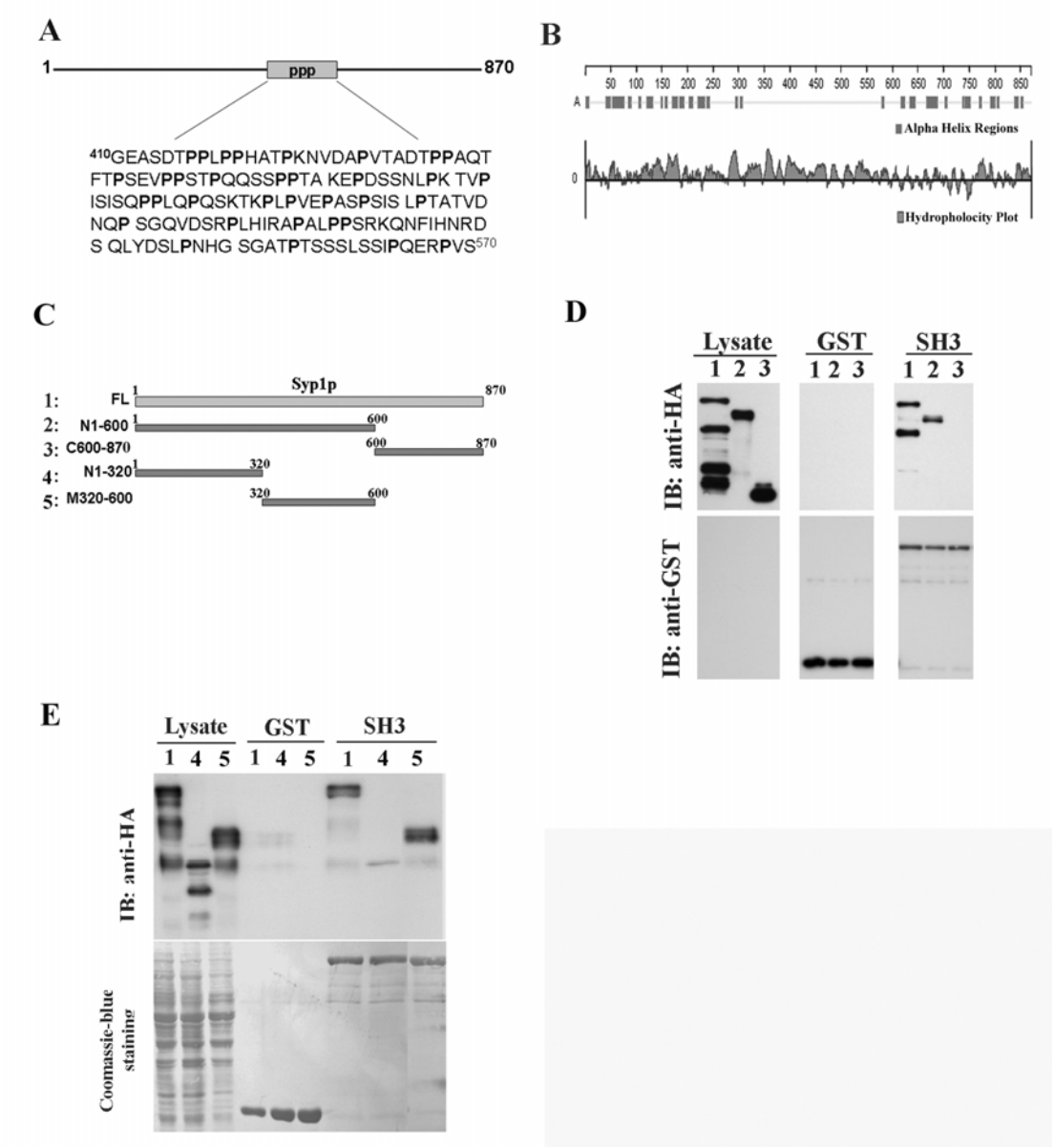


**Figure 4.11 The regions of Syp1p required for Sla1p interaction**. (A) The poly-proline region (410-570 aa) in the primary sequence of Syp1p. The proline amino acid is highlighted as the bold character "**P**". (B) The secondly structure of Syp1p analyzed by DNASTAR Protean software. The distribution of alpha helixes or hydrophilic amino acids is shown. (C) The schematic structures of Syp1p and its series truncations. The full length Syp1p and its different truncations were expressed from *GAL1* promoter. The left number 1-6 indicate the different plasmids used in the experiments below. Numbers on the top of bars indicate the amino acid positions. (D-E) Yeast lysates were extracted from different strains transformed with plasmids 1-5 respectively. The GST-SH3 fusion protein and GST alone were beads-immobilized and incubated with yeast lysates. The following binding assay procedures were the same as the one mentioned in Fig. 4.9B.

#### 4.2.3.3 No endocytosis defect in *syp1*Δ cells or cells overexpressing Syp1p

Sla1p is important for the actin-mediated endocytosis (Tang *et al.*, 2000; Warren *et al.*, 2002; Piao *et al.*, 2007). To examine whether Syp1p also plays a role in endocytosis, the *SYP1* deletion cells and Syp1p overexpressed cells were used to assay endocytic function. Uptake of the fluorescence marker Lucifer yellow (LY) was used to monitor the fluid-phase endocytosis (Dulic *et al.*, 1991). In *syp1*Δ cells, clear LY staining in the vacuoles could be observed (Fig. 4.12A). This result indicates that Syp1p was not required for the fluid-phase endocytosis. To examine whether Syp1p is required for the receptor-mediated endocytosis, Uracil uptake (Fur4p assay) was carried out (Volland *et al.*, 1994). Uracil uptake was very slow in the positive control *pan1-4* mutant which is kown to have endocytosis defect (Tang *et al.*, 1997) (Fig. 4.12B). However, both wild type and *SYP1* deletion cells had similar uracil uptake rate, although at the first time point the uptake rate of *syp1*Δ cells appeared slower (Fig. 4.12B). These results indicate that Syp1p is not required for the receptor-mediated endocytosis.

The LY uptake assay was further carried out in cells overexpressing Syp1p. The clear LY staining in the vacuoles can be observed in these cells (Fig. 4.12C), indicating that there is no endocytosis defect in cells overexpressing Syp1p. In summary, these observations imply that Syp1p is not required for endocytosis.

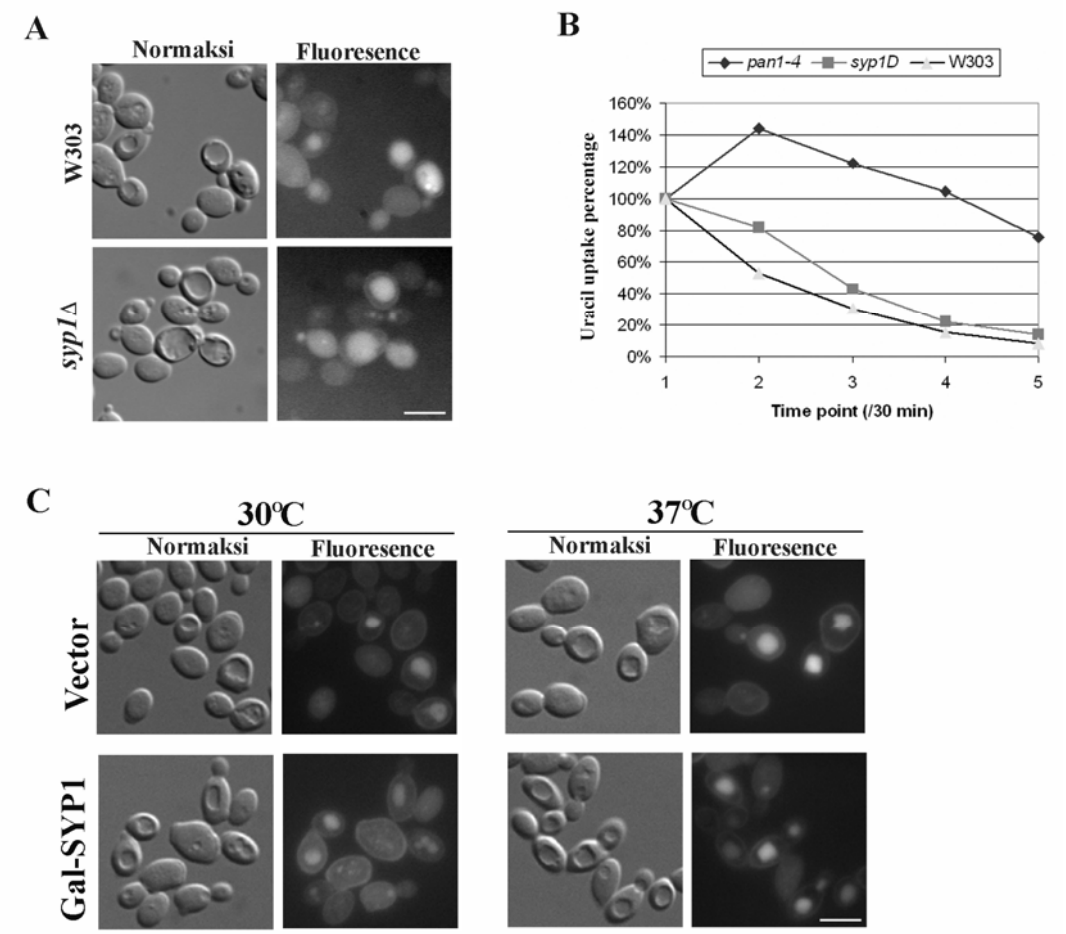


**Figure 4.12 *SYP1* deletion and overexpression did not cause endocytosis defects**. (A) LY uptake in wild-type (W303) and *syp1*Δ (YMC515) cells. The cells were grown at 30°C to log phase. After 2 h of incubation with LY, cells were examined under a microscope with fluorescein isothiocyanate and Nomarski optics. (B) Fur4p assay in the W303 (YWJ100), *syp1*Δ (YWJ101) and *pan1-4* (YWJ99) cells. Uracil uptake (permease activity) was measured at 37°C at various time points after the addition of cycloheximide. The results are expressed as a percentage of the initial activity. (C) LY uptake in YWJ63 (W303/vector) and YWJ89 (W303/Gal-*SYP1*) cells. The Strains were grown at 30°C to log phase and 2% galactose was added to induce Syp1p overexpression for 7 hours. After 2 h of incubation with LY at 25°C or 37°C, cells were examined under a microscope with fluorescein isothiocyanate and Nomarski optics. Bars, 5μm.

## 4.3 Discussion

Since its identification as a multi-copy suppressor of the *PFY1* deletion mutant (Marcoux *et al.*, 2000), the exact function of Syp1p in actin cytoskeleton has remained largely unknown. In this study, the functional relationship between Syp1p and actin cytoskeleton was investigated. Syp1p was found to have functional relationships with profilin and Bni1p. The localization of Syp1p was also revealed to be tightly related to actin cytoskeleton. Additionally, Syp1p was shown to be able to physically interact with Sla1p.

### 4.3.1 Evidence for Syp1p functioning in actin cytoskeleton organization

Although *syp1Δ* cells had no significant alterations in the organization or the function of the actin cytoskeleton, several lines of evidence suggest that Syp1p functions in actin cytoskeleton organization. Firstly, overexpressing Syp1p partially suppresses the deficient phenotypes of *bni1*Δ and *pfy1*Δ mutants. These suppressions might be due to the partial restoration of proper actin cytoskeleton organization. Secondly, overexpressing Syp1p partially depolarizes the actin patches in wild-type cells. Although actin patches were concentrated in the elongated buds of the cells overexpressing Syp1p, numerous actin patches were also found in mother cells. These findings suggest that Syp1p plays a role in actin patch organization or its regulation. Thirdly, Syp1p colocalizes with the actin cytoskeleton throughout most of the cell cycle. Additionally, the polarized localization of Syp1p is highly dependent on the integrity of actin cytoskeleton. Syp1p loses its polarized localization in the mutants of genes which are required for the actin cytoskeleton organization, such as *BNI1*, *PFY1*, *SLA1*, and *ACT1*. These observations

indicate that the function of Syp1p is linked to the actin cytoskeleton. Fourthly, Syp1p physically interacts with Sla1p *in vitro* and *in vivo*. Syp1p was found to interact with Slap directly in the two hybrid assay and can be precipitated from cell extracts by Sla1p SH3 domain. Finally, the N-terminal region of Syp1p is homologous with the domains whose functions are related to actin cytoskeleton or trafficking (Fig. 4.13 and table 3), such as Tesp/Cip4p homology domain (Lippincott and Li, 2000; Chitu and Stanley, 2007), Sec7p domain (Zeghouf *et al.*, 2005), Kinesin-like domain (Endow, 2003) and Sla2p domain (Holtzman *et al.*, 1993; Engqvist-Goldstein *et al.*, 1999). In summary, the functions of Syp1p are related to actin cytoskeleton organization.

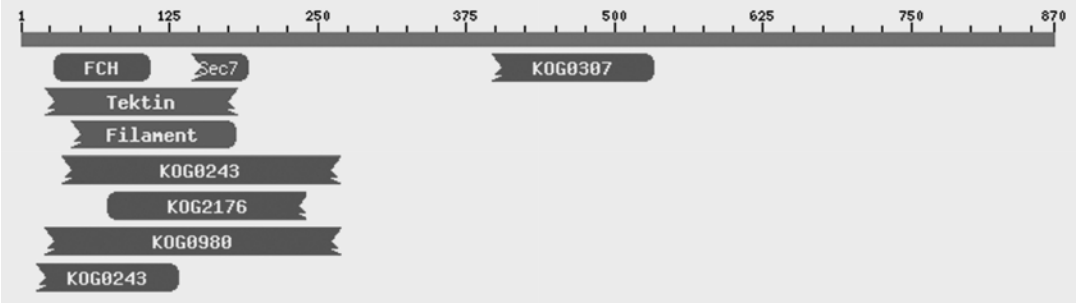


**Figure 4.13 The conserved domains in Syp1p through searching the proteins databases**. The conserved domains on the Syp1p were searched using the program in NCBI website for the conserved domains search against SMART, Pfam and KOG databases under the threshold of E-value below 10. The matching domains which have more than 10% homology with Syp1p primary sequences and function in cytoskeleton or trafficking are shown as the bars and listed in Table 3. The numbers above the scale present the length of amino acid sequence.

**Table 3. The homologous domains with Syp1p through searching against databases**

| | Homologous domains | Pct. Aligned | Match region(aa) | E-value |
|---|---|---|---|---|
| 1 | smart00055, Fes/CIP4 homology domain, cytoskeleton | 67 | 28-107 | 0.051 |
| 2 | smart00222, Sec7, Sec7 domain, trafficking | 22 | 145-191 | 2.6 |
| 3 | pfam03148, Tektin, Tektin family, cytoskeletal proteins | 40 | 20-182 | 0.88 |
| 4 | pfam00038, Filament, Intermediate filament protein | 40 | 42-180 | 1.8 |
| 5 | KOG0243, Kinesin-like protein , cytoskeleton protein | 21 | 35-268 | 0.0009 |
| 6 | KOG2176, Exocyst complex, subunit SEC15, trafficking | 23 | 74-242 | 0.3 |
| 7 | KOG0307, Vesicle coat complex COPII, trafficking | 12.9 | 397-532 | 0.38 |
| 8 | KOG0980, Actin-binding protein SLA2, cytoskeleton | 27 | 20-269 | 0.92 |
| 9 | KOG0243, Kinesin-like protein, cytoskeleton | 11.8 | 13-132 | 1.6 |

### 4.3.2 Functional relationship between Syp1p and profilin/ Bni1p

Syp1p may play a role in actin organization through regulation of profilin and Bni1p. Firstly, the localization of Syp1p is similar to many polarity proteins such as polarisome components, Bni1p, Spa2 and Bud6p (Madden and Snyder, 1998; Sheu *et al.*, 1998; Ozaki-Kuroda *et al.*, 2001). All of them first appear at the incipient bud site, then localize to the bud tip during bud growth and finally to the bud neck again during cytokinesis. Secondly, overexpressing Syp1p suppresses the ts phenotype and actin patches depolarization of the *pfy1*Δ and *bni1*Δ mutants.

Bni1p/profilin stimulates actin cable assembly. Actin cables are responsible for polarization of cortical patches. Therefore, the restoration of acitn patch polarity by Syp1p overexpression is possibly due to enhancing cable formation. However, in both *pfy1*Δ and *bni1*Δ mutants with Syp1p overexpression, the actin cable is still invisible. It is possible that cables could be partially restored but they are difficult to be observed by fluorescene microscopy.

The restoration of actin patch polarization by Syp1p overexpression in the *pfy1*Δ and *bni1*Δ mutants could also be due to other mechanisms that bypass the actin cable formation. For example, overexpressing Rho2p, a GTPase which is not required for formin activity, can restore the polarity of profilin deletion mutant by bypassing the need for actin cables (Marcoux *et al.*, 2000). Another example is that Sec3p, a protein that functions in exocytosis and does not directly regulate actin, suppressed the profilin mutation *pfy1-111* when overexpressed (Finger and Novick, 1997). Therefore, the mechanism of the suppression of *bni1*Δ and *pfy1*Δ mutants by Syp1p overexpression might be similar as the one of Rho2p or Sec3p.

### 4.3.3 Functional relationship between Syp1p and Sla1p

Sla1p plays an important role in actin patch-mediated endocytosis (Holtzman *et al.*, 1993; Warren *et al.*, 2002). This study has demonstrated that Syp1p colocalizes with Sla1p and its polarized localization is dependent on Sla1p. Syp1p is also discovered to interact with Sla1p SH3 domain. It was suspected that Syp1p might also be involved in actin-mediated endocytosis. However, although Syp1p overexpression depolarizes the localization of Sla1p, there is no endocytic defect found in the cells overexpressing

Syp1p. These results suggest that Syp1p might not be required for the function or regulation of actin-mediated endocytosis.

However, Syp1p may be involved in the Sla1p-regulated actin organization. Sla1p forms a complex with Arp2/3 activators, such as Pan1p and Las17p to regulate actin patch organization (Tang *et al.*, 2000; Warren *et al.*, 2002). It has been reported that the Sla1p SH3 domain inhibits the actin-polymerization activity of Las17p (Rodal *et al.*, 2003). As the poly-proline region of Syp1p can interact with the Sla1p SH3 domain, Syp1p might play a role in the regulation of Las17p-mediated actin assembly through its association with Sla1p. The interaction between Syp1p and Sla1p might release the inhibition of Las17p by Sla1p. This hypothesis may explain why overexpressing Syp1p results in depolarized actin patches in the mother cells. It is worthwhile to test the actin assembly activity of Las17p regulated by Syp1p and Sla1p *in vitro* and *in vivo*.

The random budding phenotype caused by Syp1p overexpression suggests that Syp1p may cooperate with Sla1p or other actin-associated proteins to achieve the bipolar bud site selection. Although the mechanism is still unknown, many actin-associated proteins, especially the proteins for regulating actin patch assembly, such as Pan1p, Sla1p and Abp1p, cause random bud site selection in the diploid cells rather than the preferential bipolar budding pattern (Tang and Cai, 1996; Yang et al., 1997). The wild type strain used in this study, W303, exhibits a higher ratio of bipolar budding pattern (Voth et al., 2005); and overexpressing Syp1p results in higher percentage of random bud site selection , which is similar to the phenotype of some mutants of actin cytoskeleton-associated proteins. These results suggest that Syp1p might play a role in bipolar bud site selection through its interaction with actin patch-associated proteins.

# Chapter 5

# Functional Relationship between Syp1p

# And the septin cytoskeleton

## 5.1 Introduction

Syp1p was first identified as a high copy suppressor of *pfy1*Δ mutant (Marcoux *et al.*, 2000). However, several observations suggest that Syp1p has other function in addition to its role in actin cytoskeleton. Firstly, the localization pattern of Syp1p is different from that of actin cytoskeleton (setion 4.2.2, Fig. 4.6). Throughout most stages of the cell cycle, a fraction of Syp1p always stays in the bud neck. Especially in the medium-budded cell, most of actin patches localize to the bud whereas a portion of Syp1p still localize at the bud neck. These findings suggest that Syp1p has some function in the bud neck. Additionally, overexpressing Syp1p results in the elongated bud phenotype, similar to those proteins that are involved in the organization of septins (Lippincott and Li, 1998a; Longtine *et al.*, 1998; Gladfelter *et al.*, 2004; Gladfelter *et al.*, 2005). Therefore, the functional relationship between Syp1p and septins was investigated in this study.

## 5.2 Results

### 5.2.1 Syp1p overexpression causes Septin disorganization

First of all, the hypothesis that the elongated bud phenotype induced by Syp1p overproduction could be attributed to septin abnormalities was examined. The strain integrated with *CDC12-GFP* was transformed with GAL1-SYP1-HA plasmid. After 7 hours of galactose induction at 30$^{o}$C, elongated buds became evident in some population of cells (Fig. 5.1A, arrow heads). Quantitative analysis showed that 46% of single nucleus (excluding the ones with very small buds) and 23% of two nuclei budded cells had elongated bud. These ratios did not change greatly after further incubation for a few

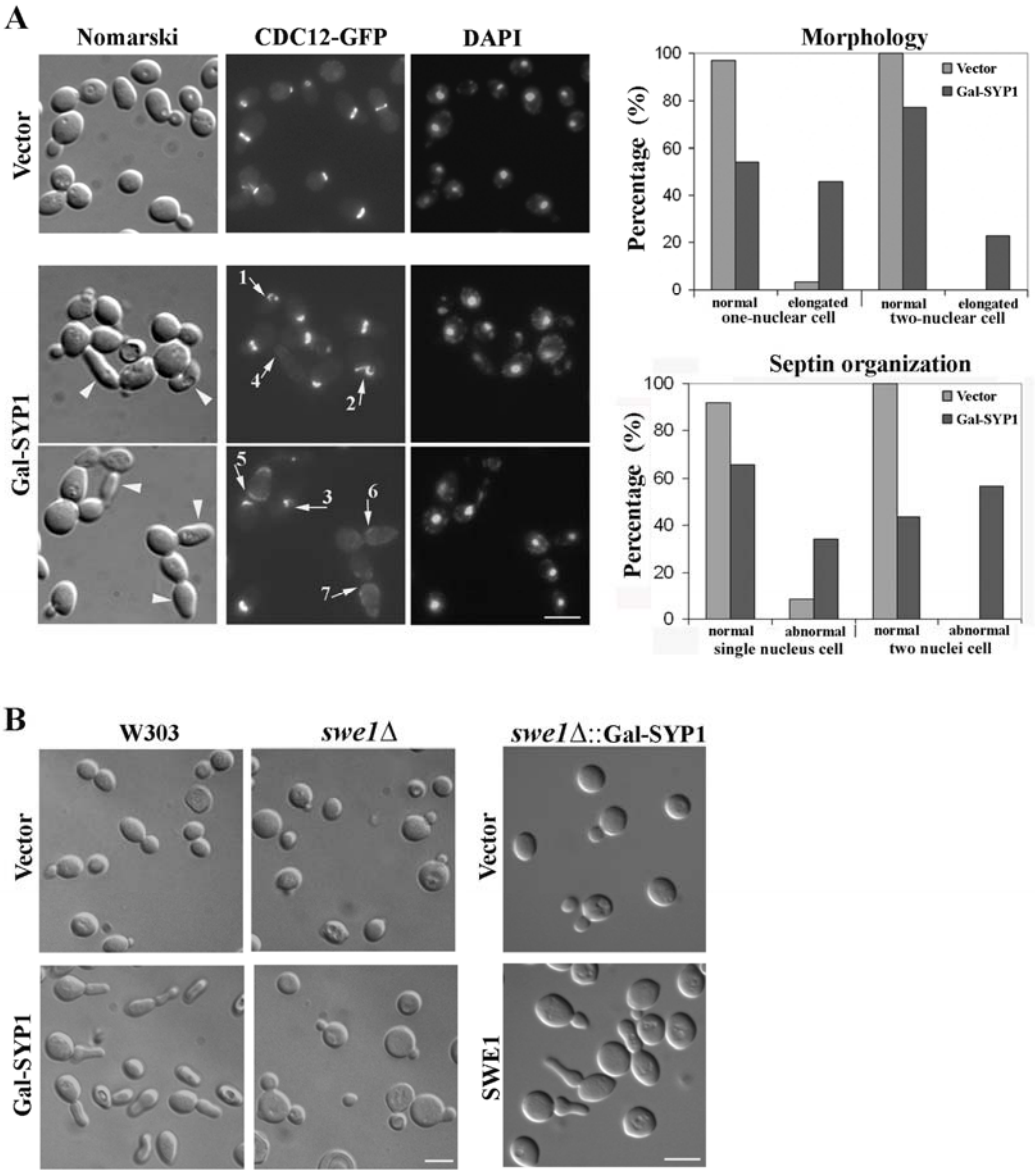


**Figure 5.1 Septin disorganization caused by Syp1p overexpression**. (A) Wild-type cell containing *CDC12-GFP* (YMC517) was transformed with pGal-SYP1-HA or the vector. The resulting strains, YMC518 (vector) and YMC519 (pGal-SYP1-HA), were cultured in raffinose at 30°C to log phase followed by addition of galactose to 2% to induce Syp1p expression. After 7 h, samples were taken, sonicated and prepared for microscopy. The elongated buds are marked by arrow heads and disorganized septin structures by arrows. The quantitative data of cell morphology and septin organization in the budded cells are shown in the right panels. (B) Left. YMC520 (W303::vector), YMC521 (W303:: *Gal-SYP1-HA*), YMC522 (*swe1Δ*::vector), YMC523 (*swe1Δ*::*Gal-SYP1-HA*) were induced for Syp1p overexpression for 7 h as stated above. The samples were taken and examined for morphology. Right. The *swe1*Δ strain integrated with Gal-SYP1 transformed with vector (YMC524) or *SWE1* (YMC525) were cultured and induced for Syp1p overexpression for 7 h and examined similarly as stated above. Bars, 5 μm.

more hours in galactose (data not shown). Interestingly, many Syp1p-overexpressing cells exhibited a septin organization defect of one kind or another (Fig. 5.1A, arrows). Some cells had deformed septin filaments at the bud neck (Fig. 5.1A, arrow 1-3); others had their septin filaments diffused to the cell membrane (Fig. 5.1A, arrow 4-7) and still others had little or no septin filaments visible. Overall, about 34% of single nucleus and 57% of two nuclear budded cells displayed abnormal septin structures. In comparison, similar septin abnormalities were rarely found in the vector-transformed control cells. This experiment indicates that Syp1p overexpression can disrupt the normal septin organization and the septin defects may be the cause of the elongated bud phenotype exhibited by some of these cells. Same results were also obtained using Cdc10-GFP as a septin filament marker (data not shown).

It has been reported that septin defects induce bud elongation through the Swe1p-dependent cell cycle delay (Longtine *et al.*, 2000; Lew, 2003). To investigate whether the elongated bud phenotype in the Syp1p overexpression cells is dependent on Swe1p, the same experiment was carried out in the *swe1*Δ mutant. As shown in Figure 5.1B, deletion of *SWE1* effectively suppressed the elongated-bud phenotype caused by overexpression of Syp1p (Fig. 5.1B), and reintroducing the *SWE1* gene back into the mutant restored the phenotype (Fig. 5.1B). This result confirms the bud elongation caused by Syp1p overexpression to be Swe1p-dependent, and thereby supports the suggestion that Syp1p may function to affect septin organization *in vivo*.

Cells experiencing Syp1p overexpression over a more prolonged period of time also exhibited cytokinesis defects. When overnight cultures in galactose were diluted into fresh galactose medium and allowed to continue the Syp1p expression for another 7

h, about 40% of cells became multi-budded (Fig. 5.2A). Accordingly, the septin organization was also abnormal in these multi-budded cells (Fig. 5.2A, arrows).

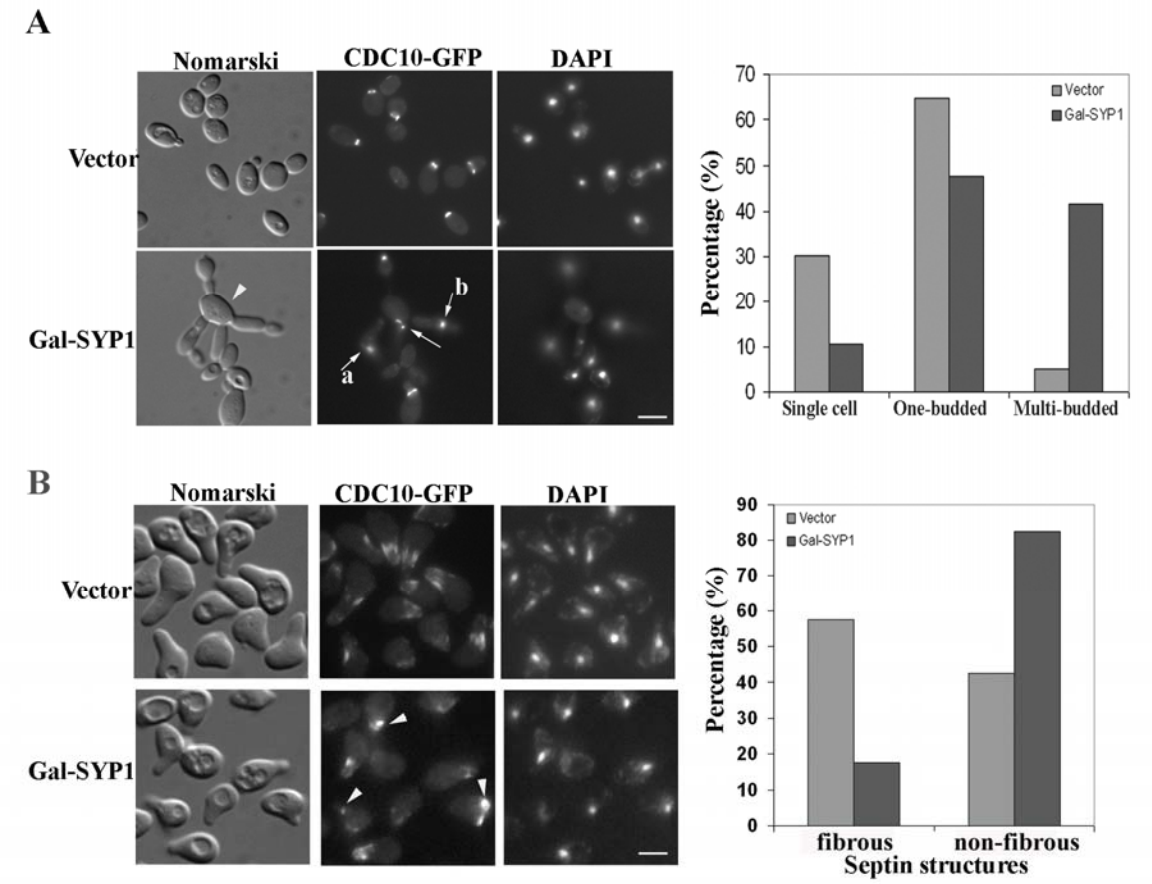


**Figure 5.2 Cytokinesis defect and septin disorganization in α-factor treated cells caused by Syp1p overexpression**. (A) Wild type cells containing *CDC10-GFP* was integrated with vector or Gal-SYP1-HA in the *ura3* locus, and the respective strains (YMC526 and YMC527) were cultured overnight at 30°C in galactose medium followed by dilution into fresh galactose medium and incubated for another 7 hr. The arrow head marks a multi-budded cell. The arrows show the septin defect in the multi-budded cells. The quantitative data of the multi-budded cells are shown in graphs in the right panel. (B) The strains described in (A) were cultured at 30°C to log phase and induced by galactose for 3 h followed by addition of α-factor for 2 h. The samples were taken for examination by microscopy. The arrow heads show the septin defect in the cell overexpressed Syp1p. The quantitative data of septin disorganization are shown in graphs in the right panel. Bars, 5 μm.

## Chapter 5 Functional Relationship between Syp1p and the septin cytoskeleton

In addition to its role in vegetative growth, the septin cytoskeleton has also been reported to take part in the mating process (Giot and Konopka, 1997). During mating pheromone treatment, the yeast cells form a projection termed "shmoo", with the septins rearranged into arrays along the projection axis (Longtine *et al.*, 1998). To examine whether overexpression of Syp1p would affect septin organization during shmoo formation, the cells were induced by galactose for 3 h before addition of α factor into the same medium. After another 2 h of incubation, remarkable septin organization defects were observed in these cells. The percentage of cells with typical fibrous septin structures was decreased to 18% from 57% in the control cells (Fig. 5.2B). The majority of the abnormal septin structures were similar to those found in the Syp1p overexpression cells without α factor treatment shown in Figure 5.1A, except that more pronounced septin aggregations were evident in this case (Fig. 5.2B, arrow heads).

Furthermore, synthetic effects between septin mutants and Syp1p overexpression were observed. Syp1p overexpression caused extraordinarily long buds in the *cdc10-1* mutant at 25$^{o}$C (Fig. 5.3, arrows), accompanied by severe septin disorganizations. There were no clear septin rings at the bud neck. Instead, the septins were present as clumps with irregular locations in these cells (Fig. 5.3, arrow head). At 31$^{o}$C, which is a permissive temperature for the *cdc10-1* mutant, Syp1p overexpression caused cell death (Fig. 5.3, right). Same synthetic effects were also observed between Syp1p overexpression and another septin mutant *cdc3* (data not shown). Taken together, these findings confirm that overexpression of Syp1p can lead to severe defects in septin organization and suggest that Syp1p is functionally related to septins in yeast.

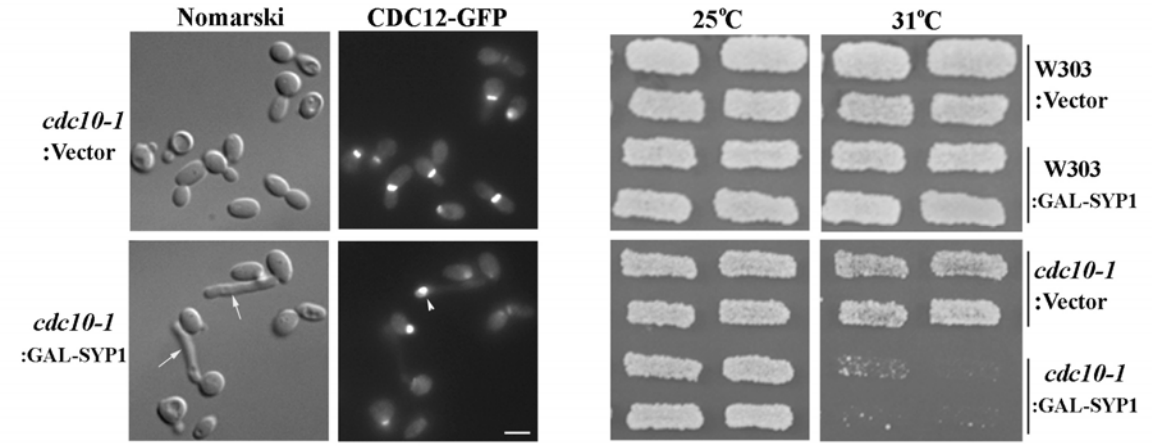


**Figure 5.3 Synthetic lethality between *cdc10* and Syp1p overexpression**. Left. The septin mutant *cdc10-1* (YEF473-1619) containing *CDC12-GFP* was integrated with vector or Gal-SYP1-HA to generate YMC528 and YMC529 respectively. The strains were cultured at 25°C to log phase and induced with galactose for 6 h. The samples were taken for examination by microscopy. The arrows indicate the elongated bud cells and arrowheads show the septin defect in the elongated bud cells. Right. YMC526 (W303::vector), YMC527 (W303::Gal-SYP1), YMC528 and YMC529 were patched on a plate and allowed to grow at 25°C for 2 days and followed by replica-plating onto a fresh plate and incubated at 31°C for 2 days. Bar, 5 μm.

### 5.2.2 Abnormal septin structures in HU-arrested *syp1*Δ cells

As reported previously (Marcoux *et al.*, 2000), deletion of the *SYP1* gene generates no obvious defects in cell growth and actin organization. In this study, *syp1*Δ cells also appeared to have normal septin structure in standard YEPD medium. However, *syp1*Δ cells arrested with the DNA synthesis inhibitor hydroxyurea (HU) displayed much more elongated buds than wild type cells (Fig. 5.4A, lower left). The mutant cells also exhibited a septin morphology different from that of wild type cells. Their septin rings at the neck were generally bigger (Fig. 5.4A, lower right). Upon careful measurement, the diameter of the septin ring at the mother-daughter neck of *syp1Δ* cells was 1.9 +/- 0.3 μm,

compared with 1.6 +/- 0.2 μm in the parental wild type cells (n>100 for each strain, Fig. 5.4B). This finding, together with the elongated bud morphology, suggests that the septin ring in the HU-arrested *syp1Δ* mutant may be functionally and structurally abnormal.

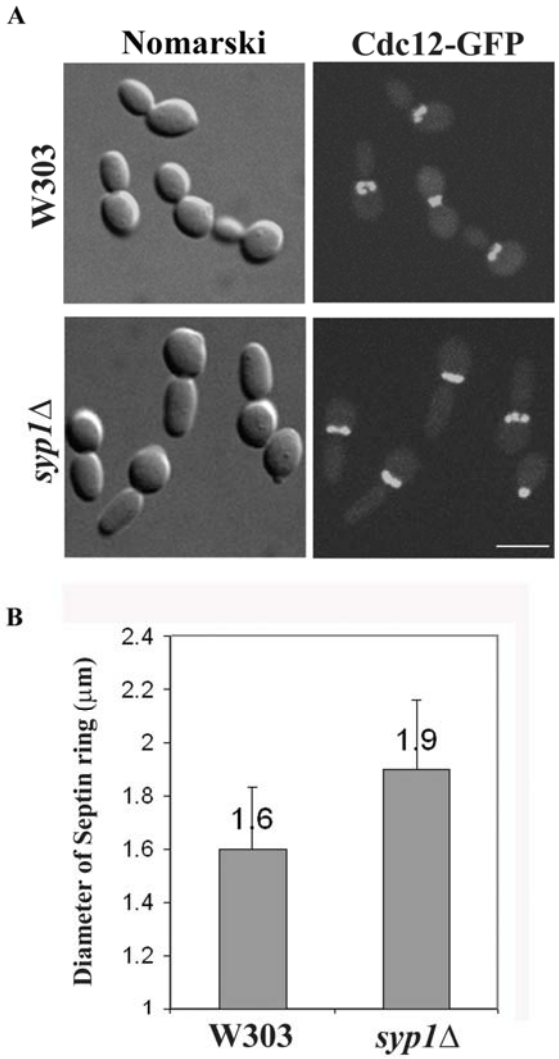


**Figure 5.4 Septin abnormality of the *syp1*Δ cells upon HU treatment**. (A) YMC517 (W303::*CDC12-GFP*) and YMC516 (*syp1*Δ::*CDC12-GFP*) were cultured to log phase and were treated with HU for 3 hr. The samples were collected to examine cell morphology and septin structures. Bars, 5 μm. (B) The Graph showing the diameter of septin rings in wild type and *syp1*Δ cells as measured by the MetaMorph software.

### 5.2.3 Association of Syp1p with septins

Although Syp1p localizes to the bud neck, its localization pattern and that of septins have not been directly compared. The localization patterns of Syp1-CFP and Cdc12-YFP in live cells were therefore examined. The two markers were found to be colocalized with each other in the cells of different cell cycle stages (Fig. 5.5A). For example, both proteins localized to the incipient bud site in unbudded cells (Fig. 5.5A, arrow 1), stayed at the mother-bud neck in small budded (Fig. 5.5A, arrow 2) and large budded cells (Fig. 5.5A, arrow 3), and remained faintly at the division sites on both mother and daughter cells after cell separation (Fig. 5.5A, arrow 4). However, the neck localization of Syp1p-CFP was diminished in large budded cells in comparison with Cdc12p-YFP (for example, Fig. 5.5A, arrow 3). When the two markers were superimposed, Syp1p-CFP was found to be localized at the exterior of the septin ring on the mother side of the collar. These results suggest that the cellular localization of Syp1p closely coincides with that of septins.

As shown in Figure 5.4A, Syp1p was not required for septins to localize to the neck region. The cellular localization of Syp1p, however, was found to be strictly dependent on septins. At the permissive temperature, the *cdc10-1* mutant grew well with normal cell morphology. Under this condition, both Syp1-CFP and Cdc12-GFP displayed normal pattern of localization similar to the one of wild type strain (Fig. 5.5B, left). At the non-permissive temperature of 37$^{o}$C, on the other hand, septins became completely diffused all over the cell (Fig. 5.5B, right), whereas Syp1p similarly lost the neck localization and was diffused as well.

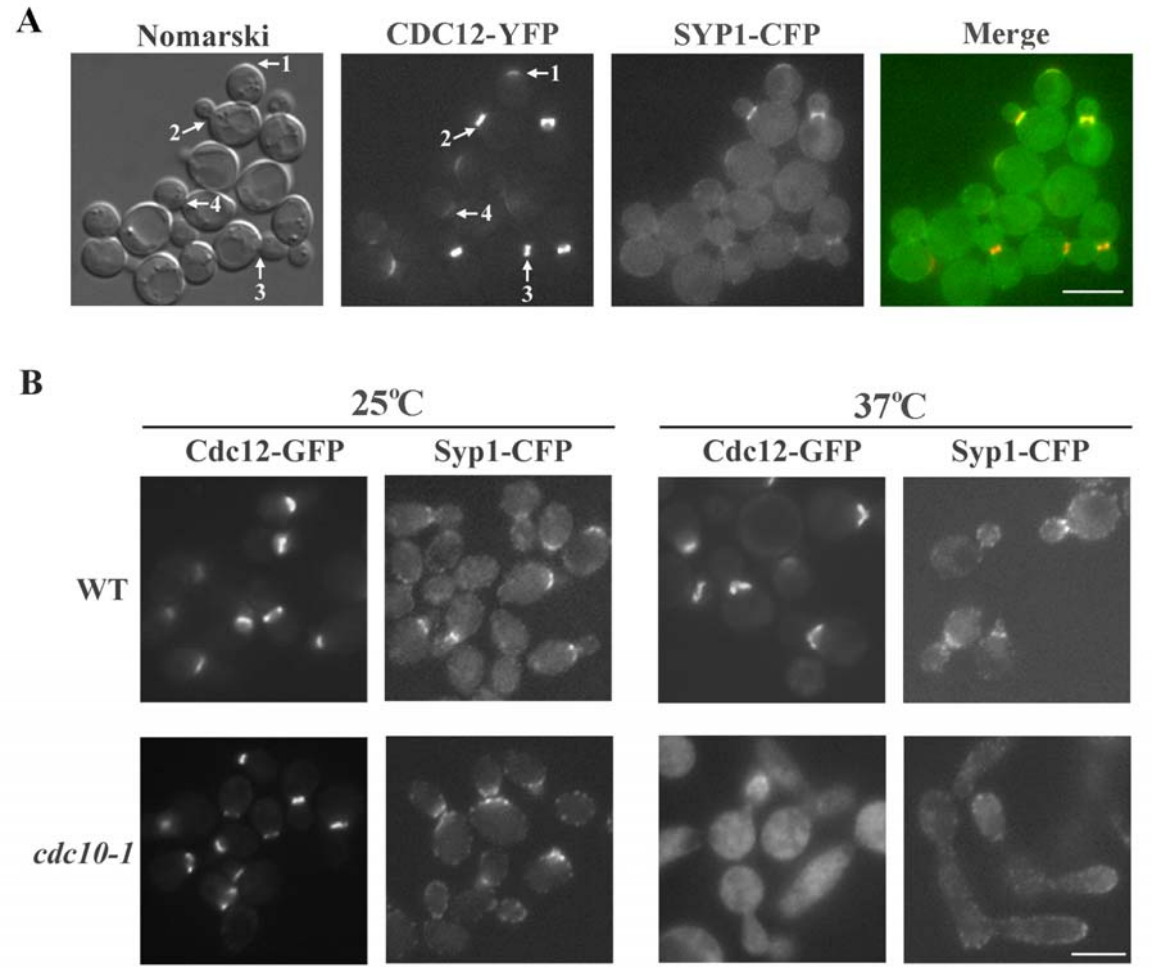


**Figure 5.5 Co-localization between Syp1p and septins**. (A) W303 strain integrated with SYP1-CFP and CDC12-YFP (YMC530) was examined for Syp1-CFP and Cdc12-YFP localizations. The arrows and numbers show the positions of the proteins at different cell cycle stages. (B) YMC517 (WT::*CDC12*-GFP), YMC531 (*cdc10-1*:: *CDC12*-GFP), YMC534 (WT::*SYP1*-CFP) and YMC535 (*cdc10-1*:: *SYP1*-CFP) was cultured at 25°C to log phase and one half of the culture was shifted to 37°C and the other half remained to be incubated at 25°C. After 5 h, the cells were collected and fixed for visualization of Syp1-CFP and Cdc12-GFP. Bars, 5 μm.

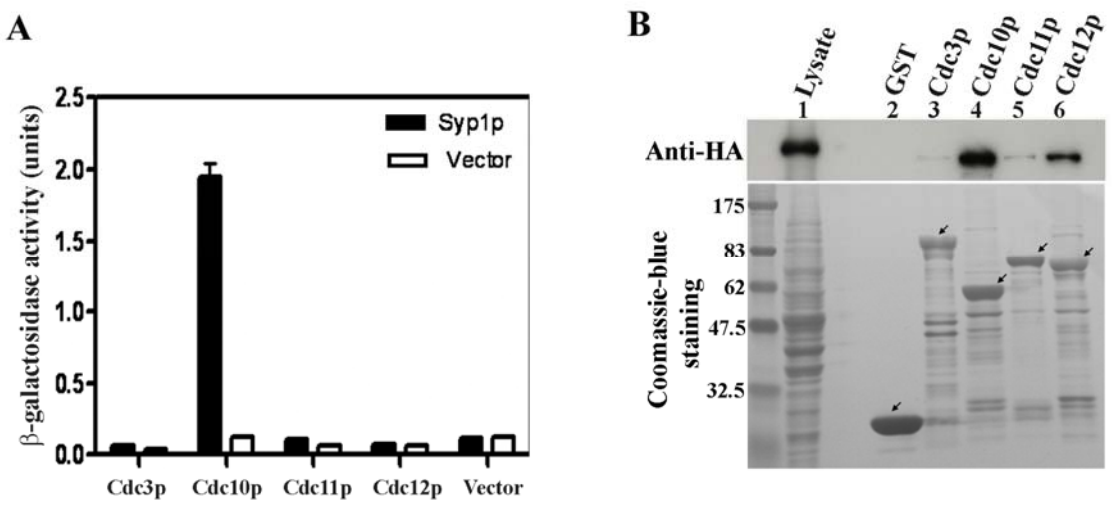


**Figure 5.6 Physical interaction between Syp1p and septins**. (A) Two-hybrid interaction between Syp1p and septins shown as the β-galactosidase activities. (B) Different septin components were expressed as GST-fusion proteins and purified from bacteria. The yeast lysate was prepared from the cell integrated with SYP1-HA (YMC532). The GST fusions were beads-immobilized and incubated with yeast lysate. The precipitates were separated by gel electrophoresis, transferred to membrane, and immunoblotted with anti-HA antibody to detect Syp1p (upper). After that, the membrane was stained with Coomassie blue to detect GST and GST-septin fusion proteins (lower). The arrows indicate different GST-septin fusion proteins.

These results suggest that Syp1p may physically associate with septins *in vivo*. To investigate this possibility, the two hybrid assay was firstly used to examine the interactions of Syp1p with different septin subunits. Indeed, Syp1p demonstrated a clear binding activity with Cdc10p (Fig. 5.6A). To further ascertain the interaction, GST-fusion protein pull-down assay was carried out to precipitate Syp1p-HA from the yeast cell lysates. As shown in Figure 5.6B, Cdc10p was able to pull down Syp1p readily (Fig. 5.6B, lane 4). Cdc12p could also pull down Syp1p in this assay, albeit somewhat less efficiently than Cdc10p (Fig. 5.6B, lane 6). Longer exposure revealed that a small

amount of Syp1p was also present in the binding reactions of Cdc3p and Cdc11p, but not in that of the GST control. These results suggest that Syp1p may bind to the septin filaments at a region involving Cdc10p as a major part of it.

### 5.2.4 Dynamic localization of Syp1p in live cells

To better understand the function of Syp1p in septins, the dynamic behavior of Syp1-GFP in live cells was studied using time-lapse fluorescent microscopy. In the early cell cycle stage, Syp1-GFP appeared at the incipient bud site about 8 minutes before bud emergence (Fig. 5.7A, arrows). After bud emergence, it stayed on as a ring at the base of the bud (Fig. 5.7A and B, arrow heads). As the bud grew bigger, a portion of Syp1-GFP started to appear on the cortex of the bud, while the signals at the bud neck were fading away and eventually disappeared completely (Fig. 5.7C, frame 8, arrow). About 16 minutes later, some Syp1-GFP signals began to congregate to the bud neck (Fig. 5.7C, frame 12, arrow head). This pattern remained until the completion of cytokinesis (Fig. 5.7C, frame 15). After cell division, Syp1-GFP re-appeared at the incipient bud site in both mother and daughter cells as the next cell cycle initiated (Fig. 5.7C, frame 16). Therefore, the dynamic behavior of Syp1p in live cells correlates very well with that of septins.

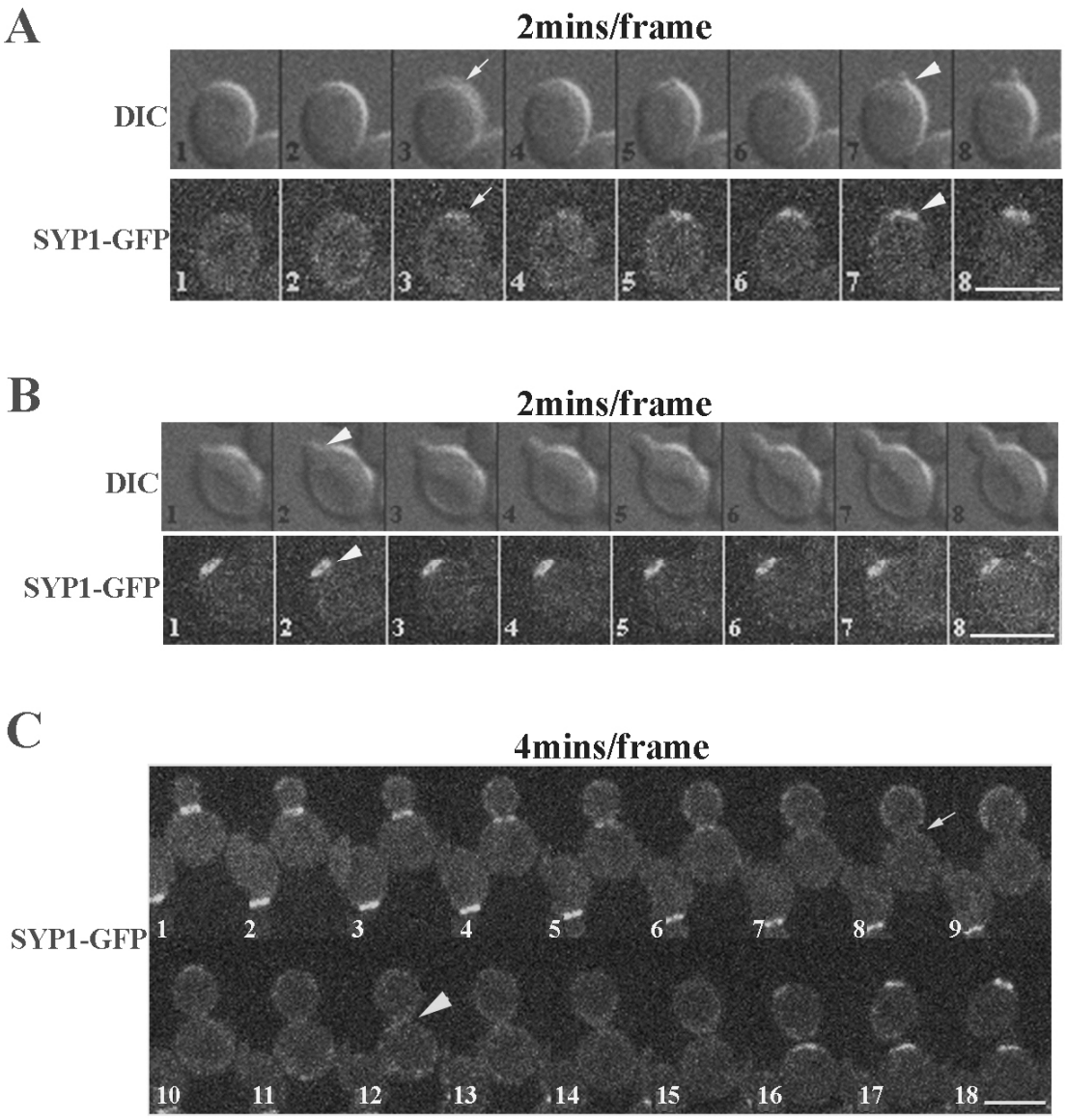


**Figure 5.7 Dynamic localization of Syp1-GFP during the cell cycle.** (A-B) Time-lapse fluorescence images of Syp1-GFP during and after bud emergence. The images were taken at 2-min intervals. The strain was YMC533. The arrows in (A) show the first appearance of Syp1-GFP at the incipient bud site. The arrowheads indicate the base of the buds. (C) Time-lapse fluorescence images of Syp1-GFP comprising the late cell cycle stages and the early stages of the next cycle. The images were taken at an interval of 4 min. YMC533 was prepared as described above. The arrow indicates the disappearance of Syp1-GFP from the neck. The arrowhead shows the reappearance of Syp1-GFP. Bars, 5 μm.

### 5.2.5 The effects of *SYP1* deletion on septin dynamics

To investigate the possible roles of Syp1p in the regulation of septin organization, the septin dynamics in *syp1*Δ cells were analyzed. Wild type and *syp1*Δ cells carrying locus-integrated CDC12-GFP were examined with time-lapse microscopy. As shown in Figure 5.8A, Cdc12-GFP first appeared in both the wild type and the *syp1*Δ cells as a hazy, irregularly shaped patch at the incipient bud site (Fig. 5.8A, arrows), which took about 4 min in the wild type to transform into a complete septin ring (Fig. 5.8A, upper, arrow head). On the other hand, the same process took nearly twice as long in the *syp1*Δ cell (Fig. 5.8A, lower, arrow head). Statistically, the average time needed for formation of a complete ring in *syp1*Δ cells (n= 21) was 8 ± 2 minutes, compared with only 5 ± 1 minutes in the wild type cells (n= 33). After the septin ring formation, the ring stayed in the mother-bud neck until its disassembly. The time was calculated from the point of ring formation to the point when the septin ring started to decrease in intensity (start of septin disassembly), and it was about 75 min in both wild type and *syp1*Δ cells (n>10 for each strain). Then the time from the start of septin disassembly to septin disappearance in either the mother or the daughter side of the neck was defined as septin disassembly time. It was found that the septin disassembly time at the daughter side was significantly longer in *syp1*Δ cells than that in wild type cells. In the wild type cell, the septin disassembly time at the mother side was about 20 min (Fig. 5.8B, upper, frame 1 through frame 10, arrowhead), while it was 28 min at the daughter side (Fig. 5.8B, upper, frame 1 through frame 14, arrowhead). In the *syp1*Δ cell, the mother side septin disassembly time was about 22 min, close to that of wild type (Fig. 5.8B, lower, frame 1 through frame 11,

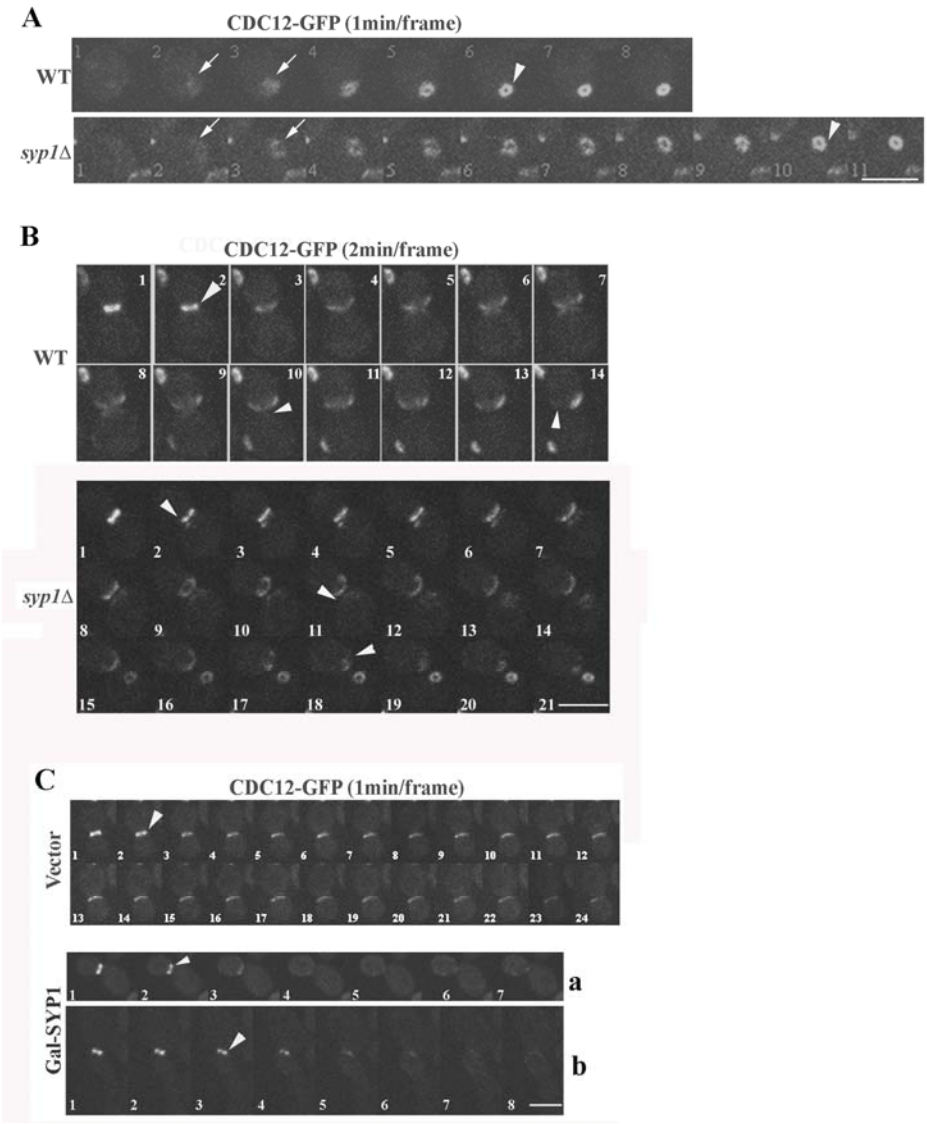


**Figure 5.8 Abnormal septin dynamics in *syp1*Δ cells and cells overexpressing Syp1p.** YMC517 (WT) and YMC516 (*syp1*Δ) containing *CDC12-GFP* were observed for live cell septin dynamics. (A) The images were taken at an interval of 1 min. The arrows indicate the nascent septin structures appearing at the incipient bud sites. The arrowheads mark the point when a complete septin ring was formed. (B) The images were taken at an interval of 2 min. The arrowheads in frame 2 mark the point when the septin ring started to decrease in intensity. The arrowheads in frame 10 and 14 of the wild type cell, and in frame 11 and 18 of the mutant, mark the point when the old septins disappeared in mother and daughter cells, respectively. (C) The images were taken at an interval of 1 min. YMC518 (vector) and YMC519 (Gal-SYP1) containing CDC12-GFP were induced for Syp1p expression by galactose for 3 h, before being examined by microscopy. The arrowheads indicate the point when septin rings begin to disassemble in the vector-containing (upper) and the GAL-SYP1 containing (lower) cells. Two representative GAL-SYP1 containing cells were shown: normal looking (a) and with an elongated bud (b). Bars, 5 μm.

arrowhead). However, the disassembly time in the daughter side was 36 min (Fig. 5.8B, lower, frame 1 through frame 18, arrowhead). The statistical data compiled from 40 wild type cells and 60 *syp1*Δ cells are consistent with the conclusion that the average time required for septin disassembly at the daughter side of the cell is about 10 minutes longer in *syp1*Δ cells (42 ± 13 minutes) than in wild type (32 ± 12 minutes). The mutant, nevertheless, had a similar time frame as the wild type for disassembly of the septin ring at the mother side of the neck, which is usually much fainter in the first place.

The above observation suggests that Syp1p may be required for septin disassembly in the late stage of cell cycle. If this was the case, one could expect to see accelerated septin disassembly in cells overexpressing Syp1p. To put this possibility to a test, the Cdc12-GFP marker was followed in live cells that contained Gal-SYP1. Wild type cells undergoing galactose shift routinely have a longer time frame of septin disassembly than in glucose. Whether this is due to a cell cycle response to galactose pulse or to other metabolic effects on the septin dynamics are not known. After 3 h in galactose, the septin ring in the vector control cell slowly and gradually decreased in intensity over a long time (more than 30 min) before completely disappeared (Fig. 5.8C, upper). Under the same condition, however, the septins in the cells overexpressing Syp1p disassembled very rapidly (Fig. 5.8C, lower). The rings disappeared as rapidly as just a few minutes, regardless whether the cell is in a normal morphology or with an elongated bud (Fig. 5.8C). Statistical data indicate that the average disassembly time was about 45 min in the control cells (n=12), and 13 min in Syp1p overexpression cells (n=20). These results are consistent with the observation of the delayed septin

disassembly in the *syp1Δ* mutant, and further support the conclusion that Syp1p functions in the disassembly of septin filaments in late cell cycle stages.

In summary, two possible functions of Syp1p in the regulation of septin dynamics have been identified. The early cell cycle function is related to the ring formation at the new budding site and the late one is the promotion of septin disassembly at the mother-daughter neck.

### 5.2.6 Effects of *SYP1* deletion on the bud site selection

The representative budding patterns of this strain manifested by new septin formation were shown in the left panel of Figure 5.9A. Interestingly, *syp1*Δ cells were observed to be more inclined to select a proximal budding pattern than their parental cells. There were at least 80% of *syp1*Δ mother cells choosing the axial budding pattern, 20% more than wild type mother cells (Fig. 5.9A, right, n>40 for each strain). However, the difference in the daughter cell budding patterns between the wild type and *syp1*Δ cells was negligible (Fig. 5.9A, right). The budding patterns of the first and second generation of budding were specifically analyzed in both wild type and *syp1*Δ cells by Calcofluor staining. For the first generation budding, the budding pattern was scored by the position of the bud in relation to the birth scar (Fig. 5.9B, left). For the second generation cells which already had a bud scar, the pattern was determined by the bud position in relation to the bud scar (Fig. 5.9B, left). The quantitative data is shown in the right panel of Figure 5.9B. It was found that in the first two cycles of cell division, *syp1*Δ cells consistently showed a higher ratio (20% more) of the axial budding pattern than wild type cells (n>100 for each strain). These results suggest that Syp1p may play a role in the bud

site selection. As septins are also required for bud site selection (Zahner *et al.*, 1996), the effect of *syp1*Δ on the bud site selection may be due to its effect on septins.

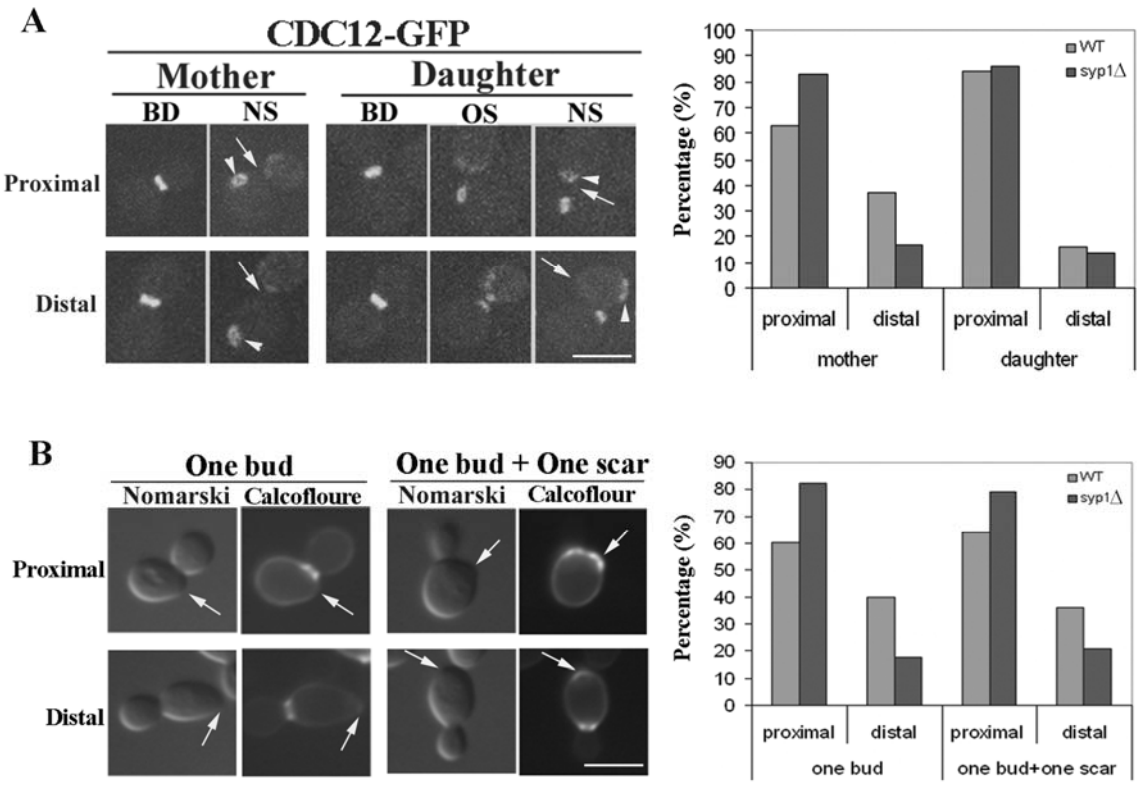


**Figure 5.9 Effect of the *syp1*Δ mutation on bud site selection**. (A) The bud site selection pattern in wild-type and *syp1*Δ cells by observing the new septin formation. YMC517 (wild type) and YMC516 (*syp1*Δ) containing *CDC12-GFP* were observed under a time-lapse microscope. The budding pattern (proximal or distal) was determined by the position of new septins relative to the division site. The arrows indicate the division site and the arrowheads show the new septin rings being assembled. BD, before division; OS, old septin; NS, new septin. The statistical data are shown in the right panel. (B) The budding selection pattern in wild-type and the *syp1*Δ cells stained with Calcofluor. W303 and YMC515 (*syp1*Δ) were grown at 30°C to log phase and fixed for Calcofluor staining as mentioned in Materials and Methods. Two kinds of cells were analyzed. One contains only one bud and no bud scar (the first generation) and the other contains one bud and one scar (the second generation). The budding pattern (proximal or distal) was determined by the position of new bud relative to the birth scar or bud scar. The arrows show the previous division sites. The statistical data are shown in the right panel. Bars, 5 μm.

## 5.3 Discussion

Inspired by the observations that Syp1p localizes to the bud neck and its overexpression causes bud elongation, its functional relationship with the septin cytoskeleton was specifically analyzed in this study. Using biochemical and live cell imaging methods, Syp1p is revealed to be a septin binding protein involved in the regulation of septin cytoskeleton dynamics during the yeast cell cycle.

### 5.3.1 Evidence for Syp1p functioning in septin organization

The evidence to support the conclusion that Syp1p functions in septin organization is multifold. Firstly, Syp1p colocalized with septins throughout most of the cell cycle. It appears at the new bud site in the early stage of cell cycle at the same time as septins, and they remain localized together at the division site after cell separation. Several other proteins in budding yeast, such as Gin4p, Bni4p, and Bnr1p, exhibit a similar pattern of cellular localization, all of which are involved in septin organization or cell morphogenesis (Gladfelter *et al.*, 2001). Secondly, Syp1p physically interacts with septins *in vitro*. Syp1p was found to interact with Cdc10p directly in the two hybrid assay. In addition to Cdc10p, Syp1p can also be precipitated from cell extracts by Cdc12p, and more weakly by other septins, suggesting that Syp1p associates with the septin complex *in vivo*. Consistent with the physical interaction between Syp1p and septin filaments, the localization of Syp1p is dependent on the integrity of septins at the neck. Thirdly, overexpression of Syp1p can dismantle the normal septin organization and induce phenotypes attributable to septins such as bud elongation and unsuccessful cytokinesis. Overexpression of Syp1p also causes cell lethality in septin mutants such as

*cdc10* and *cdc3*. Fourthly, the *syp1*Δ mutation and Syp1p overexpression both affect the septin assembly and disassembly at specific cell cycle stages. And finally, the pattern of bud site selection is altered in the *syp1*Δ mutant, a phenotype also attributable to septin organization. All these results strongly suggest a functional relationship between Syp1p and septin organization.

### 5.3.2 Interaction between Syp1p and septins

Cdc10p is the only septin protein able to interact with Syp1p in the two hybrid assay. The binding activity between Syp1p and Cdc10p is at a similar level to the binding between Cdc10p and Bni4p, which was used as a positive control in the assay (data not shown). Cdc10p is also the one that can precipitate down Syp1p from cell extracts most efficiently, although GST fusion proteins of Cdc12p, Cdc3p and Cdc11p are also able to associate with Syp1p in this assay at variably lower efficiencies. In addition, both the N-terminal region of Cdc10p, which includes the GTP binding domain, and the C-terminal region, which includes the septin unique domain, are able to pull down Syp1p with a comparable efficiency (data not shown). In this experiment, Cdc11p was also detected in the precipitates along with Syp1p. These findings strongly suggest that Syp1p binds to the septin filaments at a region where Cdc10p is a main part of the interacting interface. Similar cases have been reported before in both yeast and mammalian cells, in which septin binding proteins have been found to interact with the septin filaments (Lee *et al.*, 2002; Mortensen *et al.*, 2002; Sheffield *et al.*, 2003).

Cdc10p is a unique septin subunit in that, as the model of septin filament assembly suggests (Fig. 1.9B) (Versele *et al.*, 2004), it is not a part of the

heteropentameric complex that serves as the building block of the septin filament. Instead, Cdc10p acts as a bridge to link polymer septin complexes into paired filaments by interacting with the Cdc12p-Cdc3p complex (Versele *et al.*, 2004). Cdc10p, therefore, is ideally the best target for regulating the assembly and disassembly of septin filaments. The finding that Syp1p binds to the septin complex mainly by interacting with Cdc10p fits very well with the suggested role of Syp1p in regulating the assembly and disassembly of septin filaments.

### 5.3.3 Regulation of septin dynamics by Syp1p

The role of Syp1p in regulating the assembly and disassembly of septin filaments is also well supported by its dynamic cellular localizations. Syp1p and septins appears simultaneously during G1, localizing together at the incipient bud site about 8-10 min before bud emergence. Syp1p remains co-localized with septins at the bud neck until late at the large-budded stage. Prior to cytokinesis, Syp1p re-localizes to the bud neck and remains there until the cell has divided and septins disassembled. The dynamic behavior of Syp1p and its persistent co-localization with septins around cell cycle, suggest that Syp1p may regulate the septin organization at different cell cycle stages. Indeed, in *syp1*Δ cells, the septin dynamics are altered at least at two stages of cell cycle. Early in the cell cycle of the wild-type cells, septins first appear at the incipient bud site as cloudy and irregular structures, as has also been observed recently by Iwase *et al* (Iwase *et al.*, 2006). They then transform into a jagged ring, which further develops into a complete ring. The whole process takes about 4-5 min. However, in *syp1*Δ cells, the jagged ring persists for a longer time and the process of forming a complete ring lasts twice as long

as in the wild type. In the absence of Syp1p, therefore, the septin ring formation at the beginning of the cell cycle is delayed.

Another aspect of septin dynamics that is altered in *syp1*Δ cells is the septin disassembly at the daughter side of the neck in a late stage of the cell cycle. *syp1*Δ cells consistently show a delay of 8-10 min in this process compared with the wild type. The disassembly at the mother side of the neck appears to be unaffected. This observation, however, should be taken with caution, given the fact that the distribution of septin filaments at the two sides of the neck is overwhelmingly uneven in this strain background. Nevertheless, the finding that the septin filaments persist significantly longer in *syp1*Δ cells during the later stage of the cell cycle strongly indicates that Syp1p is required for disassembly of the old septin filaments. This notion is further supported by the result of the Syp1p overexpression experiment, in which the septin ring is found to be disassembled at a rate several times faster than in the control. The remarkably accelerated septin disassembly resulted from Syp1p overexpression may also explain the lethality caused by Syp1p overexpression to the septin mutants.

It has been reported that the septin disassembly after cytokinesis requires septin phosphorylation and dephosphorylation by the Cdc28-Cln kinase and PP2A phosphatase, respectively (Tang and Reed, 2002; Dobbelaere *et al.*, 2003; Moffat and Andrews, 2004). It will be interesting to investigate whether the Syp1p-promoted disassembly of septins is involved in the same pathway or not.

### 5.3.4 The possible links between actin cytoskeleton and septins through Syp1p

## Chapter 5 Functional Relationship between Syp1p and the septin cytoskeleton

In this study, Syp1p is demonstrated to interact with both actin cytoskeleton and septin cytoskeleton. The functional linkage between Syp1p-actin and Syp1p-septin interactions is still unclear. Nevertheless, it is found that the localization of Syp1p to the budding site and the neck is abolished by the treatment of Latrunculin A, an actin filament toxin, or by a mutation in the actin gene (Fig.4.7). Therefore, Syp1p's function in septin organization is possibly dependent on actin cytoskeleton.

The functional relationship between actin cytoskeleton and septins has emerged recently. Septin is necessary for maintenance of polarity of actin cytoskeleton (Barral *et al.*, 2000) and for the actomyosin rings contraction during the cytokinesis (Takizawa *et al.*, 2000; Lippincott *et al.*, 2001). Actin cytoskeleton is also involved in septin organization and functions. It has been reported that the initial septin ring assembly requires the actin cytoskeleton in budding yeast (Kadota *et al.*, 2004). The initial septin ring was found to be much larger in *bni1cla4* double mutant or in cell treated with LatA. These findings indicate that actin cytoskeleton can affect septin organization. However, the mechanism of how actin regulates the formation of initial septin ring is unknown. As the actin cytoskeleton associated protein Syp1p also play a role in the initial septin ring formation, it will be worthwhile to investigate whether and how Syp1p-actin interaction can regulate this septin dynamics.

Recently, the studies about how actin cytoskeleton responses to stress signals have been reported (McMillan *et al.*, 1998; Harrison *et al.*, 2001; McNulty and Lew, 2005; Clotet *et al.*, 2006). Under stressful condition, the actin cytoskeleton rearranges very quickly and then causes cell arrest to adjust to this stress environment. This stress response has been discovered as a morphogenesis checkpoint which regulates the septin-

dependent Swe1p stability upon actin disorganization (McMillan *et al.*, 1998; Keaton and Lew, 2006). As the localization of Syp1p is sensitive to mild actin disruption, it would be interesting to investigate whether Syp1p is a mediator that links the actin disorganization to Swe1p stability.

To conclude, the functional relationship between Syp1p and actin/septin cytoskeleton has been demonstrated in this study. Syp1p is shown to be a novel substrate of Prk1p and has functional relationship with both actin cable and actin patch-related proteins. Overexpressing Syp1p partially suppresses the *pfy1*Δ and *bni1*Δ mutants. Syp1p is also found to interact with actin-associated protein Sla1p. In addition to the relationship with actin cytoskeleton, Syp1p physically interacts with septin filaments and is involved in the processes of septin ring formation in the early stage of cell cycle and septin disassembly in the later stage of cell cycle. Through its functional relationship with actin and septin cytoskeletons, Syp1p may play a role in cell polarized growth and division.

# References

Adams, A.E., Botstein, D., and Drubin, D.G. (1989). A yeast actin-binding protein is encoded by SAC6, a gene found by suppression of an actin mutation. Science *243*, 231-233.

Adams, A.E., Botstein, D., and Drubin, D.G. (1991). Requirement of yeast fimbrin for actin organization and morphogenesis in vivo. Nature *354*, 404-408.

Adams, A.E., Johnson, D.I., Longnecker, R.M., Sloat, B.F., and Pringle, J.R. (1990). CDC42 and CDC43, two additional genes involved in budding and the establishment of cell polarity in the yeast Saccharomyces cerevisiae. J Cell Biol *111*, 131-142.

Adams, A.E., and Pringle, J.R. (1984). Relationship of actin and tubulin distribution to bud growth in wild-type and morphogenetic-mutant Saccharomyces cerevisiae. J Cell Biol *98*, 934-945.

Adams, A.E., and Pringle, J.R. (1991). Staining of actin with fluorochrome-conjugated phalloidin. Methods Enzymol *194*, 729-731.

Aguilar, R.C., Watson, H.A., and Wendland, B. (2003). The yeast Epsin Ent1 is recruited to membranes through multiple independent interactions. J Biol Chem *278*, 10737-10743.

Alberts, A.S. (2001). Identification of a carboxyl-terminal diaphanous-related formin homology protein autoregulatory domain. J Biol Chem *276*, 2824-2830.

Alexander, M.R., Tyers, M., Perret, M., Craig, B.M., Fang, K.S., and Gustin, M.C. (2001). Regulation of cell cycle progression by Swe1p and Hog1p following hypertonic stress. Mol Biol Cell *12*, 53-62.

Amann, K.J., and Pollard, T.D. (2001). The Arp2/3 complex nucleates actin filament branches from the sides of pre-existing filaments. Nat Cell Biol *3*, 306-310.

Amatruda, J.F., Gattermeir, D.J., Karpova, T.S., and Cooper, J.A. (1992). Effects of null mutations and overexpression of capping protein on morphogenesis, actin distribution and polarized secretion in yeast. J Cell Biol *119*, 1151-1162.

Amberg, D.C. (1998). Three-dimensional imaging of the yeast actin cytoskeleton through the budding cell cycle. Mol Biol Cell *9*, 3259-3262.

Amberg, D.C., Basart, E., and Botstein, D. (1995). Defining protein interactions with yeast actin in vivo. Nat Struct Biol *2*, 28-35.

Amberg, D.C., Zahner, J.E., Mulholland, J.W., Pringle, J.R., and Botstein, D. (1997). Aip3p/Bud6p, a yeast actin-interacting protein that is involved in morphogenesis and the selection of bipolar budding sites. Mol Biol Cell *8*, 729-753.

Anderson, B.L., Boldogh, I., Evangelista, M., Boone, C., Greene, L.A., and Pon, L.A. (1998). The Src homology domain 3 (SH3) of a yeast type I myosin, Myo5p, binds to verprolin and is required for targeting to sites of actin polarization. J Cell Biol *141*, 1357-1370.

Asano, S., Park, J.E., Sakchaisri, K., Yu, L.R., Song, S., Supavilai, P., Veenstra, T.D., and Lee, K.S. (2005). Concerted mechanism of Swe1/Wee1 regulation by multiple kinases in budding yeast. Embo J *24*, 2194-2204.

Ayscough, K. (1998). Use of latrunculin-A, an actin monomer-binding drug. Methods Enzymol *298*, 18-25.

Ayscough, K.R., Eby, J.J., Lila, T., Dewar, H., Kozminski, K.G., and Drubin, D.G. (1999). Sla1p is a functionally modular component of the yeast cortical actin cytoskeleton required for correct localization of both Rho1p-GTPase and Sla2p, a protein with talin homology. Mol Biol Cell *10*, 1061-1075.

Balasubramanian, M.K., Bi, E., and Glotzer, M. (2004). Comparative analysis of cytokinesis in budding yeast, fission yeast and animal cells. Curr Biol *14*, R806-818.

Barral, Y., Mermall, V., Mooseker, M.S., and Snyder, M. (2000). Compartmentalization of the cell cortex by septins is required for maintenance of cell polarity in yeast. Mol Cell *5*, 841-851.

Bauer, F., Urdaci, M., Aigle, M., and Crouzet, M. (1993). Alteration of a yeast SH3 protein leads to conditional viability with defects in cytoskeletal and budding patterns. Mol Cell Biol *13*, 5070-5084.

Bender, A. (1993). Genetic evidence for the roles of the bud-site-selection genes BUD5 and BUD2 in control of the Rsr1p (Bud1p) GTPase in yeast. Proc Natl Acad Sci U S A *90*, 9926-9929.

Bi, E. (2001). Cytokinesis in budding yeast: the relationship between actomyosin ring function and septum formation. Cell Struct Funct *26*, 529-537.

Bi, E., Maddox, P., Lew, D.J., Salmon, E.D., McMillan, J.N., Yeh, E., and Pringle, J.R. (1998). Involvement of an actomyosin contractile ring in Saccharomyces cerevisiae cytokinesis. J Cell Biol *142*, 1301-1312.

Blanchoin, L., Amann, K.J., Higgs, H.N., Marchand, J.B., Kaiser, D.A., and Pollard, T.D. (2000). Direct observation of dendritic actin filament networks nucleated by Arp2/3 complex and WASP/Scar proteins. Nature *404*, 1007-1011.

Bompard, G., and Caron, E. (2004). Regulation of WASP/WAVE proteins: making a long story short. J Cell Biol *166*, 957-962.

Booher, R.N., Deshaies, R.J., and Kirschner, M.W. (1993). Properties of Saccharomyces cerevisiae wee1 and its differential regulation of p34CDC28 in response to G1 and G2 cyclins. Embo J *12*, 3417-3426.

Bose, I., Irazoqui, J.E., Moskow, J.J., Bardes, E.S., Zyla, T.R., and Lew, D.J. (2001). Assembly of scaffold-mediated complexes containing Cdc42p, the exchange factor Cdc24p, and the effector Cla4p required for cell cycle-regulated phosphorylation of Cdc24p. J Biol Chem *276*, 7176-7186.

Bouquin, N., Barral, Y., Courbeyrette, R., Blondel, M., Snyder, M., and Mann, C. (2000). Regulation of cytokinesis by the Elm1 protein kinase in Saccharomyces cerevisiae. J Cell Sci *113 ( Pt 8)*, 1435-1445.

Bretscher, A. (2003). Polarized growth and organelle segregation in yeast: the tracks, motors, and receptors. J Cell Biol *160*, 811-816.

Casamayor, A., and Snyder, M. (2002). Bud-site selection and cell polarity in budding yeast. Curr Opin Microbiol *5*, 179-186.

Casamayor, A., and Snyder, M. (2003). Molecular dissection of a yeast septin: distinct domains are required for septin interaction, localization, and function. Mol Cell Biol *23*, 2762-2777.

Caviston, J.P., Longtine, M., Pringle, J.R., and Bi, E. (2003). The role of Cdc42p GTPase-activating proteins in assembly of the septin ring in yeast. Mol Biol Cell *14*, 4051-4066.

Chant, J. (1999). Cell polarity in yeast. Annu Rev Cell Dev Biol *15*, 365-391.

Chant, J., Corrado, K., Pringle, J.R., and Herskowitz, I. (1991). Yeast BUD5, encoding a putative GDP-GTP exchange factor, is necessary for bud site selection and interacts with bud formation gene BEM1. Cell *65*, 1213-1224.

Chant, J., and Herskowitz, I. (1991). Genetic control of bud site selection in yeast by a set of gene products that constitute a morphogenetic pathway. Cell *65*, 1203-1212.

Chant, J., Mischke, M., Mitchell, E., Herskowitz, I., and Pringle, J.R. (1995). Role of Bud3p in producing the axial budding pattern of yeast. J Cell Biol *129*, 767-778.

Chant, J., and Pringle, J.R. (1991). Budding and cell polarity in Saccharomyces cerevisiae. Curr Opin Genet Dev *1*, 342-350.

Chant, J., and Pringle, J.R. (1995). Patterns of bud-site selection in the yeast Saccharomyces cerevisiae. J Cell Biol *129*, 751-765.

Chen, T., Hiroko, T., Chaudhuri, A., Inose, F., Lord, M., Tanaka, S., Chant, J., and Fujita, A. (2000). Multigenerational cortical inheritance of the Rax2 protein in orienting polarity and division in yeast. Science *290*, 1975-1978.

Chien, C.T., Bartel, P.L., Sternglanz, R., and Fields, S. (1991). The two-hybrid system: a method to identify and clone genes for proteins that interact with a protein of interest. Proc Natl Acad Sci U S A *88*, 9578-9582.

Chitu, V., and Stanley, E.R. (2007). Pombe Cdc15 homology (PCH) proteins: coordinators of membrane-cytoskeletal interactions. Trends Cell Biol *17*, 145-156.

Cid, V.J., Adamikova, L., Sanchez, M., Molina, M., and Nombela, C. (2001). Cell cycle control of septin ring dynamics in the budding yeast. Microbiology *147*, 1437-1450.

Cid, V.J., Duran, A., del Rey, F., Snyder, M.P., Nombela, C., and Sanchez, M. (1995). Molecular basis of cell integrity and morphogenesis in Saccharomyces cerevisiae. Microbiol Rev *59*, 345-386.

Clotet, J., Escote, X., Adrover, M.A., Yaakov, G., Gari, E., Aldea, M., de Nadal, E., and Posas, F. (2006). Phosphorylation of Hsl1 by Hog1 leads to a G2 arrest essential for cell survival at high osmolarity. Embo J *25*, 2338-2346.

Conner, S.D., and Schmid, S.L. (2002). Identification of an adaptor-associated kinase, AAK1, as a regulator of clathrin-mediated endocytosis. J Cell Biol *156*, 921-929.

Cope, M.J., Yang, S., Shang, C., and Drubin, D.G. (1999). Novel protein kinases Ark1p and Prk1p associate with and regulate the cortical actin cytoskeleton in budding yeast. J Cell Biol *144*, 1203-1218.

Cross, F., Hartwell, L.H., Jackson, C., and Konopka, J.B. (1988). Conjugation in Saccharomyces cerevisiae. Annu Rev Cell Biol *4*, 429-457.

Crouzet, M., Urdaci, M., Dulau, L., and Aigle, M. (1991). Yeast mutant affected for viability upon nutrient starvation: characterization and cloning of the RVS161 gene. Yeast *7*, 727-743.

Cvrckova, F., De Virgilio, C., Manser, E., Pringle, J.R., and Nasmyth, K. (1995). Ste20-like protein kinases are required for normal localization of cell growth and for cytokinesis in budding yeast. Genes Dev *9*, 1817-1830.

D'Agostino, J.L., and Goode, B.L. (2005). Dissection of Arp2/3 complex actin nucleation mechanism and distinct roles for its nucleation-promoting factors in Saccharomyces cerevisiae. Genetics *171*, 35-47.

DeMarini, D.J., Adams, A.E., Fares, H., De Virgilio, C., Valle, G., Chuang, J.S., and Pringle, J.R. (1997). A septin-based hierarchy of proteins required for localized deposition of chitin in the Saccharomyces cerevisiae cell wall. J Cell Biol *139*, 75-93.

Dobbelaere, J., and Barral, Y. (2004). Spatial coordination of cytokinetic events by compartmentalization of the cell cortex. Science *305*, 393-396.

Dobbelaere, J., Gentry, M.S., Hallberg, R.L., and Barral, Y. (2003). Phosphorylation-dependent regulation of septin dynamics during the cell cycle. Dev Cell *4*, 345-357.

Dong, Y., Pruyne, D., and Bretscher, A. (2003). Formin-dependent actin assembly is regulated by distinct modes of Rho signaling in yeast. J Cell Biol *161*, 1081-1092.

Douglas, L.M., Alvarez, F.J., McCreary, C., and Konopka, J.B. (2005). Septin function in yeast model systems and pathogenic fungi. Eukaryot Cell *4*, 1503-1512.

Drubin, D.G., Jones, H.D., and Wertman, K.F. (1993). Actin structure and function: roles in mitochondrial organization and morphogenesis in budding yeast and identification of the phalloidin-binding site. Mol Biol Cell *4*, 1277-1294.

Dulic, V., Egerton, M., Elguindi, I., Raths, S., Singer, B., and Riezman, H. (1991). Yeast endocytosis assays. Methods Enzymol *194*, 697-710.

Duncan, M.C., Cope, M.J., Goode, B.L., Wendland, B., and Drubin, D.G. (2001). Yeast Eps15-like endocytic protein, Pan1p, activates the Arp2/3 complex. Nat Cell Biol *3*, 687-690.

Eden, S., Rohatgi, R., Podtelejnikov, A.V., Mann, M., and Kirschner, M.W. (2002). Mechanism of regulation of WAVE1-induced actin nucleation by Rac1 and Nck. Nature *418*, 790-793.

Endow, S.A. (2003). Kinesin motors as molecular machines. Bioessays *25*, 1212-1219.

Engqvist-Goldstein, A.E., and Drubin, D.G. (2003). Actin assembly and endocytosis: from yeast to mammals. Annu Rev Cell Dev Biol *19*, 287-332.

Engqvist-Goldstein, A.E., Kessels, M.M., Chopra, V.S., Hayden, M.R., and Drubin, D.G. (1999). An actin-binding protein of the Sla2/Huntingtin interacting protein 1 family is a novel component of clathrin-coated pits and vesicles. J Cell Biol *147*, 1503-1518.

Evangelista, M., Blundell, K., Longtine, M.S., Chow, C.J., Adames, N., Pringle, J.R., Peter, M., and Boone, C. (1997). Bni1p, a yeast formin linking cdc42p and the actin cytoskeleton during polarized morphogenesis. Science *276*, 118-122.

Evangelista, M., Klebl, B.M., Tong, A.H., Webb, B.A., Leeuw, T., Leberer, E., Whiteway, M., Thomas, D.Y., and Boone, C. (2000). A role for myosin-I in actin assembly through interactions with Vrp1p, Bee1p, and the Arp2/3 complex. J Cell Biol *148*, 353-362.

Evangelista, M., Pruyne, D., Amberg, D.C., Boone, C., and Bretscher, A. (2002). Formins direct Arp2/3-independent actin filament assembly to polarize cell growth in yeast. Nat Cell Biol *4*, 260-269.

Evangelista, M., Zigmond, S., and Boone, C. (2003). Formins: signaling effectors for assembly and polarization of actin filaments. J Cell Sci *116*, 2603-2611.

Farkasovsky, M., Herter, P., Voss, B., and Wittinghofer, A. (2005). Nucleotide binding and filament assembly of recombinant yeast septin complexes. Biol Chem *386*, 643-656.

Finger, F.P., and Novick, P. (1997). Sec3p is involved in secretion and morphogenesis in Saccharomyces cerevisiae. Mol Biol Cell *8*, 647-662.

Frazier, J.A., Wong, M.L., Longtine, M.S., Pringle, J.R., Mann, M., Mitchison, T.J., and Field, C. (1998). Polymerization of purified yeast septins: evidence that organized filament arrays may not be required for septin function. J Cell Biol *143*, 737-749.

Freeman, N.L., Lila, T., Mintzer, K.A., Chen, Z., Pahk, A.J., Ren, R., Drubin, D.G., and Field, J. (1996). A conserved proline-rich region of the Saccharomyces cerevisiae cyclase-associated protein binds SH3 domains and modulates cytoskeletal localization. Mol Cell Biol *16*, 548-556.

Fujita, A., Oka, C., Arikawa, Y., Katagai, T., Tonouchi, A., Kuhara, S., and Misumi, Y. (1994). A yeast gene necessary for bud-site selection encodes a protein similar to insulin-degrading enzymes. Nature *372*, 567-570.

Fujiwara, T., Tanaka, K., Mino, A., Kikyo, M., Takahashi, K., Shimizu, K., and Takai, Y. (1998). Rho1p-Bni1p-Spa2p interactions: implication in localization of Bni1p at the bud site and regulation of the actin cytoskeleton in Saccharomyces cerevisiae. Mol Biol Cell *9*, 1221-1233.

Gagny, B., Wiederkehr, A., Dumoulin, P., Winsor, B., Riezman, H., and Haguenauer-Tsapis, R. (2000). A novel EH domain protein of Saccharomyces cerevisiae, Ede1p, involved in endocytosis. J Cell Sci *113 ( Pt 18)*, 3309-3319.

Gavin, A.C., Bosche, M., Krause, R., Grandi, P., Marzioch, M., Bauer, A., Schultz, J., Rick, J.M., Michon, A.M., Cruciat, C.M., Remor, M., Hofert, C., Schelder, M., Brajenovic, M., Ruffner, H., Merino, A., Klein, K., Hudak, M., Dickson, D., Rudi, T., Gnau, V., Bauch, A., Bastuck, S., Huhse, B., Leutwein, C., Heurtier, M.A., Copley, R.R., Edelmann, A., Querfurth, E., Rybin, V., Drewes, G., Raida, M., Bouwmeester, T., Bork, P., Seraphin, B., Kuster, B., Neubauer, G., and Superti-Furga, G. (2002). Functional organization of the yeast proteome by systematic analysis of protein complexes. Nature *415*, 141-147.

Gimeno, C.J., Ljungdahl, P.O., Styles, C.A., and Fink, G.R. (1992). Unipolar cell divisions in the yeast S. cerevisiae lead to filamentous growth: regulation by starvation and RAS. Cell *68*, 1077-1090.

Giot, L., and Konopka, J.B. (1997). Functional analysis of the interaction between Afr1p and the Cdc12p septin, two proteins involved in pheromone-induced morphogenesis. Mol Biol Cell *8*, 987-998.

Gladfelter, A.S., Bose, I., Zyla, T.R., Bardes, E.S., and Lew, D.J. (2002). Septin ring assembly involves cycles of GTP loading and hydrolysis by Cdc42p. J Cell Biol *156*, 315-326.

Gladfelter, A.S., Kozubowski, L., Zyla, T.R., and Lew, D.J. (2005). Interplay between septin organization, cell cycle and cell shape in yeast. J Cell Sci *118*, 1617-1628.

Gladfelter, A.S., Pringle, J.R., and Lew, D.J. (2001). The septin cortex at the yeast mother-bud neck. Curr Opin Microbiol *4*, 681-689.

Gladfelter, A.S., Zyla, T.R., and Lew, D.J. (2004). Genetic interactions among regulators of septin organization. Eukaryot Cell *3*, 847-854.

Goode, B.L., and Rodal, A.A. (2001). Modular complexes that regulate actin assembly in budding yeast. Curr Opin Microbiol *4*, 703-712.

Goode, B.L., Rodal, A.A., Barnes, G., and Drubin, D.G. (2001). Activation of the Arp2/3 complex by the actin filament binding protein Abp1p. J Cell Biol *153*, 627-634.

Gourlay, C.W., Dewar, H., Warren, D.T., Costa, R., Satish, N., and Ayscough, K.R. (2003). An interaction between Sla1p and Sla2p plays a role in regulating actin dynamics and endocytosis in budding yeast. J Cell Sci *116*, 2551-2564.

Gulli, M.P., Jaquenoud, M., Shimada, Y., Niederhauser, G., Wiget, P., and Peter, M. (2000). Phosphorylation of the Cdc42 exchange factor Cdc24 by the PAK-like kinase Cla4 may regulate polarized growth in yeast. Mol Cell *6*, 1155-1167.

Haarer, B.K., Lillie, S.H., Adams, A.E., Magdolen, V., Bandlow, W., and Brown, S.S. (1990). Purification of profilin from Saccharomyces cerevisiae and analysis of profilin-deficient cells. J Cell Biol *110*, 105-114.

Haarer, B.K., and Pringle, J.R. (1987). Immunofluorescence localization of the Saccharomyces cerevisiae CDC12 gene product to the vicinity of the 10-nm filaments in the mother-bud neck. Mol Cell Biol *7*, 3678-3687.

Hall, P.A., and Russell, S.E. (2004). The pathobiology of the septin gene family. J Pathol *204*, 489-505.

Halme, A., Michelitch, M., Mitchell, E.L., and Chant, J. (1996). Bud10p directs axial cell polarization in budding yeast and resembles a transmembrane receptor. Curr Biol *6*, 570-579.

Harkins, H.A., Page, N., Schenkman, L.R., De Virgilio, C., Shaw, S., Bussey, H., and Pringle, J.R. (2001). Bud8p and Bud9p, proteins that may mark the sites for bipolar budding in yeast. Mol Biol Cell *12*, 2497-2518.

Harrison, J.C., Bardes, E.S., Ohya, Y., and Lew, D.J. (2001). A role for the Pkc1p/Mpk1p kinase cascade in the morphogenesis checkpoint. Nat Cell Biol *3*, 417-420.

Harsay, E., and Bretscher, A. (1995). Parallel secretory pathways to the cell surface in yeast. J Cell Biol *131*, 297-310.

Hartwell, L.H. (1971). Genetic control of the cell division cycle in yeast. IV. Genes controlling bud emergence and cytokinesis. Exp Cell Res *69*, 265-276.

Hartwell, L.H., and Weinert, T.A. (1989). Checkpoints: controls that ensure the order of cell cycle events. Science *246*, 629-634.

Harvey, S.L., Charlet, A., Haas, W., Gygi, S.P., and Kellogg, D.R. (2005). Cdk1-dependent regulation of the mitotic inhibitor Wee1. Cell *122*, 407-420.

Henry, K.R., D'Hondt, K., Chang, J.S., Nix, D.A., Cope, M.J., Chan, C.S., Drubin, D.G., and Lemmon, S.K. (2003). The actin-regulating kinase Prk1p negatively regulates Scd5p, a suppressor of clathrin deficiency, in actin organization and endocytosis. Curr Biol *13*, 1564-1569.

Higgs, H.N., and Pollard, T.D. (2001). Regulation of actin filament network formation through ARP2/3 complex: activation by a diverse array of proteins. Annu Rev Biochem *70*, 649-676.

Holtzman, D.A., Yang, S., and Drubin, D.G. (1993). Synthetic-lethal interactions identify two novel genes, SLA1 and SLA2, that control membrane cytoskeleton assembly in Saccharomyces cerevisiae. J Cell Biol *122*, 635-644.

Howard, J.P., Hutton, J.L., Olson, J.M., and Payne, G.S. (2002). Sla1p serves as the targeting signal recognition factor for NPFX(1,2)D-mediated endocytosis. J Cell Biol *157*, 315-326.

Huang, B., Zeng, G., Ng, A.Y., and Cai, M. (2003). Identification of novel recognition motifs and regulatory targets for the yeast actin-regulating kinase Prk1p. Mol Biol Cell *14*, 4871-4884.

Huckaba, T.M., Gay, A.C., Pantalena, L.F., Yang, H.C., and Pon, L.A. (2004). Live cell imaging of the assembly, disassembly, and actin cable-dependent movement of endosomes and actin patches in the budding yeast, Saccharomyces cerevisiae. J Cell Biol *167*, 519-530.

Imamura, H., Tanaka, K., Hihara, T., Umikawa, M., Kamei, T., Takahashi, K., Sasaki, T., and Takai, Y. (1997). Bni1p and Bnr1p: downstream targets of the Rho family small G-proteins which interact with profilin and regulate actin cytoskeleton in Saccharomyces cerevisiae. Embo J *16*, 2745-2755.

Irazoqui, J.E., Gladfelter, A.S., and Lew, D.J. (2003). Scaffold-mediated symmetry breaking by Cdc42p. Nat Cell Biol *5*, 1062-1070.

Irazoqui, J.E., Howell, A.S., Theesfeld, C.L., and Lew, D.J. (2005). Opposing roles for actin in Cdc42p polarization. Mol Biol Cell *16*, 1296-1304.

Iwase, M., Luo, J., Nagaraj, S., Longtine, M., Kim, H.B., Haarer, B.K., Caruso, C., Tong, Z., Pringle, J.R., and Bi, E. (2006). Role of a Cdc42p effector pathway in recruitment of the yeast septins to the presumptive bud site. Mol Biol Cell *17*, 1110-1125.

Jaquenoud, M., and Peter, M. (2000). Gic2p may link activated Cdc42p to components involved in actin polarization, including Bni1p and Bud6p (Aip3p). Mol Cell Biol *20*, 6244-6258.

Johnson, D.I., and Pringle, J.R. (1990). Molecular characterization of CDC42, a Saccharomyces cerevisiae gene involved in the development of cell polarity. J Cell Biol *111*, 143-152.

Kadota, J., Yamamoto, T., Yoshiuchi, S., Bi, E., and Tanaka, K. (2004). Septin ring assembly requires concerted action of polarisome components, a PAK kinase Cla4p, and the actin cytoskeleton in Saccharomyces cerevisiae. Mol Biol Cell *15*, 5329-5345.

Kaksonen, M., Sun, Y., and Drubin, D.G. (2003). A pathway for association of receptors, adaptors, and actin during endocytic internalization. Cell *115*, 475-487.

Kaksonen, M., Toret, C.P., and Drubin, D.G. (2005). A modular design for the clathrin- and actin-mediated endocytosis machinery. Cell *123*, 305-320.

Karpova, T.S., Reck-Peterson, S.L., Elkind, N.B., Mooseker, M.S., Novick, P.J., and Cooper, J.A. (2000). Role of actin and Myo2p in polarized secretion and growth of Saccharomyces cerevisiae. Mol Biol Cell *11*, 1727-1737.

Kartmann, B., and Roth, D. (2001). Novel roles for mammalian septins: from vesicle trafficking to oncogenesis. J Cell Sci *114*, 839-844.

Keaton, M.A., and Lew, D.J. (2006). Eavesdropping on the cytoskeleton: progress and controversy in the yeast morphogenesis checkpoint. Curr Opin Microbiol *9*, 540-546.

Kikyo, M., Tanaka, K., Kamei, T., Ozaki, K., Fujiwara, T., Inoue, E., Takita, Y., Ohya, Y., and Takai, Y. (1999). An FH domain-containing Bnr1p is a multifunctional protein interacting with a variety of cytoskeletal proteins in Saccharomyces cerevisiae. Oncogene *18*, 7046-7054.

Kilmartin, J.V., and Adams, A.E. (1984). Structural rearrangements of tubulin and actin during the cell cycle of the yeast Saccharomyces. J Cell Biol *98*, 922-933.

Kim, H.B., Haarer, B.K., and Pringle, J.R. (1991). Cellular morphogenesis in the Saccharomyces cerevisiae cell cycle: localization of the CDC3 gene product and the timing of events at the budding site. J Cell Biol *112*, 535-544.

Kinoshita, M. (2006). Diversity of septin scaffolds. Curr Opin Cell Biol *18*, 54-60.

Kohno, H., Tanaka, K., Mino, A., Umikawa, M., Imamura, H., Fujiwara, T., Fujita, Y., Hotta, K., Qadota, H., Watanabe, T., Ohya, Y., and Takai, Y. (1996). Bni1p implicated in

cytoskeletal control is a putative target of Rho1p small GTP binding protein in Saccharomyces cerevisiae. Embo J *15*, 6060-6068.

Kops, G.J., Weaver, B.A., and Cleveland, D.W. (2005). On the road to cancer: aneuploidy and the mitotic checkpoint. Nat Rev Cancer *5*, 773-785.

Kovar, D.R. (2006). Molecular details of formin-mediated actin assembly. Curr Opin Cell Biol *18*, 11-17.

Kovar, D.R., Harris, E.S., Mahaffy, R., Higgs, H.N., and Pollard, T.D. (2006). Control of the assembly of ATP- and ADP-actin by formins and profilin. Cell *124*, 423-435.

Kozminski, K.G., Beven, L., Angerman, E., Tong, A.H., Boone, C., and Park, H.O. (2003). Interaction between a Ras and a Rho GTPase couples selection of a growth site to the development of cell polarity in yeast. Mol Biol Cell *14*, 4958-4970.

Kubler, E., and Riezman, H. (1993). Actin and fimbrin are required for the internalization step of endocytosis in yeast. Embo J *12*, 2855-2862.

Lechler, T., Shevchenko, A., and Li, R. (2000). Direct involvement of yeast type I myosins in Cdc42-dependent actin polymerization. J Cell Biol *148*, 363-373.

Lee, P.R., Song, S., Ro, H.S., Park, C.J., Lippincott, J., Li, R., Pringle, J.R., De Virgilio, C., Longtine, M.S., and Lee, K.S. (2002). Bni5p, a septin-interacting protein, is required for normal septin function and cytokinesis in Saccharomyces cerevisiae. Mol Cell Biol *22*, 6906-6920.

Lee, W.L., Bezanilla, M., and Pollard, T.D. (2000). Fission yeast myosin-I, Myo1p, stimulates actin assembly by Arp2/3 complex and shares functions with WASp. J Cell Biol *151*, 789-800.

Lew, D.J. (2003). The morphogenesis checkpoint: how yeast cells watch their figures. Curr Opin Cell Biol *15*, 648-653.

Li, F., and Higgs, H.N. (2003). The mouse Formin mDia1 is a potent actin nucleation factor regulated by autoinhibition. Curr Biol *13*, 1335-1340.

Li, R. (1997). Bee1, a yeast protein with homology to Wiscott-Aldrich syndrome protein, is critical for the assembly of cortical actin cytoskeleton. J Cell Biol *136*, 649-658.

Li, R., Zheng, Y., and Drubin, D.G. (1995). Regulation of cortical actin cytoskeleton assembly during polarized cell growth in budding yeast. J Cell Biol *128*, 599-615.

Lippincott, J., and Li, R. (1998a). Dual function of Cyk2, a cdc15/PSTPIP family protein, in regulating actomyosin ring dynamics and septin distribution. J Cell Biol *143*, 1947-1960.

Lippincott, J., and Li, R. (1998b). Sequential assembly of myosin II, an IQGAP-like protein, and filamentous actin to a ring structure involved in budding yeast cytokinesis. J Cell Biol *140*, 355-366.

Lippincott, J., and Li, R. (2000). Involvement of PCH family proteins in cytokinesis and actin distribution. Microsc Res Tech *49*, 168-172.

Lippincott, J., Shannon, K.B., Shou, W., Deshaies, R.J., and Li, R. (2001). The Tem1 small GTPase controls actomyosin and septin dynamics during cytokinesis. J Cell Sci *114*, 1379-1386.

Longtine, M.S., and Bi, E. (2003). Regulation of septin organization and function in yeast. Trends Cell Biol *13*, 403-409.

Longtine, M.S., DeMarini, D.J., Valencik, M.L., Al-Awar, O.S., Fares, H., De Virgilio, C., and Pringle, J.R. (1996). The septins: roles in cytokinesis and other processes. Curr Opin Cell Biol *8*, 106-119.

Longtine, M.S., Fares, H., and Pringle, J.R. (1998). Role of the yeast Gin4p protein kinase in septin assembly and the relationship between septin assembly and septin function. J Cell Biol *143*, 719-736.

Longtine, M.S., Theesfeld, C.L., McMillan, J.N., Weaver, E., Pringle, J.R., and Lew, D.J. (2000). Septin-dependent assembly of a cell cycle-regulatory module in Saccharomyces cerevisiae. Mol Cell Biol *20*, 4049-4061.

Louvet, O., Doignon, F., and Crouzet, M. (1997). Stable DNA-binding yeast vector allowing high-bait expression for use in the two-hybrid system. Biotechniques *23*, 816-818, 820.

Madden, K., and Snyder, M. (1998). Cell polarity and morphogenesis in budding yeast. Annu Rev Microbiol *52*, 687-744.

Marcoux, N., Cloutier, S., Zakrzewska, E., Charest, P.M., Bourbonnais, Y., and Pallotta, D. (2000). Suppression of the profilin-deficient phenotype by the RHO2 signaling pathway in Saccharomyces cerevisiae. Genetics *156*, 579-592.

Marsh, L., Neiman, A.M., and Herskowitz, I. (1991). Signal transduction during pheromone response in yeast. Annu Rev Cell Biol *7*, 699-728.

Martinez, C., and Ware, J. (2004). Mammalian septin function in hemostasis and beyond. Exp Biol Med (Maywood) *229*, 1111-1119.

Mayer, B.J. (2001). SH3 domains: complexity in moderation. J Cell Sci *114*, 1253-1263.

McMillan, J.N., Longtine, M.S., Sia, R.A., Theesfeld, C.L., Bardes, E.S., Pringle, J.R., and Lew, D.J. (1999). The morphogenesis checkpoint in Saccharomyces cerevisiae: cell cycle control of Swe1p degradation by Hsl1p and Hsl7p. Mol Cell Biol *19*, 6929-6939.

McMillan, J.N., Sia, R.A., and Lew, D.J. (1998). A morphogenesis checkpoint monitors the actin cytoskeleton in yeast. J Cell Biol *142*, 1487-1499.

McNulty, J.J., and Lew, D.J. (2005). Swe1p responds to cytoskeletal perturbation, not bud size, in S. cerevisiae. Curr Biol *15*, 2190-2198.

Mendoza, M., Hyman, A.A., and Glotzer, M. (2002). GTP binding induces filament assembly of a recombinant septin. Curr Biol *12*, 1858-1863.

Mitchell, D.A., and Sprague, G.F., Jr. (2001). The phosphotyrosyl phosphatase activator, Ncs1p (Rrd1p), functions with Cla4p to regulate the G(2)/M transition in Saccharomyces cerevisiae. Mol Cell Biol *21*, 488-500.

Mockrin, S.C., and Korn, E.D. (1980). Acanthamoeba profilin interacts with G-actin to increase the rate of exchange of actin-bound adenosine 5'-triphosphate. Biochemistry *19*, 5359-5362.

Moffat, J., and Andrews, B. (2004). Late-G1 cyclin-CDK activity is essential for control of cell morphogenesis in budding yeast. Nat Cell Biol *6*, 59-66.

Moore, L.B., and Campbell, R.D. (1973). Bud initiation in a non-budding strain of hydra: role of interstitial cells. J Exp Zool *184*, 397-408.

Moreau, V., Madania, A., Martin, R.P., and Winson, B. (1996). The Saccharomyces cerevisiae actin-related protein Arp2 is involved in the actin cytoskeleton. J Cell Biol *134*, 117-132.

Mortensen, E.M., McDonald, H., Yates, J., 3rd, and Kellogg, D.R. (2002). Cell cycle-dependent assembly of a Gin4-septin complex. Mol Biol Cell *13*, 2091-2105.

Moseley, J.B., and Goode, B.L. (2005). Differential activities and regulation of Saccharomyces cerevisiae formin proteins Bni1 and Bnr1 by Bud6. J Biol Chem *280*, 28023-28033.

Moseley, J.B., and Goode, B.L. (2006). The yeast actin cytoskeleton: from cellular function to biochemical mechanism. Microbiol Mol Biol Rev *70*, 605-645.

Moseley, J.B., Sagot, I., Manning, A.L., Xu, Y., Eck, M.J., Pellman, D., and Goode, B.L. (2004). A conserved mechanism for Bni1- and mDia1-induced actin assembly and dual regulation of Bni1 by Bud6 and profilin. Mol Biol Cell *15*, 896-907.

Mulholland, J., Konopka, J., Singer-Kruger, B., Zerial, M., and Botstein, D. (1999). Visualization of receptor-mediated endocytosis in yeast. Mol Biol Cell *10*, 799-817.

Munn, A.L., Stevenson, B.J., Geli, M.I., and Riezman, H. (1995). end5, end6, and end7: mutations that cause actin delocalization and block the internalization step of endocytosis in Saccharomyces cerevisiae. Mol Biol Cell *6*, 1721-1742.

Newpher, T.M., Smith, R.P., Lemmon, V., and Lemmon, S.K. (2005). In vivo dynamics of clathrin and its adaptor-dependent recruitment to the actin-based endocytic machinery in yeast. Dev Cell *9*, 87-98.

Novick, P., and Botstein, D. (1985). Phenotypic analysis of temperature-sensitive yeast actin mutants. Cell *40*, 405-416.

Okuzaki, D., Watanabe, T., Tanaka, S., and Nojima, H. (2003). The Saccharomyces cerevisiae bud-neck proteins Kcc4 and Gin4 have distinct but partially-overlapping cellular functions. Genes Genet Syst *78*, 113-126.

Ozaki-Kuroda, K., Yamamoto, Y., Nohara, H., Kinoshita, M., Fujiwara, T., Irie, K., and Takai, Y. (2001). Dynamic localization and function of Bni1p at the sites of directed growth in Saccharomyces cerevisiae. Mol Cell Biol *21*, 827-839.

Park, H.O., Bi, E., Pringle, J.R., and Herskowitz, I. (1997). Two active states of the Ras-related Bud1/Rsr1 protein bind to different effectors to determine yeast cell polarity. Proc Natl Acad Sci U S A *94*, 4463-4468.

Park, H.O., Chant, J., and Herskowitz, I. (1993). BUD2 encodes a GTPase-activating protein for Bud1/Rsr1 necessary for proper bud-site selection in yeast. Nature *365*, 269-274.

Peter, B.J., Kent, H.M., Mills, I.G., Vallis, Y., Butler, P.J., Evans, P.R., and McMahon, H.T. (2004). BAR domains as sensors of membrane curvature: the amphiphysin BAR structure. Science *303*, 495-499.

Piao, H.L., Machado, I.M., and Payne, G.S. (2007). NPFXD-mediated endocytosis is required for polarity and function of a yeast cell wall stress sensor. Mol Biol Cell *18*, 57-65.

Pollard, T.D., and Beltzner, C.C. (2002). Structure and function of the Arp2/3 complex. Curr Opin Struct Biol *12*, 768-774.

Pollard, T.D., Blanchoin, L., and Mullins, R.D. (2000). Molecular mechanisms controlling actin filament dynamics in nonmuscle cells. Annu Rev Biophys Biomol Struct *29*, 545-576.

Pollard, T.D., and Cooper, J.A. (1984). Quantitative analysis of the effect of Acanthamoeba profilin on actin filament nucleation and elongation. Biochemistry *23*, 6631-6641.

Pring, M., Evangelista, M., Boone, C., Yang, C., and Zigmond, S.H. (2003). Mechanism of formin-induced nucleation of actin filaments. Biochemistry *42*, 486-496.

Pringle, J.R., Preston, R.A., Adams, A.E., Stearns, T., Drubin, D.G., Haarer, B.K., and Jones, E.W. (1989). Fluorescence microscopy methods for yeast. Methods Cell Biol *31*, 357-435.

Pruyne, D., and Bretscher, A. (2000). Polarization of cell growth in yeast. I. Establishment and maintenance of polarity states. J Cell Sci *113 ( Pt 3)*, 365-375.

Pruyne, D., Evangelista, M., Yang, C., Bi, E., Zigmond, S., Bretscher, A., and Boone, C. (2002). Role of formins in actin assembly: nucleation and barbed-end association. Science *297*, 612-615.

Pruyne, D., Gao, L., Bi, E., and Bretscher, A. (2004a). Stable and dynamic axes of polarity use distinct formin isoforms in budding yeast. Mol Biol Cell *15*, 4971-4989.

Pruyne, D., Legesse-Miller, A., Gao, L., Dong, Y., and Bretscher, A. (2004b). Mechanisms of polarized growth and organelle segregation in yeast. Annu Rev Cell Dev Biol *20*, 559-591.

Pruyne, D.W., Schott, D.H., and Bretscher, A. (1998). Tropomyosin-containing actin cables direct the Myo2p-dependent polarized delivery of secretory vesicles in budding yeast. J Cell Biol *143*, 1931-1945.

Ram, A.F., Wolters, A., Ten Hoopen, R., and Klis, F.M. (1994). A new approach for isolating cell wall mutants in Saccharomyces cerevisiae by screening for hypersensitivity to calcofluor white. Yeast *10*, 1019-1030.

Ricotta, D., Conner, S.D., Schmid, S.L., von Figura, K., and Honing, S. (2002). Phosphorylation of the AP2 mu subunit by AAK1 mediates high affinity binding to membrane protein sorting signals. J Cell Biol *156*, 791-795.

Roberts, R.L., and Fink, G.R. (1994). Elements of a single MAP kinase cascade in Saccharomyces cerevisiae mediate two developmental programs in the same cell type: mating and invasive growth. Genes Dev *8*, 2974-2985.

Robinson, L.C., Bradley, C., Bryan, J.D., Jerome, A., Kweon, Y., and Panek, H.R. (1999). The Yck2 yeast casein kinase 1 isoform shows cell cycle-specific localization to sites of polarized growth and is required for proper septin organization. Mol Biol Cell *10*, 1077-1092.

Rodal, A.A., Manning, A.L., Goode, B.L., and Drubin, D.G. (2003). Negative regulation of yeast WASp by two SH3 domain-containing proteins. Curr Biol *13*, 1000-1008.

Roemer, T., Madden, K., Chang, J., and Snyder, M. (1996a). Selection of axial growth sites in yeast requires Axl2p, a novel plasma membrane glycoprotein. Genes Dev *10*, 777-793.

Roemer, T., Vallier, L.G., and Snyder, M. (1996b). Selection of polarized growth sites in yeast. Trends Cell Biol *6*, 434-441.

Rohatgi, R., Ho, H.Y., and Kirschner, M.W. (2000). Mechanism of N-WASP activation by CDC42 and phosphatidylinositol 4, 5-bisphosphate. J Cell Biol *150*, 1299-1310.

Romero, S., Le Clainche, C., Didry, D., Egile, C., Pantaloni, D., and Carlier, M.F. (2004). Formin is a processive motor that requires profilin to accelerate actin assembly and associated ATP hydrolysis. Cell *119*, 419-429.

Sagot, I., Klee, S.K., and Pellman, D. (2002a). Yeast formins regulate cell polarity by controlling the assembly of actin cables. Nat Cell Biol *4*, 42-50.

Sagot, I., Rodal, A.A., Moseley, J., Goode, B.L., and Pellman, D. (2002b). An actin nucleation mechanism mediated by Bni1 and profilin. Nat Cell Biol *4*, 626-631.

Sakchaisri, K., Asano, S., Yu, L.R., Shulewitz, M.J., Park, C.J., Park, J.E., Cho, Y.W., Veenstra, T.D., Thorner, J., and Lee, K.S. (2004). Coupling morphogenesis to mitotic entry. Proc Natl Acad Sci U S A *101*, 4124-4129.

Sanders, S.L., and Herskowitz, I. (1996). The BUD4 protein of yeast, required for axial budding, is localized to the mother/BUD neck in a cell cycle-dependent manner. J Cell Biol *134*, 413-427.

Santos, B., and Snyder, M. (1997). Targeting of chitin synthase 3 to polarized growth sites in yeast requires Chs5p and Myo2p. J Cell Biol *136*, 95-110.

Shaw, J.A., Mol, P.C., Bowers, B., Silverman, S.J., Valdivieso, M.H., Duran, A., and Cabib, E. (1991). The function of chitin synthases 2 and 3 in the Saccharomyces cerevisiae cell cycle. J Cell Biol *114*, 111-123.

Sheffield, P.J., Oliver, C.J., Kremer, B.E., Sheng, S., Shao, Z., and Macara, I.G. (2003). Borg/septin interactions and the assembly of mammalian septin heterodimers, trimers, and filaments. J Biol Chem *278*, 3483-3488.

Sheu, Y.J., Santos, B., Fortin, N., Costigan, C., and Snyder, M. (1998). Spa2p interacts with cell polarity proteins and signaling components involved in yeast cell morphogenesis. Mol Cell Biol *18*, 4053-4069.

Sia, R.A., Bardes, E.S., and Lew, D.J. (1998). Control of Swe1p degradation by the morphogenesis checkpoint. Embo J *17*, 6678-6688.

Sia, R.A., Herald, H.A., and Lew, D.J. (1996). Cdc28 tyrosine phosphorylation and the morphogenesis checkpoint in budding yeast. Mol Biol Cell *7*, 1657-1666.

Sikorski, R.S., and Hieter, P. (1989). A system of shuttle vectors and yeast host strains designed for efficient manipulation of DNA in Saccharomyces cerevisiae. Genetics *122*, 19-27.

Sloat, B.F., and Pringle, J.R. (1978). A mutant of yeast defective in cellular morphogenesis. Science *200*, 1171-1173.

Small, J.V., and Kaverina, I. (2003). Microtubules meet substrate adhesions to arrange cell polarity. Curr Opin Cell Biol *15*, 40-47.

Smythe, E., and Ayscough, K.R. (2003). The Ark1/Prk1 family of protein kinases. Regulators of endocytosis and the actin skeleton. EMBO Rep *4*, 246-251.

Song, S., and Lee, K.S. (2001). A novel function of Saccharomyces cerevisiae CDC5 in cytokinesis. J Cell Biol *152*, 451-469.

Sparks, A.B., Rider, J.E., Hoffman, N.G., Fowlkes, D.M., Quillam, L.A., and Kay, B.K. (1996). Distinct ligand preferences of Src homology 3 domains from Src, Yes, Abl, Cortactin, p53bp2, PLCgamma, Crk, and Grb2. Proc Natl Acad Sci U S A *93*, 1540-1544.

Spiliotis, E.T., and Nelson, W.J. (2006). Here come the septins: novel polymers that coordinate intracellular functions and organization. J Cell Sci *119*, 4-10.

Sun, Y., Kaksonen, M., Madden, D.T., Schekman, R., and Drubin, D.G. (2005). Interaction of Sla2p's ANTH domain with PtdIns(4,5)P2 is important for actin-dependent endocytic internalization. Mol Biol Cell *16*, 717-730.

Sun, Y., Martin, A.C., and Drubin, D.G. (2006). Endocytic internalization in budding yeast requires coordinated actin nucleation and myosin motor activity. Dev Cell *11*, 33-46.

Taheri, N., Kohler, T., Braus, G.H., and Mosch, H.U. (2000). Asymmetrically localized Bud8p and Bud9p proteins control yeast cell polarity and development. Embo J *19*, 6686-6696.

Takizawa, P.A., DeRisi, J.L., Wilhelm, J.E., and Vale, R.D. (2000). Plasma membrane compartmentalization in yeast by messenger RNA transport and a septin diffusion barrier. Science *290*, 341-344.

Tan, P.K., Howard, J.P., and Payne, G.S. (1996). The sequence NPFXD defines a new class of endocytosis signal in Saccharomyces cerevisiae. J Cell Biol *135*, 1789-1800.

Tang, C.S., and Reed, S.I. (2002). Phosphorylation of the septin cdc3 in g1 by the cdc28 kinase is essential for efficient septin ring disassembly. Cell Cycle *1*, 42-49.

Tang, H.Y., and Cai, M. (1996). The EH-domain-containing protein Pan1 is required for normal organization of the actin cytoskeleton in Saccharomyces cerevisiae. Mol Cell Biol *16*, 4897-4914.

Tang, H.Y., Munn, A., and Cai, M. (1997). EH domain proteins Pan1p and End3p are components of a complex that plays a dual role in organization of the cortical actin cytoskeleton and endocytosis in Saccharomyces cerevisiae. Mol Cell Biol *17*, 4294-4304.

Tang, H.Y., Xu, J., and Cai, M. (2000). Pan1p, End3p, and S1a1p, three yeast proteins required for normal cortical actin cytoskeleton organization, associate with each other and play essential roles in cell wall morphogenesis. Mol Cell Biol *20*, 12-25.

Theesfeld, C.L., Zyla, T.R., Bardes, E.G., and Lew, D.J. (2003). A monitor for bud emergence in the yeast morphogenesis checkpoint. Mol Biol Cell *14*, 3280-3291.

Tolliday, N., VerPlank, L., and Li, R. (2002). Rho1 directs formin-mediated actin ring assembly during budding yeast cytokinesis. Curr Biol *12*, 1864-1870.

Toshima, J., Toshima, J.Y., Martin, A.C., and Drubin, D.G. (2005). Phosphoregulation of Arp2/3-dependent actin assembly during receptor-mediated endocytosis. Nat Cell Biol *7*, 246-254.

Trilla, J.A., Cos, T., Duran, A., and Roncero, C. (1997). Characterization of CHS4 (CAL2), a gene of Saccharomyces cerevisiae involved in chitin biosynthesis and allelic to SKT5 and CSD4. Yeast *13*, 795-807.

Vallen, E.A., Caviston, J., and Bi, E. (2000). Roles of Hof1p, Bni1p, Bnr1p, and myo1p in cytokinesis in Saccharomyces cerevisiae. Mol Biol Cell *11*, 593-611.

Valtz, N., and Herskowitz, I. (1996). Pea2 protein of yeast is localized to sites of polarized growth and is required for efficient mating and bipolar budding. J Cell Biol *135*, 725-739.

Versele, M., Gullbrand, B., Shulewitz, M.J., Cid, V.J., Bahmanyar, S., Chen, R.E., Barth, P., Alber, T., and Thorner, J. (2004). Protein-protein interactions governing septin heteropentamer assembly and septin filament organization in Saccharomyces cerevisiae. Mol Biol Cell *15*, 4568-4583.

Versele, M., and Thorner, J. (2004). Septin collar formation in budding yeast requires GTP binding and direct phosphorylation by the PAK, Cla4. J Cell Biol *164*, 701-715.

Versele, M., and Thorner, J. (2005). Some assembly required: yeast septins provide the instruction manual. Trends Cell Biol *15*, 414-424.

Vojtek, A., Haarer, B., Field, J., Gerst, J., Pollard, T.D., Brown, S., and Wigler, M. (1991). Evidence for a functional link between profilin and CAP in the yeast S. cerevisiae. Cell *66*, 497-505.

Volland, C., Urban-Grimal, D., Geraud, G., and Haguenauer-Tsapis, R. (1994). Endocytosis and degradation of the yeast uracil permease under adverse conditions. J Biol Chem *269*, 9833-9841.

Voth, W.P., Olsen, A.E., Sbia, M., Freedman, K.H., and Stillman, D.J. (2005). ACE2, CBK1, and BUD4 in budding and cell separation. Eukaryot Cell *4*, 1018-1028.

Vrabioiu, A.M., and Mitchison, T.J. (2006). Structural insights into yeast septin organization from polarized fluorescence microscopy. Nature *443*, 466-469.

Wallar, B.J., and Alberts, A.S. (2003). The formins: active scaffolds that remodel the cytoskeleton. Trends Cell Biol *13*, 435-446.

Wang, Y.L. (1985). Exchange of actin subunits at the leading edge of living fibroblasts: possible role of treadmilling. J Cell Biol *101*, 597-602.

Warren, D.T., Andrews, P.D., Gourlay, C.W., and Ayscough, K.R. (2002). Sla1p couples the yeast endocytic machinery to proteins regulating actin dynamics. J Cell Sci *115*, 1703-1715.

Watanabe, N., Arai, H., Iwasaki, J., Shiina, M., Ogata, K., Hunter, T., and Osada, H. (2005). Cyclin-dependent kinase (CDK) phosphorylation destabilizes somatic Wee1 via multiple pathways. Proc Natl Acad Sci U S A *102*, 11663-11668.

Watanabe, N., Kato, T., Fujita, A., Ishizaki, T., and Narumiya, S. (1999). Cooperation between mDia1 and ROCK in Rho-induced actin reorganization. Nat Cell Biol *1*, 136-143.

Watson, H.A., Cope, M.J., Groen, A.C., Drubin, D.G., and Wendland, B. (2001). In vivo role for actin-regulating kinases in endocytosis and yeast epsin phosphorylation. Mol Biol Cell *12*, 3668-3679.

Weiss, E.L., Bishop, A.C., Shokat, K.M., and Drubin, D.G. (2000). Chemical genetic analysis of the budding-yeast p21-activated kinase Cla4p. Nat Cell Biol *2*, 677-685.

Welch, M.D., and Mullins, R.D. (2002). Cellular control of actin nucleation. Annu Rev Cell Dev Biol *18*, 247-288.

Wendland, B., and Emr, S.D. (1998). Pan1p, yeast eps15, functions as a multivalent adaptor that coordinates protein-protein interactions essential for endocytosis. J Cell Biol *141*, 71-84.

Wendland, B., Steece, K.E., and Emr, S.D. (1999). Yeast epsins contain an essential N-terminal ENTH domain, bind clathrin and are required for endocytosis. Embo J *18*, 4383-4393.

Wertman, K.F., Drubin, D.G., and Botstein, D. (1992). Systematic mutational analysis of the yeast ACT1 gene. Genetics *132*, 337-350.

Winter, D., Lechler, T., and Li, R. (1999a). Activation of the yeast Arp2/3 complex by Bee1p, a WASP-family protein. Curr Biol *9*, 501-504.

Winter, D., Podtelejnikov, A.V., Mann, M., and Li, R. (1997). The complex containing actin-related proteins Arp2 and Arp3 is required for the motility and integrity of yeast actin patches. Curr Biol *7*, 519-529.

Winter, D.C., Choe, E.Y., and Li, R. (1999b). Genetic dissection of the budding yeast Arp2/3 complex: a comparison of the in vivo and structural roles of individual subunits. Proc Natl Acad Sci U S A *96*, 7288-7293.

Witke, W. (2004). The role of profilin complexes in cell motility and other cellular processes. Trends Cell Biol *14*, 461-469.

Wolven, A.K., Belmont, L.D., Mahoney, N.M., Almo, S.C., and Drubin, D.G. (2000). In vivo importance of actin nucleotide exchange catalyzed by profilin. J Cell Biol *150*, 895-904.

Yang, S., Ayscough, K.R., and Drubin, D.G. (1997). A role for the actin cytoskeleton of Saccharomyces cerevisiae in bipolar bud-site selection. J Cell Biol *136*, 111-123.

Zahner, J.E., Harkins, H.A., and Pringle, J.R. (1996). Genetic analysis of the bipolar pattern of bud site selection in the yeast Saccharomyces cerevisiae. Mol Cell Biol *16*, 1857-1870.

Zeghouf, M., Guibert, B., Zeeh, J.C., and Cherfils, J. (2005). Arf, Sec7 and Brefeldin A: a model towards the therapeutic inhibition of guanine nucleotide-exchange factors. Biochem Soc Trans *33*, 1265-1268.

Zeng, G., and Cai, M. (1999). Regulation of the actin cytoskeleton organization in yeast by a novel serine/threonine kinase Prk1p. J Cell Biol *144*, 71-82.

Zeng, G., and Cai, M. (2005). Prk1p. Int J Biochem Cell Biol *37*, 48-53.

Zeng, G., Yu, X., and Cai, M. (2001). Regulation of yeast actin cytoskeleton-regulatory complex Pan1p/Sla1p/End3p by serine/threonine kinase Prk1p. Mol Biol Cell *12*, 3759-3772.

Zheng, Y., Bender, A., and Cerione, R.A. (1995). Interactions among proteins involved in bud-site selection and bud-site assembly in Saccharomyces cerevisiae. J Biol Chem *270*, 626-630.

Zheng, Y., Cerione, R., and Bender, A. (1994). Control of the yeast bud-site assembly GTPase Cdc42. Catalysis of guanine nucleotide exchange by Cdc24 and stimulation of GTPase activity by Bem3. J Biol Chem *269*, 2369-2372.